Cholinergic projections to the preBötzinger Complex

by

Xiaqiu Yang

A thesis submitted in partial fulfillment of the requirements for the degree of

Master of Science

Department of Physiology
University of Alberta

Abstract

Breathing is a vital behavior regulated by the brainstem neurons. To maintain the regular ventilation, these neurons need to establish proper interactions with other neurons and process signals transmitted by various neurotransmitters. Located in the ventrolateral medulla, the neurons in the preBötzinger Complex (preBötC) are essential for respiratory rhythmogenesis. Cholinergic neurotransmission influences the activity of preBötC and affects the activity of rhythmic respiratory neurons. However, the source of cholinergic inputs to the preBötC and the roles of those projections are not fully understood. Using transgenic ChAT-Cre mouse line, Cre-depended viruses, combinatorial genetics and state-of-the-art technologies, we investigated the cholinergic connections of the preBötC. In our study, we injected the HSV into the preBötC of ChAT-Cre mice to non-specifically label the neurons projecting to the preBötC, and the retrograde Cre-dependent virus to specifically label cholinergic neurons. Then, we use the microscopy to qualitatively and quantitatively analyze the distribution of the retrogradely labeled neurons. Furthermore, we injected the anterograde Cre dependent virus into the pedunculopontine tegmental nucleus and laterodorsal tegmentum (PPT/LDT), two cholinergic structures proposed to provide cholinergic inputs to preBötC neurons of ChAT-Cre mice and analyzed the labeled axons within the preBötC. We observed that cholinergic inputs to the preBötC are primarily from the neighboring regions include lateral paragigantocellular nucleus (LPGi) and nucleus ambiguus (NA), while the preBötC receives few cholinergic inputs

from the brainstem major cholinergic nuclei PPT/LDT. Our study provides the anatomical foundation to help researcher to further investigate the cholinergic modulation of respiration, the physiological roles of cholinergic neurons adjacent to the preBötC, and the cardiorespiratory disorders related to cholinergic dysfunction.

Acknowledgements

To my supervisor Dr. Silvia Pagliardini who gives me the opportunity to work on this project and supports me from beginning to end. I wouldn't be able to finish the master's program without her continuous support.

To acknowledge all the participants who contribute to this study. Especially Dr. Silvia Pagliardini and Pagliardini's lab members, who teach me everything and help me to overcome all the obstacles.

To Dr. Vivian Biancardi and Xiuqing Ding for their help with the RNAscope, cryosection, and immunofluorescence staining.

To my supervisory committee members (Dr. Gregory D Funk, Dr. Jesse Jackson) for their constructive feedback and advice on this project.

To Mitacs for providing me the funding and the opportunity to study abroad.

To my friends for all of their love and my family for being always supportive.

Table of Content

Chapter 1 Introduction 1
1.1 The central control of respiration 1
1.2 Respiratory rhythm oscillators 2
1.2.1 The preBötC 2
1.2.2 The retrotrapezoid nucleus, the paraFacial respiratory group and the Post-inspiratory Complex 6
1.3 Current theories on respiratory rhythmogenesis 7
1.4 Connections of the preBötC 8
1.5 Cholinergic system 10
1.5.1 Acetylcholine 10
1.5.2 Cholinergic neurons 11
1.5.3 Brainstem cholinergic nuclei 12
1.6 Cholinergic control of breathing 14
1.6.1 Cholinergic transmission affects the respiratory rate and motor output 14
1.6.2 Cholinergic transmission affects the respiratory chemosensitivity 17
1.6.3 Cholinergic transmission and the state-dependent modulation of breathing 18
1.7 Cholinergic projections to the preBotC 20
Chapter 2 Hypothesis 22
Chapter 3 Methods 23
3.1 Experimental animals 23
3.2 Viral injections 23
3.3 Stereotaxic surgery 25
3.4 Histology 26
3.5 RNAScope in situ hybridization 27
3.6 Data analysis and anatomical landmarks 28
Chapter 4 Results 30
4.1 Targeting the Cholinergic afferent projections to the preBötC 30
4.2 Verification of the ChAT-Cre mouse line 31
4.3 Afferent projections to the preBötC 34
4.3.1 Medullary projections to the preBötC 36
4.3.2 Pontine projections to the preBötC 44
4.4 Cre-dependent retrograde tracing 49
4.5 Cre dependent anterograde tracing 69
Chapter 5 Discussion 78
5.1 Technical considerations 78
5.2 Cholinergic inputs to preBötC 80
5.3 Future Directions 84
5.4 Conclusion 85
Reference 87

List of tables

Chapter 1 Introduction

Table 1. 1 Principal connections of the pedunculopontine tegmental nucleus; representative references are given for each cluster(Gut, 2016).....13

Chapter 3 Methods

Table 3. 1 Serotype, catalogue number and source of the viruses used for the retrograde studies. 23

Table 3. 2 Serotype, catalogue number and source of viruses used for the anterograde studies.....24

Chapter 4 Results

Table 4. 1 HSV labeling in the major cholinergic nuclei 47

Table 4. 2 HSV labeling in other regions 47

Table 4. 3 Brainstem regions with retrogradely labeled cholinergic neurons. 50

Table 4. 4 AAV2-retro-EF1a-DIO-mCherry retrogradely labeled neurons in LPGi and NA 55

Table 4. 5 AAV2-retro-hSyn-DIO-EGFP retrogradely labeled neurons in LPGi and NA.....61

Table 4. 6 AAV9-EF1a-DIO-EYFP retrogradely labeled neurons in LPGi and NA 67

Table 4. 7 AAV2-EF1a-DIO-EYFP anterogradely labelled neurons in PPT and LDT - Unilateral injections.....71

Table 4. 8 AAV2-EF1a-DIO-EYFP anterogradely labeled neurons in PPT and LDT - Bilateral injections 71

Table 4. 9 The tracing results of the additional anterograde AAVs 76

List of figures

Chapter 1 Introduction

Figure 1. 1 | The Parasagittal view of the brainstem containing the breathing CPG. 1

Figure 1. 2 | Effects of microinjection of nicotine (Nic, 20 μM, 10 nl) on integrated XIIn activity (∫XIIn).....15

Chapter 4 Results

Figure 4. 1 | The injection procedure and the Cre-DIO system. 31

Figure 4. 2The expression of Cre in ChAT immune-positive neurons. 34

Figure 4. 3 | Stereotaxic injection of HSV into the right preBötC of the ChAT-Cre mouse. 36

Figure 4. 4 | Retrogradely labeled neurons in the contralateral preBötC with HSV retrograde virus. 39

Figure 4. 5 | HSV retrogradely labeled neurons in the ventral respiratory column. 40

Figure 4. 6 | HSV retrogradely labeled neurons in ventral medulla. 41

Figure 4. 7 | HSV retrogradely labeled neurons in dorsal and middle medulla. ...44

Figure 4. 8 | HSV retrogradely labeled neurons in pontine structures. 46

Figure 4. 9 | Stereotaxic injection of AAV2-retro-EF1a-DIO-mCherry into the right preBötC of the ChAT-Cre mouse. 52

Figure 4. 10 | Retrogradely labeled neurons in brainstem (AAV2-retro-EF1a-DIO-mCherry). 54

Figure 4. 11 | The distribution of AAV2-retro-EF1a-DIO-mCherry retrogradely labeled cholinergic neurons in the LPGi and NA. 56

Figure 4. 12 | The injection site in one of the mice used with AAV2-retro-hSyn-DIO-EGFP. 58

Figure 4. 13 | Retrogradely labeled neurons in brainstem (AAV-retro-hSyn-DIO-EGFP). 60

Figure 4. 14 | The graphs illustrate distribution of AAV-retro-hSyn-DIO-EGFP retrogradely labeled cholinergic neurons in the LPGi and NA. 62
Figure 4. 15 | The injection site of AAV9-EF1a-DIO-EYFP. 64
Figure 4. 16 | Retrogradely labeled neurons in brainstem (AAV9-EF1a-DIO-EYFP). 66
Figure 4. 17 | The distribution of AAV9-EF1a-DIO-EYFP retrogradely labeled cholinergic neurons in the LPGi and NA. 68
Figure 4. 18 | Anterograde tracing with rAAV2-EF1a-DIO-EYFP. 70
Figure 4. 19 | The distribution of rAAV2-EF1a-DIO-EYFP anterogradely labeled cholinergic neurons in the bilateral LDT and PPT. 72
Figure 4. 20 | Retrogradely labeled axons in brainstem (rAAV2-EF1a-DIO-EYFP). 75
Figure 4. 21 | Anterograde tracing with and retrogradely labeled axons in brainstem (rAAV2-EF1a-DIO-p2A-mCherry). 77

List of symbols, nomenclature abbreviations

respiratory central pattern generator	rCPG
rostral ventral respiratory group	rVRG
caudal ventral respiratory group	cVRG
preBötzinger Complex	preBötC
Bötzinger Complex	BötC
postinspiratory complex	PiCO
lateral parafacial region	pF_L
ventral parafacial region	pF_V
parafacial respiratory group/lateral parafacial	pFRG/pF_L
retrotrapezoid nucleus/ ventral parafacial	RTN/pF_V
spinal trigeminal nucleus, interpolar part	Sp5I
spinal trigeminal nucleus, oral part	Sp5O
spinal trigeminal nucleus, caudal part	Sp5C
lateral paragigantocellular nucleus	LPGi
dorsal paragigantocellular nucleus	DPGi
ventrolateral medulla	VLM
rostral ventrolateral medulla	RVLM
medial portion of the rostral ventrolateral medulla	mRVLM
gigantocellular reticular nucleus	Gi
gigantocellular reticular nucleus, alpha part	GiA
gigantocellular reticular nucleus, ventral part	GiV
intermediate reticular nucleus	IRt
parvicellular reticular nucleus	PCRt
parvicellular reticular nucleus, alpha part	PCRtA
raphe pallidus nucleus	RPa
raphe obscurus nucleus	Rob
raphe magnus nucleus	RMg

raphe interpositus nucleus	RIP
genu of the facial nerve	g7
nucleus ambiguus	NA
oculomotor nucleus	3N
trochlear nucleus	4N
trigeminal motor nucleus	5N
abducens nucleus	6N
the facial motor nucleus	7N
dorsal motor nucleus of vagus	10N
hypoglossal motor nucleus	12N
nucleus of Roller	Ro
vestibular nuclei	Ve
medial vestibular nucleus, parvicellular part	MVePC
prepositus nucleus	Pr
locus coeruleus	LC
nucleus of the solitary tract	NTS
mesencephalic tract of the trigeminal nerve	Me5
trigeminal nucleus	MO5
Kolliker-Fuse nuclei	KF
parabrachial nuclei	PB
lateral parabrachial nucleus	LPB
inferior colliculus	IC
superior colliculus	SC
superior olive	SO
periaqueductal gray	PAG
subcoeruleus nucleus	SubC
subcoeruleus nucleus, ventral part	SubCV
laterodorsal tegmental nuclei	LDT
pedunculopontine tegmental nuclei	PPT

parabigeminal nucleus	PBG
dorsomedial tegmental area	DMTg
pontine reticular nucleus	Pn
pontine reticular nucleus, oral part	PnO
tensor tympani part of the motor trigeminal nucleus	5TT
motor root of the trigeminal nerve	m5
nucleus accumbens	NAc
medial habenula	MHb
basal forebrain	BF
medial septal nucleus	MSN
diagonal band of broca	DB
nucleus basalis	NB
bed nucleus of the stria terminali	BNST
lateral preoptic area	LPO
substantia nigra pars reticulate	SNR

acetylcholine	ACh
choline acetyl-transferase	ChAT
vesicular acetylcholine transporter	VAChT
nicotinic acetylcholine receptors	nAChRs
muscarinic acetylcholine receptors	mAChRs
local cholinergic interneuron	CIN
cholinomimetic carbachol	CCH
Phaseolus vulgaris-leucoagglutinin	PHA-L
carbon dioxide	CO_2
Developing brain homeobox 1	Dbx1
Early growth response protein 2	EGR2/Krox20
neurokinin 1 receptor	NK1R
somatostatin	SST

vesicular-glutamate transporter 2	vGluT2
Gamma-aminobutyric acid	GABA
Gamma-Amino Butyric Acid-A	$GABA_A$
glutamate decarboxylase	GAD
glycine transporter 2	GlyT2
serotonin/5-hydroxytryptamine	5-HT
Paired-like homeobox 2b	Phox2b
fluorogold	FG
adeno-associated virus	AAV
Herpes simplex virus	HSV
Double-floxed Inverted Orientation	DIO
Flip-Excision	FLEx
respiratory-related local field potentials	LPFs
enhanced green fluorescent protein	EYFP
paraformaldehyde	PFA
phosphate-buffered saline	PBS

Chapter 1 Introduction

1.1 The central control of respiration

Breathing is one of the most fundamental physiological functions that allows for oxygenation of the body and eliminates the carbon dioxide. It is characterized by three phases: inspiration, post-inspiration (post-I), and late expiration(Ramirez & Baertsch, 2018b). The respiratory central pattern generator (rCPG), together with the sensory input system and the respiratory musculature, are three essential elements of the respiratory control system(Brinkman & Sharma, 2019). As the kernel of respiratory control system, the rCPG includes the dorsal respiratory group (nucleus of the solitary tract, NTS), the ventral respiratory group (that includes the rostral ventral respiratory group (rVRG), caudal ventral respiratory group (cVRG), the preBötzinger Complex (preBötC), the Bötzinger Complex (BötC) and the pontine respiratory group (Figure 1. 1) (Kölliker-Fuse nucleus (KF), parabrachial nuclei (PB)) in the brainstem(J. C. Smith et al., 2013).

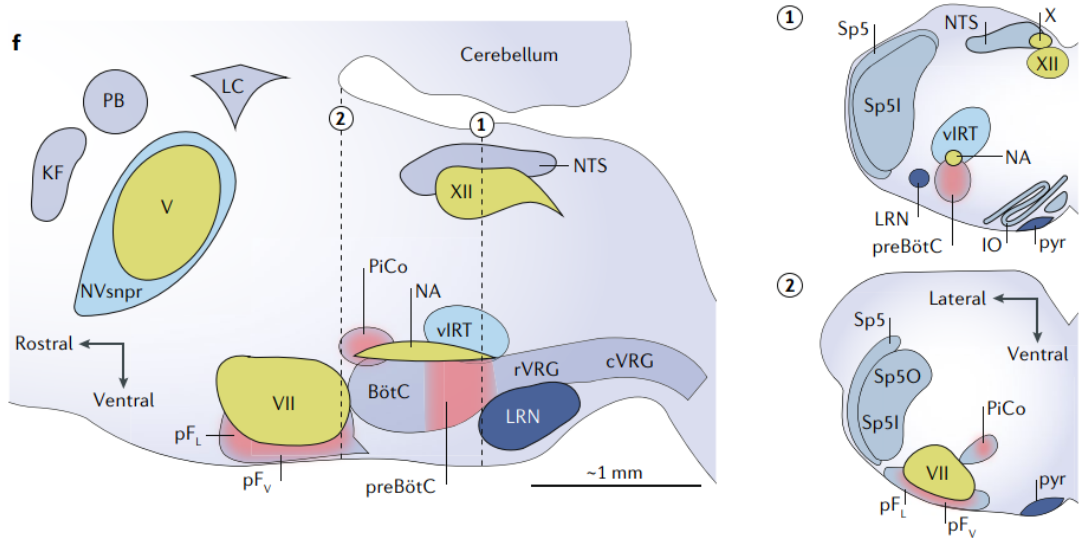

Figure 1. 1 | The Parasagittal view of the brainstem containing the breathing CPG. Insets 1 and 2 show transverse sections at the level of the preBötC (1) and parafacial region (2)(Del Negro et al., 2018).

1.2 Respiratory rhythm oscillators

1.2.1 The preBötC

The preBötzinger Complex (preBötC) was first identified in 1991 by Smith and his colleagues in the neonatal rat as a group of rhythmically active neurons responsible for respiratory rhythmogenesis. It is located in the ventrolateral medulla, ventral to the nucleus ambiguus (NA), just caudal to the BötC and rostral to the rVRG(J. Smith et al., 1991).

The transverse slice preparation in this study has been used as the principal experimental model for investigating respiratory rhythm *in vitro*(Muñoz-Ortiz et al., 2019). A 350-600μm thick transverse medullary slice which includes the preBötC, NA, hypoglossal motor nucleus (12N), and hypoglossal nerve was collected, and the activities of the preBötC neurons were examined either directly with whole-cell patch-clamp recording techniques or indirectly by recording the activity of the hypoglossal nerve roots, because the preBötC excites the 12N and transmits the excitatory signals to the tongue musculature. The oscillatory neuronal activity of the preBötC, the rhythmic activity of the slice, and that generated in less reduced, *en bloc* preparations (brainstem with spinal cord to record phrenic nerve activity) also contributed to identify electrophysiological properties of preBötC neurons(Del Negro et al., 2018; J. C. Smith et al., 2013), demonstrating the essential role of preBötC neurons as respiratory rhythm generator.

During embryogenesis, a subpopulation of interneurons in hindbrain rhombomere 6 (r6) forms and develops into the preBötC, expressing key transcription factors such as the Developing brain homeobox 1 (Dbx1) and the Early growth response protein 2 (EGR2/Krox20)(Heijden & Zoghbi, 2020). In adult rodents, the preBötC contains ~3000 neurons, including intrinsically bursting neurons, tonically firing neurons and silent

neurons(Carroll & Ramirez, 2013; Feldman & Kam, 2015). The synaptic interactions between these neurons help the preBötC to generate the inspiratory drive potential on top of synchronic depolarization which lasts up to 0.8 seconds in vitro(Del Negro et al., 2005; Morgado-Valle et al., 2015). There are three major hypotheses for rhythmogenesis, based on pace-maker properties in a subpopulation of preBötC neurons, reciprocal inhibition, and synchronization properties, whereas the network synchronization and synchrony propagation is the most recent one(Ashhad & Feldman, 2019) (discussed below).

Glutamate is the main excitatory neurotransmitter in the preBötC(Greer et al., 1991; Wallén-Mackenzie et al., 2010). Applying the glutamate receptor antagonist to the preBötC abolishes the respiratory oscillations(J. Smith et al., 1991). *In vivo*, nonspecific photo-stimulation of the preBötC neurons increased the respiratory frequency, reset the inspiratory rhythm in a phase-independent manner, and entrained the rhythm at a frequency up to 4-fold the baseline rhythm(Alsahafi et al., 2015), which substantiates that excitatory mechanisms within the preBötC can pace the inspiratory rhythm. On the contrary, optogenetic inhibition of glutamatergic preBötC neurons in neonatal medullary slices *in vitro* and in adult mouse in situ brainstem-spinal cord preparations significantly reduced the inspiratory frequency(Koizumi et al., 2016).

Genetically, the preBötC glutamatergic neurons can be classified by their expression of Dbx1, neurokinin 1 receptor (NK1R), somatostatin (SST), and other proteins which partially overlap with each other(Gray et al., 2010; Picardo et al., 2013; Stornetta et al., 2003; Tupal et al., 2014). Dbx1 is a transcription factor expressed in preBötC glutamatergic neurons(Gray et al., 2010), some of which show a pre-inspiratory firing patten which starts before the onset of hypoglossal nerve burst in slice preparation of neonatal rodent(Picardo et al., 2013). This pre-inspiratory activity suggests that these Dbx1+ neurons appears to be critical to initiate the inspiration(Kam et al., 2013).

Additionally, *in vivo* photostimulation of the preBötC Dbx1+ neurons largely increases both breathing frequency and tidal volume in mouse(Cui et al., 2016). Recent study indicates that DBX1 preBötC neurons include the "Type-1" putative rhythmogenic neurons and the "Type-2" pattern neurons which generate the preBötC output(Kallurkar et al., 2021). NK1R and SST are other two neuronal markers of the preBötC neurons that are expressed in conjunction with the onset of rhythmic respiratory-related activity at embryonic day 17 (E17) in rat(Pagliardini et al., 2003). Similarly, the expression of NK1R and the emergence of respiratory rhythm commences at E15 in the mouse embryo(Thoby-Brisson, 2005). Ablation of the preBötC NK1R-expressing neurons induces breathing disorders in adult unanesthetized awake rat and apneas during sleep(Gray et al., 2001; McKay et al., 2005). Acute silencing (~4 min) of the preBötC SST+ neurons also produces persistent apnea in the intact eupneic rat(Tan et al., 2008), while short-pulse photo-stimulation of preBötC SST+ neurons induces an increased burst in early inspiration in mouse(Cui et al., 2016). These studies support the hypothesis that the preBötC excitatory neurons participate the generation of respiratory rhythm and pattern.

In addition to the excitatory preBötC rhythmogenic neurons expressing the vesicular-glutamate transporter 2 (vGluT2), there are also inhibitory neurons in the preBötC that express the Gamma-aminobutyric acid (GABAergic), the glutamate decarboxylase (GAD) enzyme and the glycine transporter 2 (GlyT2). An estimated of 40% inspiratory neurons in the preBötC are inhibitory(Baertsch & Ramirez, 2019; Oke et al., 2018; Winter et al., 2009), and they have been proposed to participate in inspiratory signal transmission, modulation of respiratory pattern and apneas(Ashhad & Feldman, 2019; Cui et al., 2016; Yang et al., 2019).

Distinct inhibitory currents have been recorded from the presumptive preBötC neurons in cats and rodents(Ballantyne & Richter, 1984; Richter & Smith, 2014). Nonetheless, it is

still debated whether inhibitory neurons are essential for the preBötC rhythmogenesis(Baertsch et al., 2018, 2019). Recent studies indicated that the inhibitory neurons affect the breathing frequency by regulating the excitatory neurons and limiting the synchronization during inspiratory burst, while the inhibitory interactions subsequently reduce the network refractoriness(Baertsch et al., 2018; Harris et al., 2017). However, another study showed that blocking $GABA_A$ and glycine receptors in the preBötC of anesthetized rats suppressed the lung inflation-induced Breuer–Herring inspiratory inhibitory reflex, but did not alter or stopped the breathing rhythm, suggesting that postsynaptic inhibition modulates the lung inflation reflex but is not critical for the respiratory rhythm generation(Janczewski et al., 2013). Furthermore, brief photostimulation of preBötC glycinergic neurons during inspiratory-phase terminated inspiratory burst prematurely; if stimulation occurred during expiratory-phase the occurrence of subsequent inspiration was delayed, whereas prolonged photo-stimulation induced persistent apnea during the light pulse(Sherman et al., 2015). On the other hand, photoinhibition of those neurons during inspiratory-phase augmented the tidal volume, while during expiratory-phase shortened the interval before the next inspiration. However, during persistence apnea, prolonged photoinhibition reinstated the breathing rhythm(Sherman et al., 2015). Based on these results, the authors concluded that inhibitory neurons primarily adjust the breathing pattern but are not rhtyhmogenic(Sherman et al., 2015).

In a nutshell, these *in vivo* and *in vitro* studies suggest that the preBötC is vital for generating respiratory rhythm and modulating respiratory pattern.

Further, acetylcholine (ACh) receptors, serotonin/5-hydroxytryptamine (5-HT) receptors, opioid receptors, adrenergic and purinergic receptors have been identified in the preBötC region as well(Muñoz-Ortiz et al., 2019), which suggest that these neurotransmitters may

have a role in modulating preBötC activity.

1.2.2 The retrotrapezoid nucleus, the paraFacial respiratory group and the Post-inspiratory Complex

Lying under the facial nuclei, the retrotrapezoid nucleus (RTN, also identified anatomically as ventral parafacial, pF_V)(Weston et al., 2004) is a central chemosensitive site that modulates the central respiratory chemoreflex(Souza et al., 2018) to maintain arterial pH and carbon dioxide (CO_2) level. Paired-like homeobox 2b (Phox2b) is a defining marker for respiratory chemoreceptor neurons of the RTN as well as the whole chemoreflex and autonomic circuits(Goridis et al., 2010; Levy et al., 2019). Interestingly, phox2b-expressing neurons in the parafacial region of both neonate and adult rats were found to be CO_2-sensitive and tonically active, and 84% of prenatal neurons fire during pre-inspiration(Onimaru et al., 2008)·(Guyenet, 2005). Extensive research demonstrate that RTN neurons provide a CO2-driven tonic drive to the generation of breathing rhythm in adult rat(Guyenet, 2005).

Within the parafacial region, another structure has been identified: the para-facial respiratory group (pFRG; also termed, lateral parafacial, pF_L). The pFRG and the RTN have indistinctive boundaries but separate function, although they may anatomically overlap to some extent(Onimaru et al., 2008), Nevertheless, studies shows that the pFRG glutamatergic expiratory neurons lack Phox2b expression and CO2/H+ sensitivity(Magalhães et al., 2021). The pFRG was initially described in *in vitro* optical recordings as a group of pre-inspiratory (Pre-I) and inspiratory neurons located ventrolateral to the facial nucleus in the neonatal rat (post-natal day, P,0-1)(Onimaru & Homma, 2003). In adult anesthetized rats, pharmacological disinhibition or photostimulation of the pFRG area, activated silent pFRG neurons to rhythmic late

expiratory neurons, generated active expiration, and reset the respiratory rhythm(Pagliardini et al., 2011). The pFRG is thus proposed to be the oscillator of active expiration during high metabolic demand stages in adulthood(Pagliardini et al., 2011). These studies suggest that the parafacial region participates the respiratory rhythmogenesis as well.

The postinspiratory complex (PiCo) is a group of glutamatergic-cholinergic neurons located rostral and dorsal to the preBötC, and caudal to the facial nucleus in mice. Postinspiratory activity was recorded from the PiCo region of the horizontal mouse brain slice. Bath application of atropine (a muscarinic receptor antagonist) depressed postinspiratory frequency, DAMGO (a μ-opioid receptor agonist) and SST eliminated PiCo population bursts *in vitro*, whereas photostimulation of cholinergic neurons elicited postinspiratory activities and evoked post-inspiratory bursts in the cervical vagal nerve. *In vivo*, injection of DAMGO or SST into PiCo reduced the duration and amplitude of vagal post-inspiratory burst. Thus, PiCo was proposed to be a third respiratory oscillator that generates the post-inspiratory activity(Anderson et al., 2016), although this hypothesis is still under debated because of limited evidence(Dhingra et al., 2021; Hülsmann, 2021).

1.3 Current theories on respiratory rhythmogenesis

How the rCPG controls the three-phase respiratory activity is still a controversial topic. One hypothesis is that the preBötC, since it contains both excitatory and inhibitory neurons, generates both respiratory rhythm and pattern, proposes that an inhibitory ring within the preBötC and the neighboring nuclei (e.g. the BötC) forms the core circuit, while the other respiratory areas provide tonic inputs to the core or relay the outputs to modulate respiratory activities(Ausborn et al., 2018; Dhingra et al., 2019; Rybak, n.d.; J. C. Smith et al., 2009). Additionally, a triple oscillator hypothesis has been proposed, in which three

breathing phases are controlled by three different oscillators, the preBötC (inspiration)(Feldman et al., 2013), the PiCo(Anderson et al., 2016)or other pontine regions containing the KF(Dutschmann & Herbert, 2006) (Post-I), and the pFRG (late-E). These three oscillators coupled each other via excitatory and inhibitory interactions to modulate the breathing activity(Del Negro et al., 2018; Ramirez & Baertsch, 2018a).

The pacemaker hypothesis indicates that a group of excitatory 'pacemaker' neurons within the preBötC, which are dependent on the persistent Na+ current (I_{NaP}) and the Ca^{2+}-activated nonspecific cationic current (I_{CAN}). However, theses ion currents are expressed in other excitatory and inhibitory neurons beside pacemaker neurons, and attenuation of the I_{NaP} and I_{CAN} affect the membrane potential and the synaptic transmission does not interrupt respiratory rhythms(Del Negro et al., 2018). Thus, the pacemaker hypothesis is insufficient to support respiratory rhythmogenesis. Recently, another hypothesis has been proposed and it involves burstlets and percolation of activity in preBötC neuron. In vitro studies indicated that the rhythmogenic neurons initiate the pre-inspiration which further triggers the inspiratory burst, then followed by the recruitment of pattern-related neurons which drive motor output(Del Negro et al., 2018; Kallurkar et al., 2020; Kam et al., 2013). Researchers posited the SST-expressing neurons to be the pattern/output neurons(Cui et al., 2016; Stornetta et al., 2003; Tan et al., 2010; Yang & Feldman, 2018), and recording the membrane potential of SST+ neurons revealed that the synchronization of preBötC rhythmogenic neurons leads to the inspiratory bursts(Ashhad & Feldman, 2020). In all these hypotheses, the preBötC plays a vital role in breathing control.

1.4 Connections of the preBötC

The preBötC neurons communicate with other brain nuclei to synchronize and modulate breathing in order to maintain the adequate ventilation across sleep and wakefulness, while

coordinate breathing with other orofacial functions such as chewing, swallowing, speaking, sighing, whisking, sniffing, coughing and sneezing as well as with emotions(Dick et al., 1993; F. Li et al., 2021; P. Li et al., 2016; Moore et al., 2013, 2014). Studying the functions of the preBötC and its interaction (anatomically and functionally) with other nuclei are crucial for understanding the regulation of respiration.

Several studies have investigated the afferent projections to the preBötC that may influence its function, even before anatomical landmarks and genetic identification of preBötC cells were obtained. Unilateral injection of the traditional tracer WGA-HRP into a region of the VRG that includes the now identified preBötC area(Schwarzacher et al., 1995) retrogradely labeled cells in the PB/KF, the NTS, the raphe nuclei, the retrofacial nucleus, the NA, the parafacial region (RTN) and the upper cervical spinal cord(Gang et al., 1995). Microinjection of another traditional retrograde tracer fluorogold (FG) into the mouse preBötC retrogradely labeled neurons in BötC, contralateral preBötC, the NTS, parafacial and facial nuclei, PB/KF, trigeminal nucleus (MO5), substantia nigra, red nucleus, superior colliculus, central amygdala, lateral hypothalamus, and zona incerta, paraventricular hypothalamus, bed nucleus of the stria terminalis (BNST), lateral preoptic area (LPO), and cortex(Yang et al., 2019). Furthermore, modified rabies tracing studies in mice illustrated monosynaptic connections to SST+ and GlyT2+ preBötC neurons, demonstrate the presence of projection to comparable areas including local and contralateral preBötC, BötC, intermediate reticular region (IRt), NTS, PB/KF, Periaqueductal gray (PAG), superior colliculus (SC), substantia nigra, central amygdala, cortex, etc.(Yang et al., 2019). These results indicate that the preBötC receives projections not only from the neighboring medullary nuclei but also from the rostral brainstem and subcortical areas.

Efferent projections of preBötC neurons have also been intensively investigated with both

classical tracers and more modern viral approaches. Microinjection of WGA-HRP into the VRG of cat anterogradely labeled neuronal fibers in the PB/KF, the contralateral retrofacial nucleus, the ventrolateral NTS, the NA and retro ambiguus, the upper cervical spinal cord, the RTN and the raphe magnus(Gang et al., 1995). Moreover, to label the axons and terminal fields of phenotype-specific SST+ preBötC neurons, an adeno-associated virus (AAV) with enhanced yellow fluorescent protein (EYFP) gene driven by the somatostatin promoter was injected into the rat preBötC. The results demonstrated that the SST+ preBötC neurons project to the contralateral preBötC, the ipsilateral and contralateral BötC, the cVRG, the RTN/pFRG, the para12N, NTS, PB/KF, and the PAG(Tan et al., 2010). More recently, AAV-FLEX-EGFP was injected into the preBötC of SST-Cre and GlyT2-Cre mice to label efferent projections of excitatory (SST+) and inhibitory (GlyT2+) preBötC neurons(Yang & Feldman, 2018). Interestingly, these neurons have parallel efferent projections to the NTS, the BötC, the parafacial, the dorsal rostral pons (PB, KF), as well as the suprapontine nuclei which may attune emotional states and other behaviors including the PAG, the thalamus, the lateral and dorsomedial hypothalamus, the lateral preoptic area, etc.(Yang & Feldman, 2018).

These tracing studies are not specific to neuronal subtypes of the retrograde labeled connections, although some of which selectively infected selected subtype of neurons in the preBötC.

1.5 Cholinergic system

1.5.1 Acetylcholine

Acetylcholine (ACh) serves as a chiefly excitatory neurotransmitter in the peripheral nervous system that participates in sensory, autonomic and motor control, and acts as a neuromodulator in the central nervous system(Picciotto et al., 2012). Cholinergic neuronal

transmissions in the brain generally modulates the presynaptic release of other neurotransmitters, alters the excitability of neurons, and coordinate the activities of neuronal groups(Picciotto et al., 2012).

There are two types of receptors that mediate the effects of the Ach: the muscarinic (M) and the nicotinic (N) receptors, which are named after the ligands that contributed to their studies(Carlson & Kraus, 2018). The muscarinic acetylcholine receptors, or the mAChRs, are G protein-coupled receptors which can be further divided into 5 subtypes, M1 through M5(Caulfield, 1993). On the other hand, the nicotinic acetylcholine receptors (nAChRs) are ion channels with various subtypes that composed of α, β, δ, and ε subunits, whereases the nAChRs of neurons are particularly formed in αβ combinations(Dani & Bertrand, 2007).

1.5.2 Cholinergic neurons

Neurons release the neurotransmitter ACh have been defined as cholinergic neurons(Wessler & Kirkpatrick, 2008). For example, the cranial motor neurons release the ACh into the neuromuscular junction to control muscles involved in head movements, speech and facial expression, etc.(Guthrie, 2007). In central nervous system, cholinergic neurons are distributed in discrete regions mainly in the striatum, the basal forebrain, as well as the brainstem(X. Li et al., 2018), with axons extending throughout the brain(Dautan et al., 2016; X. Li et al., 2018). Cholinergic neurons participate the attunement of excitatory and inhibitory synaptic inputs(Zhou et al., 2017), the maintenance of brain function(Bonsi et al., 2011) including sleep and arousal(Van Dort et al., 2015; Xu et al., 2015), and the coordination of the sensory processing(Ballinger et al., 2016; Minces et al., 2017).

Cholinergic neurons can be divided into two categories based on their synapsing and

projecting patterns: the local cholinergic interneurons (CINs) and the projecting cholinergic neurons(Allaway & Machold, 2017). CINs are mainly located in the striatum(Lim et al., 2014), the nucleus accumbens (NAc)(Meredith et al., 1989; Warner-Schmidt et al., 2012) and the neocortex(Benagiano et al., 2003; Von Engelhardt et al., 2007). Whereas projection cholinergic neurons have been identified in the pedunculopontine and laterodorsal tegmental areas (PPT and LDT)(H.-L. Wang & Morales, 2009), the medial habenula (MHb)(Ren et al., 2011), the basal forebrain (BF) complex(Zaborszky et al., 2008) which comprises the medial septal nucleus (MSN), the vertical and horizontal limbs of the diagonal band of broca (DB), and the nucleus basalis (NB) of Meynert.

Although all cholinergic neurons have similar properties, such as the expression of choline acetyl-transferase (ChAT) and vesicular acetylcholine transporter (vAChT), the diversity within cholinergic cell populations still exists, which is related to their different developmental origins (E.g. the caudal ganglionic eminence, CGE; the medial ganglionic eminence, MGE; the preoptic area, POA; the septal neuroepithelium, SE) and the influence of various genetic factors (E.g. Nkx2.1, Isl1, Lhx8, Fgf8, Fgf17, Dbx1, Zic4, Otx2, etc.)(Ahmed et al., 2019). Thus, cholinergic neurons exhibit heterogeneity in connectivity, morphology, and electrophysiological properties(Ahmed et al., 2019; Muñoz-Manchado et al., 2018).

1.5.3 Brainstem cholinergic nuclei

In the brainstem, there are two main categories of cholinergic neurons(Datta, 2009):

1) The motor neurons, which receive inputs from upper motor neurons in the cerebral cortex, sensory neurons and interneurons, with axons terminating in the peripheral nervous system to contract muscles and stimulate glands(Zayia & Tadi, 2020). These cholinergic

motor neurons principally populate the cranial nuclei including the 12N, the NA, the dorsal motor nucleus of the vagus nerve (10N), the facial nucleus (7N), the salivatory and lacrimatory complexes, the motor nucleus of the trigeminal nerve (5N), the trochlear nucleus (4N), the oculomotor nucleus (3N), and the Edinger-Westphal nucleus(Datta, 2009).

2) The projecting cholinergic neurons which are completely restrained within the central nervous system(Mesulam et al., 1983) mainly located in the PPT and LDT(Datta, 2009), with long-range axons projecting to the forebrain, ascending reticular activating system, midbrain, brainstem, cerebellum, and spinal cord (Table 1. 1) (French & Muthusamy, 2018; Gut, 2016). Cholinergic neurons in the PPT and LDT participate in the regulation of REM sleep, wakefulness, goal-directed locomotion, behavioral context and cortical activation processes(Datta, 2009; Mena-Segovia, 2016; Van Dort et al., 2015).

Table 1. 1 Principal connections of the pedunculopontine tegmental nucleus; representative references are given for each cluster(Gut, 2016).

Midbrain, brain stem, cerebellum, and spinal cord	
Inferior and superior colliculus (reciprocal)	96-98
Pontine and medial reticular formation; nucleus pontis oralis	99-102
Motor trigeminal	103-105
Medulla	99,106
Spinal cord (reciprocal)	107-109
Ascending reticular activating system	
Dorsal raphe, locus coeruleus, laterodorsal tegmental nucleus	70,107,110,111
Forebrain	
Thalamus	112-114,125
Basal ganglia—striatum; globus pallidus (internal and external); subthalamic nucleus; substantia nigra pars reticulata; and projections to midbrain dopamine-containing neurons	47,107,115-120
Extended amygdala, basal forebrain, lateral hypothalamus	113,118,121,122

Cortical influence is mainly via connections through the thalamus. There is some evidence for direct projections to medial and sulcal frontal cortical areas.[117] Auditory[123] and motor[124] cortex send projections to pedunculopontine tegmental nucleus.

Additionally, sparse cholinergic neurons with different expression levels of ChAT and vAChT are found in the medullary reticular formation (intermediate, lateral, and parvicellular parts)(Jones, 1990), in the dorsomedial region of the caudal NTS, around the superior olivary nucleus, in the medullary paragigantocellular area, the medial portion of the rostral ventrolateral medulla (mRVLM), the ventral surface of medulla, and the nucleus of the mesencephalic tract of the trigeminal nerve (Me5)(Kubin & Fenik, 2004; Schäfer et al., 1998; X. M. Shao & Feldman, 2009; Stornetta et al., 2013).

1.6 Cholinergic control of breathing

Generally, cholinergic neurotransmission within the brainstem controls several aspects of breathing: the respiratory rate and motor output, the state-dependent modulation, the post-inspiratory activity, the active expiration, the central and peripheral chemosensitivity(Anderson et al., 2016; R. C. T. Boutin et al., 2017; M. D. Burton et al., 1995; Kubin & Fenik, 2004; Nurse, 2010). Deficit of brainstem cholinergic system disturbed the central control of respiration and it has been proposed to be related to sudden infant death syndrome (SIDS)(Kinney et al., 1995; Mallard et al., 1999).

1.6.1 Cholinergic transmission affects the respiratory rate and motor output

ACh modulates respiratory frequency, pattern and motor output(X. M. Shao & Feldman, 2009). *In vitro* bath application of ACh increased respiratory-related frequency in the brainstem-spinal cord preparation from neonatal rats, which can be reduced by anti-muscarinic atropine, and completely abolished by further application of nicotinic receptor antagonist (DHβ-E)(Murakoshi et al., 1985). *In vivo*, the acetylcholinesterase (AChE) inhibitor sarin caused respiratory arrest while injected into the ventrolateral medulla of the

anesthetized rabbit. When applied more dorsally, sarin caused respiratory stimulation, and the effect could be reversed by the injection of atropine(STEWART & ANDERSON, 1968). However, in rat medullary slice preparations, unilateral microinjections of physostigmine, another AChE inhibitor, into the preBötC increased breathing frequency(X. M. Shao & Feldman, 2005), suggesting that the effects of ACh may depend on its site of action and the selective activation of ACh receptors.

Specifically, application of nicotine (the classic nAChR agonist) either into the lateral ventricles or at the ventral surface of medulla, increases the overall activity (especially the amplitude) of genioglossus muscles and inspiratory muscles(Haxhiu et al., 1984; Mitchell et al., 1963). The localized preBötC microinjection of nicotine increased the respiratory frequency and decreased the motor output of 12N(J. Smith et al., 1991). On the other hand, application of nicotine into the 12N induced a tonic activity with increased amplitude, leaving the breathing frequency intact (Figure 1. 2) (X. M. Shao & Feldman, 2001, 2005). Together, these findings suggest that nicotine act on the preBötC to potentiate the respiratory rhythm, and on the 12N to potentiate the inspiratory amplitude(X. M. Shao & Feldman, 2009).

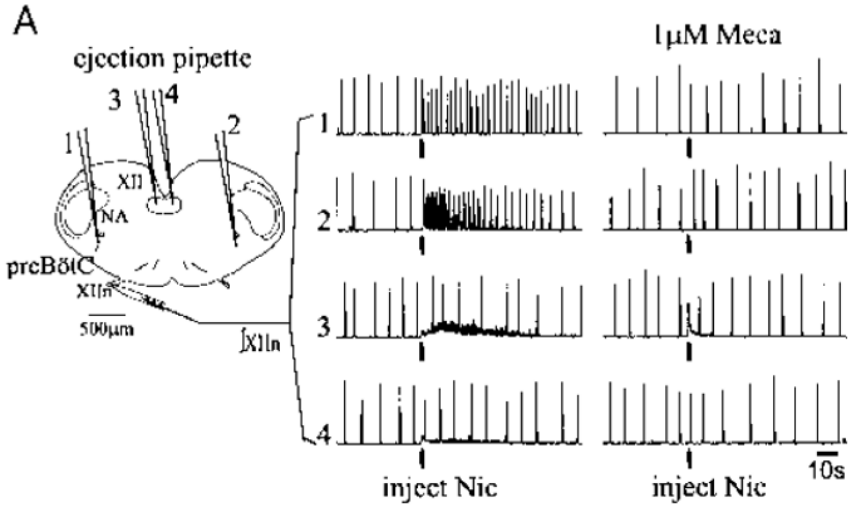

Figure 1. 2 | Effects of microinjection of nicotine (Nic, 20 μM, 10 nl) on integrated

XIIn activity (∫XIIn).

A: arrows indicate the time of injection. The numbers 1, 2, 3, and 4 indicate injections into the ipsilateral preBötC, contralateral preBötC, ipsilateral XII nucleus, and contralateral XII nucleus, respectively. The injection pipettes were inserted into the loci 100–200 μm below the surface of the slice. Left XIIn activity was recorded with the medullary slice caudal side up. All data traces were from the same slice. First set of injections was prior to, and the 2nd set was at least 4.5 min after bath application of 1 μM mecamylamine (Meca)(X. M. Shao & Feldman, 2001).

Anatomically, both mRNA of α4 and β2 nAChRs subunits have been identified in the ventral lateral medulla (including the preBötC) by *in situ* hybridization(WADA, 1989; Wada et al., 1990), while α7 nAChR subunit immunoreactivity was detected in more than half (57%) of the presuming NK1R immunoreactive preBötC neurons in rat(Dehkordi et al., 2004; del Toro et al., 1994). However, the immunohistochemistry results are less convincing because the antibodies against the nAChR subunits lack specificity(Moser et al., 2007). The mRNA of M2 and M3 mAChRs, as well as a small amount of M1, M4, and M5 receptor mRNA was detected by the polymerase chain reaction (PCR) in the preBötC, the BötC and the NA(Lai et al., 2001). In the rostral ventrolateral medulla of cat, the M2 receptors were found to regulate the cardiovascular activity, while the M3 receptors could affect breathing via mediating the excitatory effects of ACh on the activity of preBötC neurons(E. E. Nattie & Li, 1990; X. Shao & Feldman, 2000).

Cholinergic transmission also affects the post-inspiratory activity. The proposed post inspiratory activity generator, PiCo, comprises neurons that express both cholinergic and glutamatergic markers. Bath application of atropine (a muscarinic receptor antagonist) depressed post-inspiratory frequency *in vitro*, whereas in horizontal slices， photo-stimulation of cholinergic neurons elicited post-inspiratory activities recorded from PiCo,

and evoked bursts in the cervical vagal nerve(Anderson et al., 2016).

Cholinergic transmission is also important in active expiration. *In vivo*, microinjection of physostigmine into the pFRG gradually increased the expiratory activity, while local application of cholinomimetic carbachol (CCH) elicited persistent active expiration, decreased respiratory rate, increased tidal volume and consequently increased minute ventilation(R. C. T. Boutin et al., 2017). Along with the potentiation of active expiration, not only the abdominal expiratory muscles were recruited, but also the inspiratory activity of the diaphragm and the genioglossal muscles were promoted as well, which suggests interaction between oscillators and possibly the presence of connections between the pFRG and the preBötC and respiratory premotoneurons(R. C. T. Boutin et al., 2017; Pagliardini et al., 2011). Additionally, application of muscarinic antagonist, (M3 receptor antagonist) reduced these effect, which suggest that the cholinergic muscarinic transmission also modulate the activity of pFRG and active expiration(R. C. T. Boutin et al., 2017). The source of this cholinergic inputs is currently unknown as recent studies indicate that a major cholinergic structure, the PPT, do not project directly to the pFRG (Silva et al., 2019; Takakura et al., 2014)

1.6.2 Cholinergic transmission affects the respiratory chemosensitivity

Breathing exhibits diverse characteristics to maintain homeostasis when the mammal is freely moving, exposed to room air, hypoxic or hypercapnic gas mixtures(E. Nattie & Li, 2011), which is called respiratory chemosensitivity, and the cholinergic transmission plays an important role in it(M. D. Burton et al., 1997; Monteau et al., 1990).

Cholinergic transmission modulates the function of RTN chemoreceptor. The Ach level within the brainstem chemosensitive areas increased under hypercapnia(Metz, 1966).

Similarly, both *in vivo* and *in vitro* studies show that cholinergic transmission at the level of ventral surface of medulla (RTN region) is necessary for maintenance of respiratory activity and involved in chemosensitivity(M. Burton et al., 1994; Fukuda & Loeschcke, 1979; Monteau et al., 1990; E. Nattie et al., 1989). Application of cholinergic agonist or acetylcholinesterase inhibitor affected the respiratory chemosensitivity(Eugenín & Nicholls, 1997; Monteau et al., 1990), and ACh stimulated the respiratory activity when it was applied near the RTN. On the other hand, atropine or specifically blocking M1 and M3 receptors depressed the ventilatory response to CO_2(Coddou et al., 2009; Fukuda & Loeschcke, 1979; Monteau et al., 1990; E. Nattie et al., 1989; E. E. Nattie & Li, 1990), which suggest that mAChRs modulate central chemosensitivity.

Furthermore, *in vivo* study demonstrates that ACh stimulates RTN chemoreceptor by M1/M3 mAChR-mediated inositol 1,4,5-trisphosphate (IP_3)/Ca^{+2} signaling pathway and inhibits the downstream KCNQ channels, which is independent of CO_2/H^+ levels(Sobrinho et al., 2016). In brain slice preparation, ACh activate RTN chemosensitive neurons even when glutamate, $GABA_A$ and glycine receptors were blocked, and application of muscarinic receptor blockers barely affected RTN chemosensitivity, which imply that RTN chemoreceptors are directly and independently activated by ACh(Sobrinho et al., 2016).

1.6.3 Cholinergic transmission and the state-dependent modulation of breathing

The levels of ACh in the brain change with the sleep-wake cycle and mainly consolidate the memory(Hasselmo & McGaughy, 2004). ACh levels in the hippocampus decrease during slow wave sleep, and increase recurrent activity related to cortical inputs to promote memory consolidation. Conversely, in REM sleep or awake, elevated ACh levels enhances the inputs to the hippocampus and stimulates memory encoding(Hasselmo & McGaughy,

2004; Newman et al., 2012). On the other hand, cholinergic pathways produce activation directly and locally in the neocortex, and ACh is essential for cortical activation(Dringenberg & Vanderwolf, 1998). The cholinergic system is in close relationship with the change of brain states. Particularly, a group of cholinergic neurons in PPT/LDT exhibit state-specific discharge patterns as mentioned before.

Breathing varies with states (quiet wake, none-REM or REM sleep) and anesthetic levels (freely behaving or different anesthetics)(Bellingham & Ireland, 2002; de Sousa Abreu et al., 2021). Breathing disorders are more likely to occur during sleep(Fleming et al., 1980), when chemosensory(Burke et al., 2015), propriosensory, and neuromodulatory systems are less perceptive to maintain respiratory activities(Douglas, 2005; Marcus, 2001). Additionally, the activity of genioglossus muscles which is key for the maintenance of upper airway patency, reduces during non-REM and dramatically declines during REM sleep(Horner, 2008a). Cholinergic transmission directly or indirectly modulates breathing changes across states in three major ways: 1) motor output of respiratory motor neurons; 2) rhythmogenesis and pattern of rCPG; 3) chemosensitivity of rCPG(E. Nattie & Li, 2010; Bellingham & Ireland, 2002).

Most physiological characteristics of rats under urethane anesthesia are similar to that of animals in natural sleep(Pagliardini et al., 2012). Moreover, most anesthetics normally caused a dose-related depression of the breathing, which is mediated by multiple receptors such as $GABA_A$, glycine, N-methyl-d-aspartate and nicotinic acetylcholinergic (nACh) receptors distributed within the respiratory system(Teppema & Baby, 2011). Specifically, the nACh receptor with α4β2 subunits is highly sensitive to a variety of inhaled and intravenous anesthetics, while the same goes for the muscarinic receptors(Eger et al., 2002). Thus, cholinergic neurotransmission contributes to the behavioral effects of anesthetics and may modulate the respiratory depression caused by anesthetics(Teppema & Baby,

2011).

1.7 Cholinergic projections to the preBotC

Little is known about the source of cholinergic inputs to the preBötC, although it has been assumed in many publications that the source is from the major brainstem cholinergic nuclei, such as the PPT, LDT, and possibly the motor nuclei, which contain a large number of cholinergic neurons(X. Li et al., 2018). As for the cranial motor nuclei, the hypoglossal nucleus and the nucleus ambiguus control the airway resistance muscles, whereas the facial nucleus and the trigeminal motor nucleus control the facial muscles(Del Negro et al., 2018). However, it is more likely that the preBötC interneurons project to the breathing related cranial motor nuclei rather than the opposite(Gang et al., 1995; Montandon et al., 2016; Zayia & Tadi, 2020).

Evidence shows that the PPT/LDT send cholinergic projections to the medullary reticular formation, possibly containing the preBötC(X. M. Shao & Feldman, 2009). Infusion of traditional anterograde tracer plant lectin Phaseolus vulgaris-leucoagglutinin (PHA-L) into the PPT labeled fibers mainly in the pontine reticular nuclei oralis and caudalis, ventromedial portions (pars alpha and pars ventralis) of the gigantocellular reticular nucleus as well as a smaller number of fibers distributed to more dorsal regions of the gigantocellular nucleus, lateral paragigantocellular, ventral reticular nucleus of the medulla, lateral reticular nucleus and the lateral facial motor neurons(Spann & Grofova, 1992). Furthermore, retrograde tracing study with FG labeled cholinergic projections from rostral PPT to the RTN (but not pFRG) in rat(Silva et al., 2019). Functionally, general stimulation of PPT suppressed respiratory output(Lydic & Baghdoyan, 1993), while activation of the PPT cholinergic neurons increased respiratory irregularity(Gilbert & Lydic, 1990, 1994; Kubin, 2001), while bilaterally inhibition of the rostral PPT increased

the inspiratory activity and induced active expiration(Silva et al., 2019). In addition, sparse cholinergic neurons are identified in the brainstem and exhibit respiratory related activity(French & Muthusamy, 2018; Mesulam et al., 1983), Endogenous cholinergic inputs terminating on the preBötC may also derive from cholinergic neurons in neighboring regions of the reticular formation(Kubin & Fenik, 2004).

Since the source of cholinergic inputs to the preBötC is yet to be clarified, the aim of this study was determining the source of cholinergic inputs to the preBötC. Results from this anatomical tracing study will direct further functional identification of cholinergic modulation of preBötC neurons.

Chapter 2 Hypothesis

The neuromodulation of breathing is usually sleep and state-dependent. For example, respiratory rhythm disturbances of central origin mostly occurs during sleep especially in the perinatal period(Aserinsky, 1965; Horner, 2008b, 2008a). Similarly, the activity of several cholinergic neurons in the brainstem is state dependent (active in wakefulness and REM sleep, quiet in NREM sleep)(R. C. Boutin et al., 2017) as well as the release of the neurotransmitter Ach, which modulates the activity of respiratory neurons and upper airway motoneurons(Grace et al., 2013, 2014). As reported in the previous section, the source of the cholinergic inputs to the preBotC and the effects of those cholinergic projections are not fully understood(Bellingham & Funk, 2000; Kubin & Fenik, 2004; X. M. Shao & Feldman, 2009).

This study aims to investigate the anatomical connections between the PPT, the LDT and the breathing related nuclei (primarily the preBötC). We hypothesize that the PPT and the LDT send cholinergic projections to the kernel respiratory center to provide state-dependent modulation of breathing.

Chapter 3 Methods

3.1 Experimental animals

Experimental procedures were approved by the Health Science Animal Policy and Welfare Committee of the University of Alberta (AUP#461) according to the guidelines established by the Canadian Council on Animal Care. B6J.129S6-Chat$^{tm2(cre)Lowl}$/MwarJ (Stock No: 028861)(Rossi et al., 2011) mice (ChAT-Cre mice) obtained from The Jackson Laboratory were bred in the Health Sciences Laboratory Animal Services Facility at the University of Alberta, maintained on an ad libitum diet and 12 hours dark/light cycle. Male and female adult ChAT-Cre mice (>8 weeks) were used for tracing experiments.

3.2 Viral injections

In order to trace projections from cholinergic structures into the preBötC we used both a retrograde and an anterograde approach. For retrograde virus tracing, we infected cholinergic projections from ChAT-Cre mice in the preBötC region with three types of Cre-dependent Adeno-associated viruses (AAVs) as follows: AAV-EF1a-double floxed-hChR2(H134R)-mCherry-WPRE-HGHpA (#20297-AAVrg; Addgene), AAV-retro-hSyn-DIO-EGFP (#50457-AAVrg; Addgene) and pAAV-EF1a-double floxed-hChR2(H134R)-EYFP-WPRE-HGHpA (AAV9) (#20298-AAV9; Addgene).

Another group of ChAT-Cre mice (n=4) was transfected with HSV-hEF1a-eYFP-IRES-Cre (Massachusetts Institute of Technology [MIT] vector core) with the same experimental procedure (Table 3. 1).

Table 3. 1 Serotype, catalogue number and source of the viruses used for the retrograde studies.

Virus for retrograde tracing	Serotype	Item ID	Source
pAAV-EF1a-double floxed-hChR2(H134R)-mCherry-WPRE-HGHpA	AAV2-retro	20297-AAVrg	Addgene
pAAV-hSyn-DIO-EGFP	AAV2-retro	50457-AAVrg	Addgene
pAAV-EF1a-double floxed-hChR2(H134R)-EYFP-WPRE-HGHpA (AAV9)	AAV9	20298-AAV9	Addgene
HSV-hEF1a-eYFP-IRES-Cre	HSV	RN411	MIT vector core

For the anterograde virus tracing experiments, we infected cholinergic neurons in the PPT and LDT with four types of Cre-dependent AAVs as follows: rAAV2/Ef1a-DIO-hChR2(H134R)-EYFP (AV4378J and AV4378O, UNC Vector Core), AAV2/eF1a-DIO-hChR2-(E123T/T159C)-p2A-mCherry-WPRE (UNC Vector Core), AAV5/eF1a-DIO-hChR2(H134R)-mCherry (UNC Vector Core), and rAAV2/ hSyn-DIO-mCherry (Addgene) (Table 3. 2).

Table 3. 2 Serotype, catalogue number and source of viruses used for the anterograde studies.

Virus for anterograde tracing	Serotype	lot number	Source
rAAV2/Ef1a-DIO-hchR2(H134R)-EYFP	AAV2	AV4378J	UNC GTC Vector Core
rAAV2/Ef1a-DIO-hchR2(H134R)-eYFP	AAV2	AV4378O	UNC GTC Vector Core

rAAV2/Ef1a-DIO-hChR2-(E123T/T159C)-p2A-mCherry-WPRE	AAV2	AV5470B	UNC GTC Vector Core
AAV2/hSyn-DIO-mCherry	AAV2	v7854	Addgene
rAAV5/Ef1a-DIO-hchR2(H134R)-mcherry	AAV5	AV4314G	UNC GTC Vector Core

In order to verify the location of the injection site, fluorescent carboxylate-modified microspheres (absorbance /emission spectra: 350/440nm), 2% solids, size 0.1 μm; dilution 1:200; Invitrogen, Paisley, UK) were added to the viral solution.

3.3 Stereotaxic surgery

ChAT-Cre mice of both sexes (8–24 weeks old) were anesthetized with isoflurane and positioned on a stereotaxic device (Kopf Instruments, Tujunga, CA, United States) with isoflurane continuously delivered at 1.5-2% in room air. Following aseptic procedures, the mouse head was shaved, an incision was made along the midline of the scalp and the skull was exposed. The landmarks of bregma and lambda were used to set appropriate stereotaxic coordinates.

A sharp glass micropipette (5-000-2005, Wiretrol II, Drummond Scientific Company) was used to inject 50-100 nl of viral solution into either the preBötC (stereotaxic coordinates relative to Bregma: posterior [P], 6.60 mm; medial [M], ±1.45 mm; and relative to the surface of the brain: ventral [V], -4.85 to-4.95 mm,), the PPT (P, 4.72 mm; M, ±1.30 mm; V, 3.60 mm; relative to Bregma) or the LDT (P, 5.02 mm; M, ±0.50 mm; V, 3.45 mm; relative to Bregma), Following injection, the micropipette remained in place for 10 min to avoid backflow of the viral particles. The incision was then sutured with 4-0 silk thread (REF B66D, Havel's inc). Local Buprenorphine (DIN: 02443694, SteriMax) and systemic

Metacam (DIN: 02237715, Boehringer Ingelheim) were given for postoperative pain management. Mice were housed for ≥3 weeks to achieve the robust expression of the viruses in the brain.

3.4 Histology

Mice were transcardially perfused under isoflurane anesthesia (4-5%) with 20ml. of 0.9% saline followed by 4% paraformaldehyde (PFA) in phosphate-buffered saline (PBS) (20ml). Following perfusion, the brains were gently removed and post-fixed in 4% PFA overnight at 4℃ and cryoprotected in 30% sucrose in PBS for 48 hours.

The brains were then embedded in O.C.T. compound, frozen and sectioned with a CM1950 cryostat (Leica Biosystems, Buffalo Grove, IL). Free-floating coronal sections (50 μm) were collected and stored in cryoprotectant solution (1L cryoprotectant solution contains 500 ml PBS (0.01M/1×), 300g sucrose, 10g PVP-40, and 300ml ethylene glycol) at -20℃ until further processing.

Mouse brain slices were transferred to 96-micro well plates, washed in PBS 5 times, and incubated in blocking solution containing 0.3% Triton X-100, 10% normal donkey serum (NDS) in PBS for one hour at room temperature to minimize the nonspecific binding. After that, the blocking solution was directly replaced by the blocking solution containing the following primary antibodies: anti-somatostatin (SST; 1:200; rabbit; Thermo Fisher Scientific), anti-choline acetyltransferase (ChAT; 1:500; goat; EMD Millipore), anti-green fluorescent protein (GFP; 1:800; chicken; Aves Labs Inc.), anti-mCherry (1:1000; chicken; EMD Millipore) in PBS (1×) for 24 hours at room temperature. On the next day, sections were rinsed with PBS for 5 times and incubated with the secondary antibody dilution buffer, which contained 0.3% Triton X-100, 1% NDS, and a 1:200 dilution of specific secondary

antibodies (Cy2-donkey anti-rabbit (711-225-152, Jackson ImmunoResearch) or Cy3-donkey anti-rabbit (711-165-152, Jackson ImmunoResearch); Cy5-donkey anti-goat (705-175-147, Jackson ImmunoResearch); Cy3-donkey anti-chicken (703-166-155, Jackson ImmunoResearch) or Cy2-donkey anti-chicken (703-225-155, Jackson ImmunoResearch)) in PBS for 2 hours at room temperature. Brain sections were then washed with PBS before mounting and coverslipping with Fluorsave mounting medium (EMD Millipore).

3.5 RNAscope in situ hybridization

To determine the accuracy of Cre expression by the cholinergic neurons of the transgenic mice, RNAscope technique combined with the immunofluorescence were performed according to a modified Advanced Cell Diagnostics-ACDBio RNAscope protocol(Biancardi et al., 2020). Selected sections of medulla and pontine were mounted on microscope slides and stored at -80℃ until use. On the day of the experiments, the slides were thawed at room temperature and immersed in 4% PFA at 4℃ for 1 hour. After 2 washed in PBS(1×), slides were baked at 60℃ for 15mins and dehydrated in gradient ethanol (50%, 70% and 100%, each time for 5 mins) before heating them again at 60℃ for 15mins and pretreating them H_2O_2. After pretreatment, slides were dried in room temperature, incubated in protease III at 40℃ for 30 mins and rinsed in distilled water before incubating them with the RNAscope oligonucleotide probes for Cre (CRE; #312281, ACDBio) at 40℃ for 2 hours. Next, slides were treated with the RNAscope Multiplex Fluorescent Assay Kit version 2 (ACDBio) according to the manufacturer's instructions.

Immediately after this procedure, the immunofluorescence staining for ChAT was performed immediately to identify the cholinergic neurons. Similar to the protocol mentioned above, slides were washed in PBS(1×), incubated in the blocking solution for 1 hour followed by the primary antibody solution (ChAT; 1:500; goat; EMD Millipore)

overnight. On the next day, the slides were washed with PBS(1×) and incubated in the secondary solution with Cy5-donkey anti-goat (705-175-147, Jackson ImmunoResearch) for 2 hours. Finally, the slides were washed again with PBS(1×), dried and coverslipped. The immunofluorescence protocol was performed at room temperature.

3.6 Data analysis and anatomical landmarks

The Evos FL fluorescent microscope (Thermofisher) and Confocal Laser Scanning Microscope (Leica) were used to observe and analyze the results of the immunofluorescence staining with reference to mouse brain atlas(Franklin et al., 2008). Only neuron profile that included a nucleus and axons labelled by the reporter protein was counted as a labelled neuron.

ChAT staining portrayed the major cholinergic nuclei in the brainstem, including the motor nuclei, the PPT and LDT. Cholinergic neurons of the PPT and LDT form a longitudinally oriented column starting from the substantia nigra pars reticulate (SNR) and end at the lateral central gray matter in the periventricular area(Mena-Segovia, 2016). Because there is no clear dividing line between PPT and LDT(Mena-Segovia, 2016), and there are cholinergic neurons in the transition region, for the convenience of data analysis, we defined the cholinergic neurons rostral to Bregma -4.9 mm as the PPT neurons, and the caudal cholinergic groups belong to the LDT based on the mouse brain atlas(Franklin et al., 2008).

The facial nucleus (7N) and the nucleus ambiguus (NA) were used as anatomical landmarks to localize the preBötC (350~600 μm caudal to the facial nucleus, directly ventral to the semi-compact NA), in reference to the shape of the inferior olivary nuclei (maximum). The SST-expressing neurons assemble in the preBötC were used for

localization as well.

Chapter 4 Results

4.1 Targeting the Cholinergic afferent projections to the preBötC

In order to target cholinergic projections terminating on preBötC neurons, we used two different approaches: 1) a retrograde virus, herpes simplex virus (HSV) that is not dependent on the phenotype and characteristics of infected neurons and is also shown to provide good tropism toward different neuronal phenotype; 2) Cre dependent anterograde and retrograde viruses in ChAT-Cre mice. In this second strategy, a battery of AAVs, including 3 types of retrograde Cre dependent viruses injected into the preBötC and 4 types of anterograde Cre dependent viruses (Figure 4. 1 A) injected into the PPT and LDT(Tervo et al., 2016), were used in this study. The viral constructs contained a Double-floxed Inverted Orientation (DIO) sequence (also known as Flip-Excision, FLEx) which utilizes oppositely oriented loxP and lox2272 sites as the mediator to regulate the gene transcription. In the presence of Cre, the reporter mRNA in between (mCherrry/EGFP/EYFP) can be inverted, recombined and transcribed with reference to the promoter sequence(Saunders & Sabatini, 2015) (Figure 4. 1 B).

The ChAT-Cre mice used in this project express Cre recombinase in ChAT + neurons(Rossi et al., 2011), which means that all the cholinergic neurons in the transgenic mouse expressed Cre recombinase.

Because we opted to use viral tracers expressing fluorescent reporter proteins, we did not tag Cre recombinase with a fluorescent reporter. We therefore verified selective expression of Cre recombinase in ChAT-expressing neurons in a series of preliminary experiments.

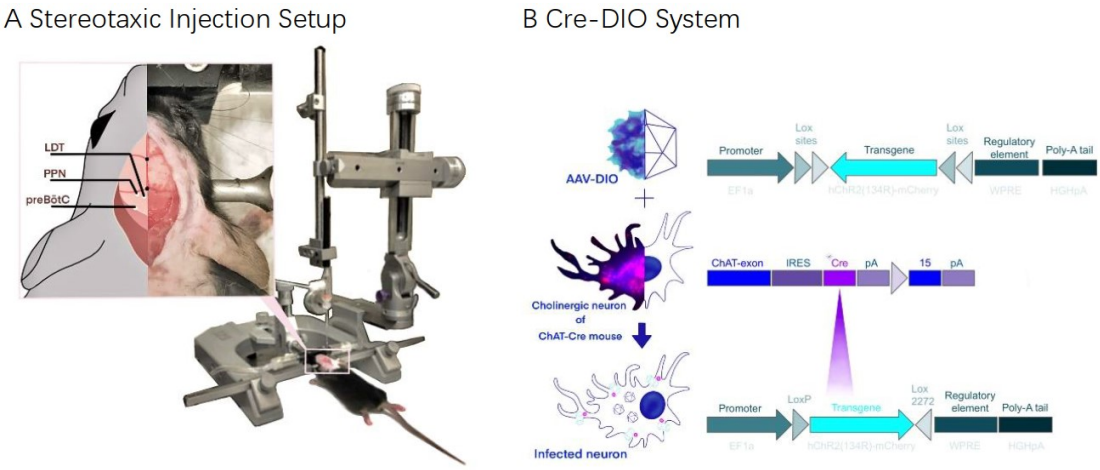

Figure 4. 1 | The injection procedure and the Cre-DIO system.

(A) The stereotaxic injection setup and approximate location of the area of interest. (B) The Cre-DIO system allows for the virus to be expressed exclusively in cholinergic neurons.

4.2 Verification of the ChAT-Cre mouse line

Brain sections of ChAT-Cre mice (n=2 mice) were processed for the multiplex fluorescent in situ hybridization (RNAscope) to verify the expression of Cre recombinase in ChAT immuno-positive neurons of the transgenic ChAT-Cre mice. Dense and bright Cre mRNA signals (red) were found in every ChAT+ neurons within the brainstem motor nuclei, the PPT, the LDT, and the parabigeminal nucleus (PBG)(X. Li et al., 2018). In addition, we found Cre signal within other regions that contained sparse cholinergic neurons as reported by previous studies: the NTS(D. Ruggiero et al., 2019; D. A. Ruggiero et al., 1990a), the prepositus nucleus (Pr)(Barmack et al., 1992; Sugimura & Saito, 2021), the lateral paragigantocellular nucleus (LPGi)(Stornetta et al., 2013), the vestibular nuclei (Ve)(Poppi et al., 2020; Takeshita et al., 1999), the superior olive (SO)(Simmons et al., n.d.), the Me5(Schäfer et al., 1998; H.-L. Wang & Morales, 2009), and the KF(Bonis et al., 2010; Varga et al., 2021). Additionally, several double-positive neurons (Cre+/ChAT+) were

scattered within the reticular formation(Fuller et al., 2007; Toor et al., 2019; Volgin et al., 2008) (including the IRt, parvicellular reticular nucleus (PCRt), pontine reticular nucleus, etc.) throughout the brainstem (Figure 4. 2). We did not find any ectopic expression of Cre in ChAT-negative neurons.

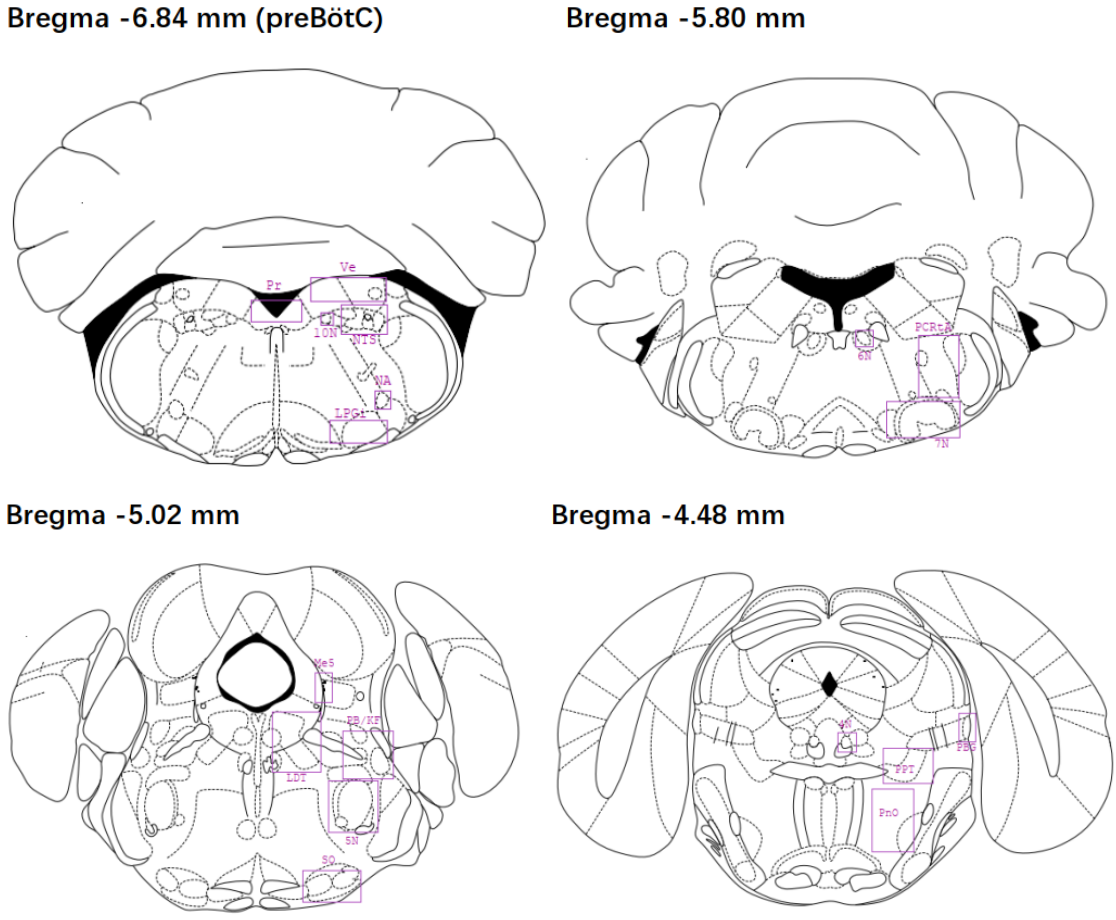

A Cre signals in cholinergic motor nuclei

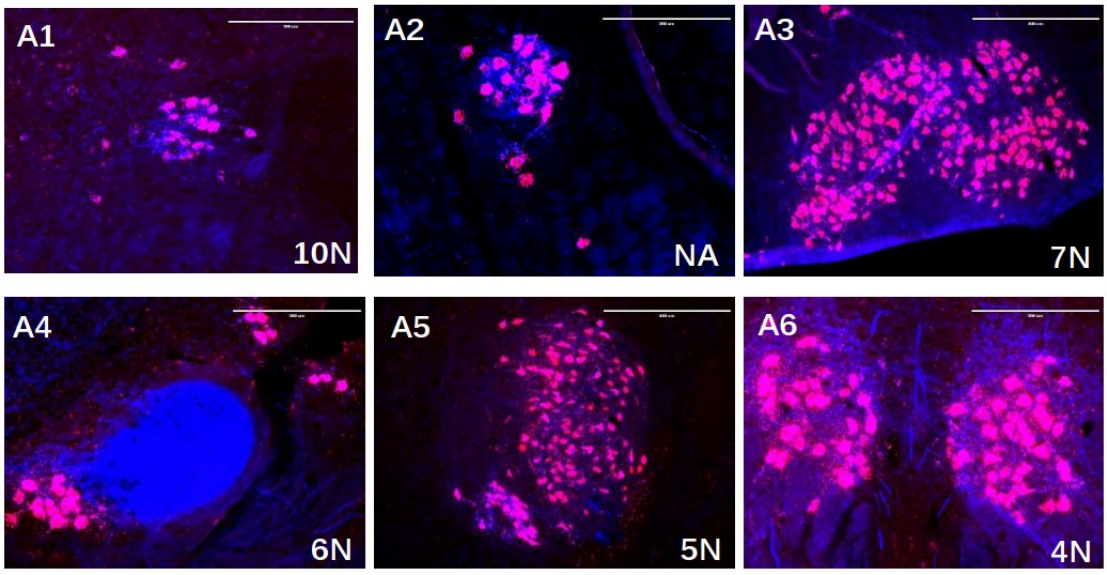

B Cre signals in pontine major cholinergic nuclei

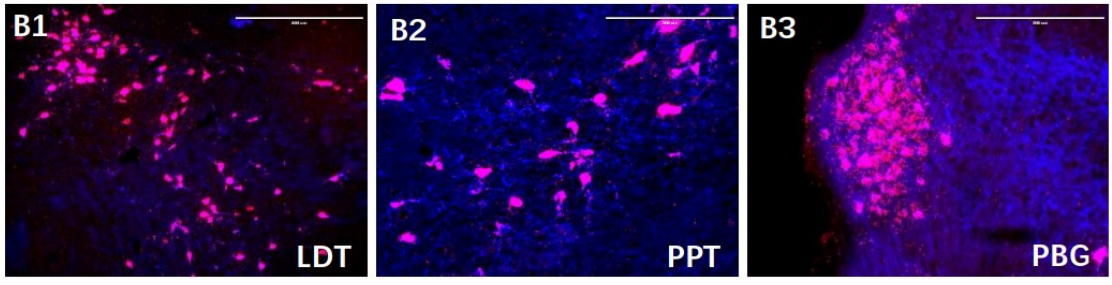

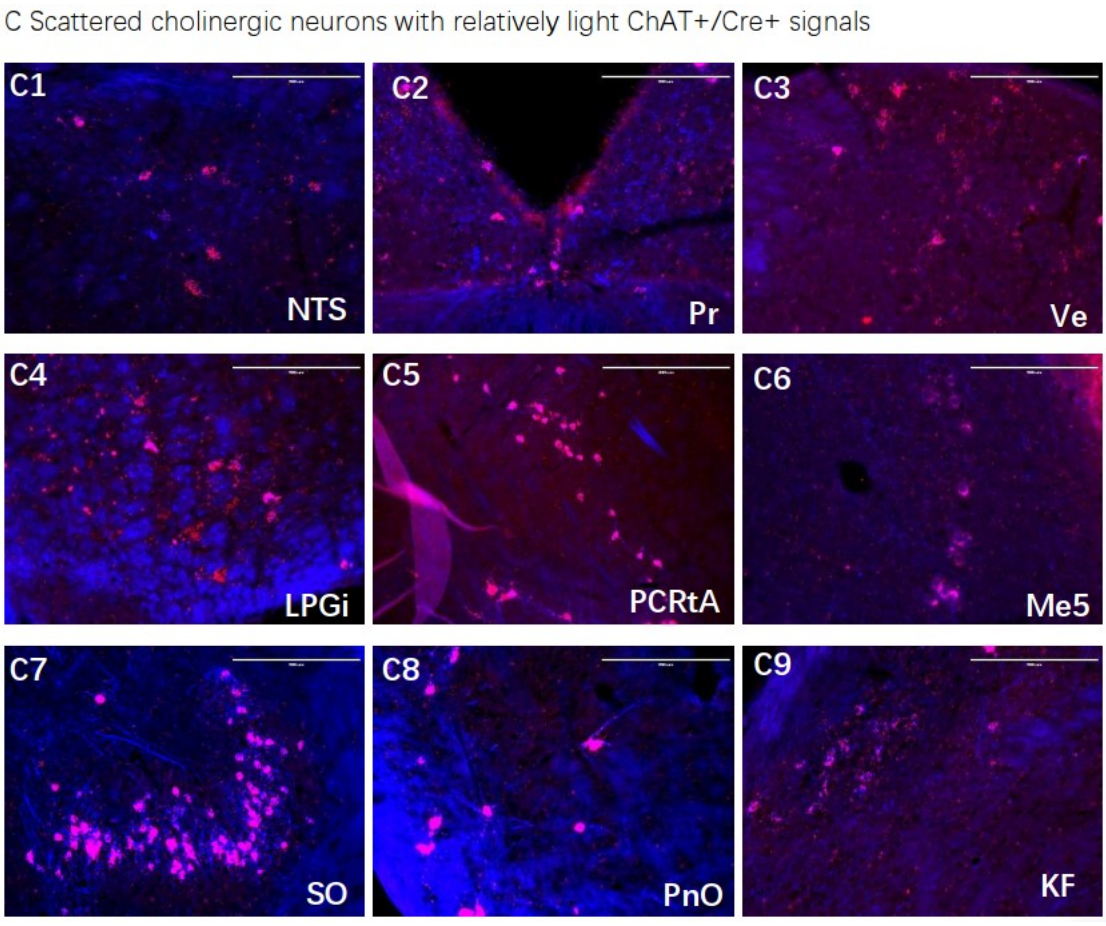

Figure 4. 2The expression of Cre in ChAT immune-positive neurons.

Coronal sections from the ChAT-Cre mice show cholinergic neurons that express ChAT (blue) and Cre (red). Cre was expressed in the cholinergic neurons of major cholinergic nuclei (A, B) including the 10N, NA, 7N, 6N, 5N, 4N, PPT, LDT, PBG, as well as in the cholinergic neurons scattered (C) in the NTS, Pr, Ve, LPGi, PCRtA, Me5, SO, PnO, KF, etc. Scale bar=400μm (A3, A5, B1, C5); Rest scale bar=200μm.

4.3 Afferent projections to the preBötC

We initially use a non-Cre dependent HSV to identify retrograde projections to the preBötC. HSV has endogenous retrograde properties, which can be used to label projections to the preBötC from various neuronal structures(Bearer et al., 2000; Biancardi

et al., 2020; Ugolini et al., 1987), including cholinergic neurons(Boskovic et al., 2018; Peng et al., 2019). In this study, HSV-hEF1a-eYFP-IRES-Cre virus with retrograde properties(Biancardi et al., 2020; Gremel et al., 2016) was injected into the preBötC of ChAT-Cre mice (n=4 mice) to label circuit-specific projections to the preBötC (Figure 4. 3). The fluorescent carboxylate-modified microspheres added to the viral solution confirmed that the injection site was within the boundary of the preBötC, defined as the area containing SST-expressing neurons within specific anatomical landmarks (Figure 4. 3): 350~600 μm caudal to the facial nucleus, directly ventral to the semi-compact NA, and at the level where the inferior olivary nuclei reached maximum. Injections with obvious track leakage and out-of-target locations were removed from the analysis although we can't exclude the possibility of false positive labelling in our samples due to the spread of the virus to adjacent area(Gang et al., 1995; Yang et al., 2019) and false negatives given the toxicity and preferential viral tropism of HSV(Nectow & Nestler, 2020; Tokumaru, 1968).

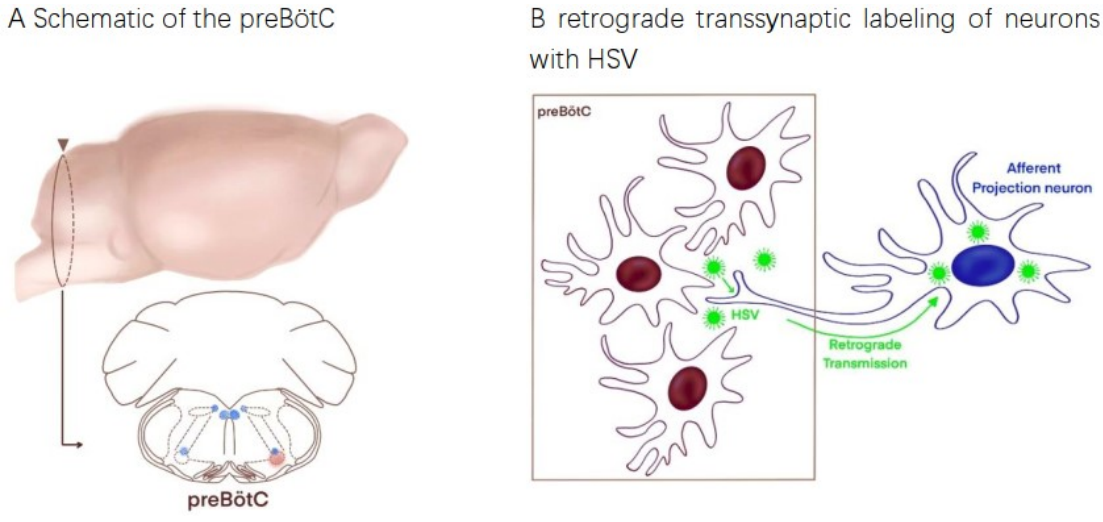

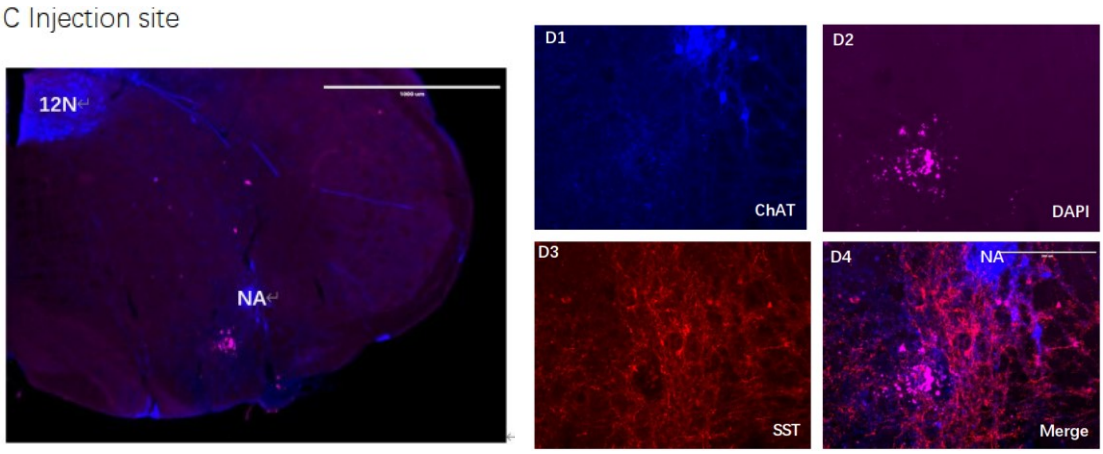

Figure 4. 3 | Stereotaxic injection of HSV into the right preBötC of the ChAT-Cre mouse.

(A) Schematic of the brain slice at the level of preBötC. (B) Schematic of the retrograde transmission of HSV-hEF1a-eYFP-IRES-Cre. (C) Immunofluorescence staining results of brain slice at the level of preBötC. (D) Magnified images of the injection site. Blue-ChAT (D1); Purple-DAPI (fluorobeads) (D2); Red-SST (D3), and the merged image (D4). Panel C scale bar=1000μm; Panel D scale bar=200μm.

4.3.1 Medullary projections to the preBötC

Similar to previous studies, retrogradely labeled neurons (labeled by the non-cell-type-specific traditional tracer FG(Yang et al., 2019) and WGA-HRP(Gang et al., 1995) which have been injected into the preBötC and VRG respectively) were identified in the contralateral preBötC, the BötC, the NTS, the reticular nuclei, the raphe nuclei, the parafacial and facial nuclei, the PB/KF, and the NA. Interestingly, we found neurons in additional areas that were also retrogradely labeled by HSV. In general, there were quite a few labeled neurons in the VRG, the paraNA, the LPGi, the gigantocellular reticular nucleus (Gi), the medullary reticular formation, the RTN/pFv, the NTS, the transition region of the caudal part (Sp5C) and interpolar part (Sp5I) of the spinal trigeminal nucleus (Sp5), the PB/KF, the PAG, the regions around tensor tympani part of the motor trigeminal

nucleus/ motor root of the trigeminal nerve (5TT/m5), and the regions around 5N. Additionally, there are sparse labeled neurons in the NA, the 7N, the 10N, the para10N, the 12N, the para12N, the raphe nucleus, the vestibular nucleus (Ve), the prepositus nucleus (Pr), the dorsal marginal layer of medulla, the pFRG, the locus coeruleus (LC), the LDT/PPT, and the pontine reticular nucleus, oral part (PnO).

4.3.1.1 Ventral medulla

The VRC lies in the ventrolateral medulla which includes 6 subdivisions: the cVRG, the rVRG, the preBötC, the BötC, the RTN/pF$_V$ and the pFRG. We identified the preBötC based on the anatomical landmarks indicated above and SST expression in a subpopulation of preBötC neurons(Cui et al., 2016; Stornetta et al., 2003; Yang & Feldman, 2018). Some GFP expressing neurons were identified in the VRG (n=4 mice), including the contralateral preBötC (n=4 mice) (Figure 4. 4). Normally, GFP+ neurons were concentrated in the ipsilateral side, but in some cases (n=2 mice), labeled neurons were fewer in the ipsilateral BötC compared to the contralateral side, because of the ability of the HSV to be taken up by presynaptic terminals and not infect neurons directly at the injection site. Several GFP+ neurons were also observed in parafacial region (n=4 mice) including the RTN/pF$_V$ and the pFRG, while most of them were in the ipsilateral RTN/pF$_V$(Figure 4. 5). There were occasionally labelled neurons in the RTN/pF$_V$ expressing ChAT signals (n=2 mice) and some labeled neurons around NA (N=4 mice) along its rostral-caudal axis, which concentrated in the region lateral to the caudal NA (Figure 4. 5), while a small number of them express light ChAT signals (n=3 mice). However, not many labelled neurons were located within NA, and we identified several GFP+/ChAT+ neurons in the caudal NA only in one case.

In addition, we observed some GFP+ neurons in the LPGi (n=4 mice), and in the Gi (both

ventral part (GiV) and the alpha part (GiA)) (Figure 4.6) at the level of BötC and 7N (n=4 mice). However, only few of them express ChAT signal (n=1 mice and n=3 mice respectively). In the middle, we found sparse GFP+ neurons in all four subdivisions of the raphe nucleus (n=4 mice, including the raphe interpositus nucleus (RIP), raphe magnus nucleus (RMg), raphe obscurus nucleus (ROb), raphe pallidus nucleus (RPa)), while some of the labelled neurons in Rob also express ChAT signals (n=2 mice) (Figure 4.6).

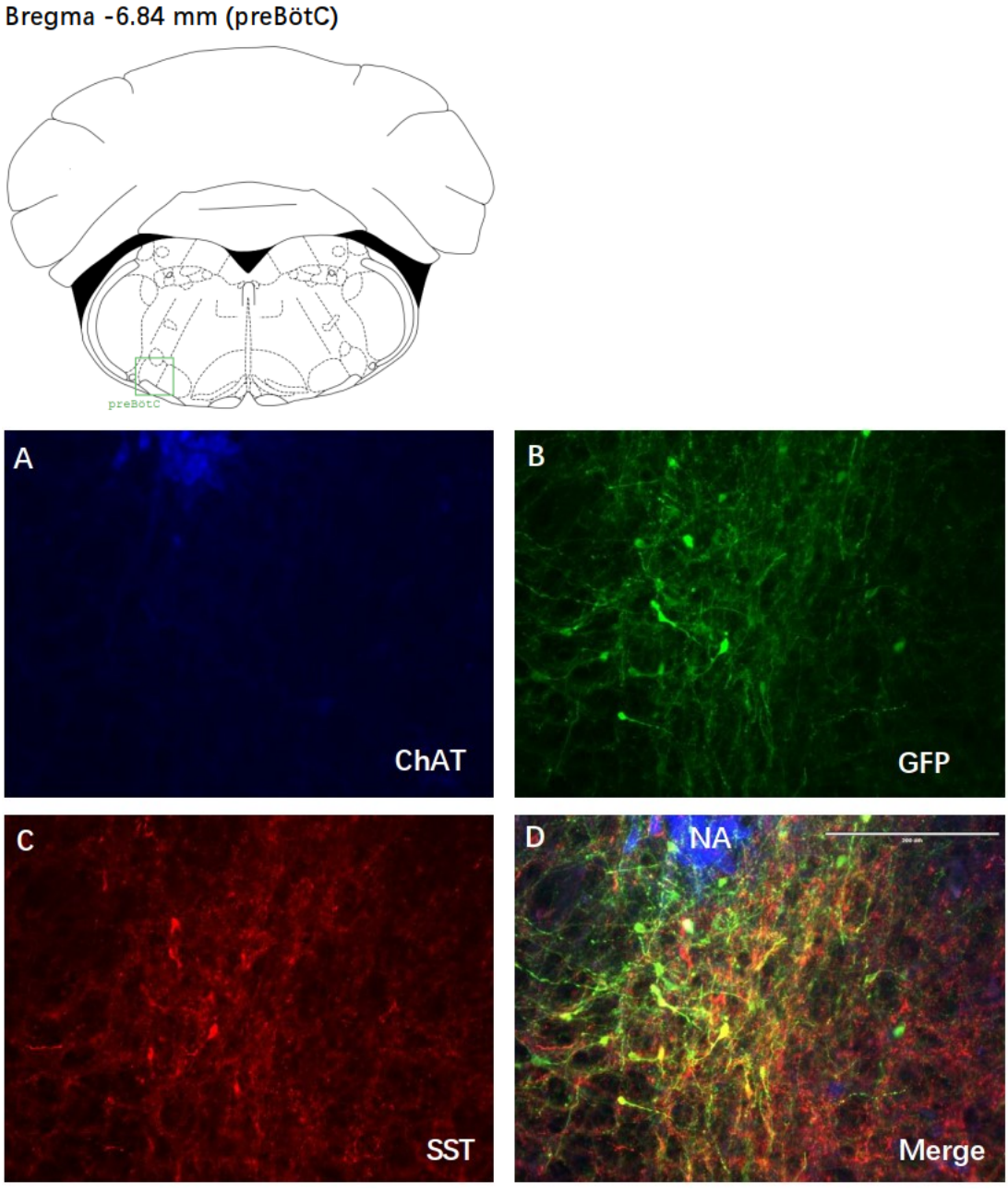

Figure 4. 4 | Retrogradely labeled neurons in the contralateral preBötC with HSV retrograde virus.

Images of the contralateral preBötC. Blue-ChAT (A); Green-GFP (HSV reporter protein) (B); Red-SST (C), and the merged image (D). Scale bar=200μm.

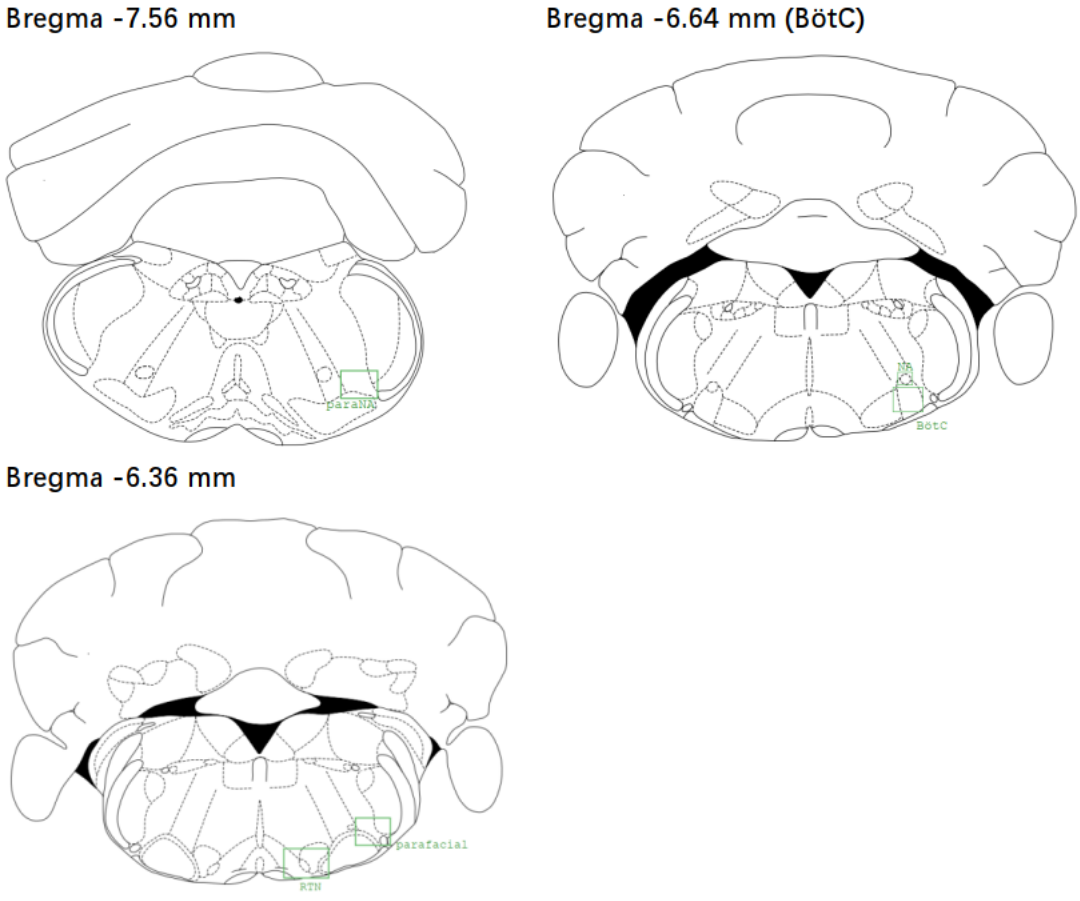

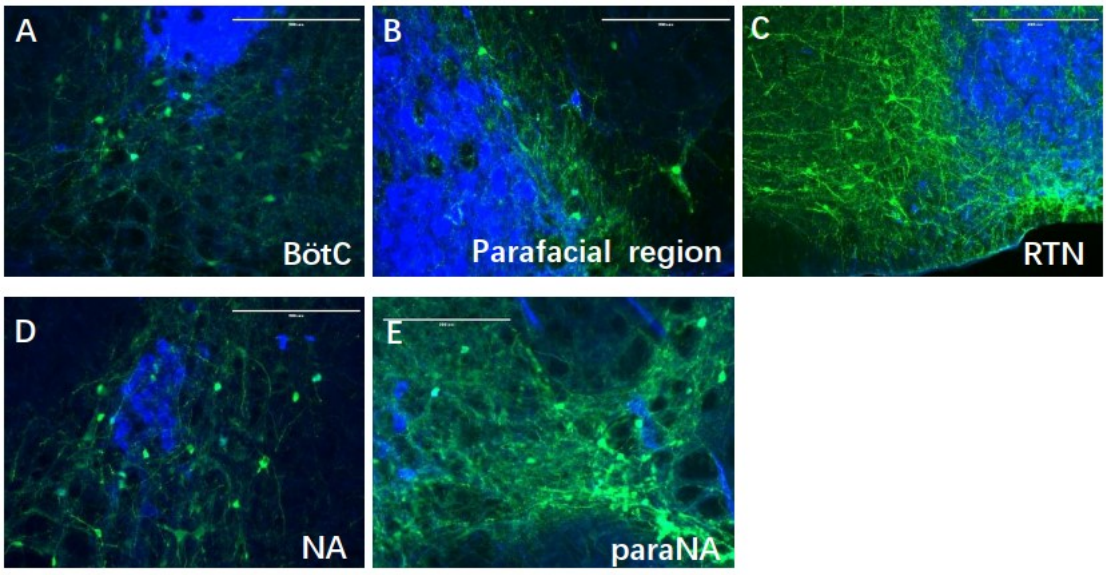

Figure 4. 5 | HSV retrogradely labeled neurons in the ventral respiratory column.

We found labeled neurons in the BötC (A), pFRG (B), RTN (C), NA (D), and paraNA (E, F). Blue-ChAT; Green-GFP. Panel C scale bar=400μm; Rest scale bar=200μm.

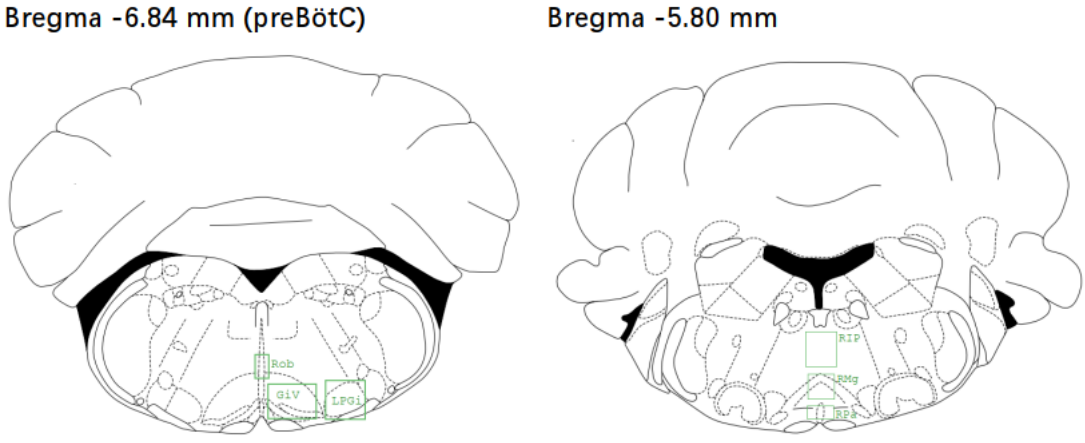

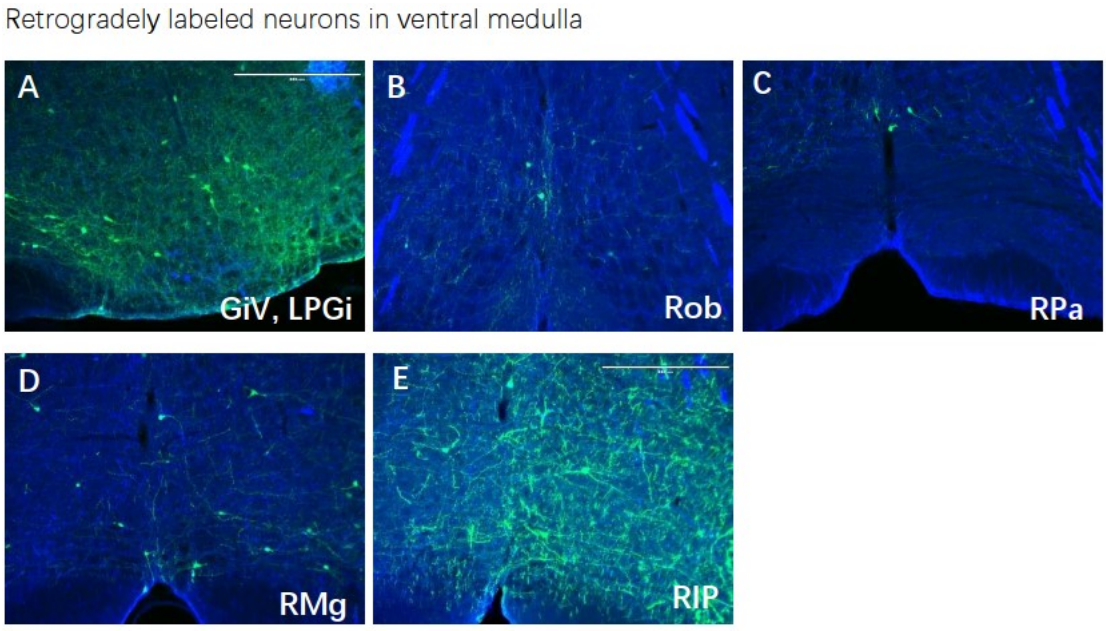

Figure 4. 6 | HSV retrogradely labeled neurons in ventral medulla.

We found labeled neurons in the GiV and LPGi (A), Rob (B), RPa (C), RMg (D), and RIP (E). Blue-ChAT; Green-GFP. Scale bar=400μm

4.3.1.2 Middle and dorsal medulla

Laterally, we identified some labeled neurons bilaterally in the transition region between Sp5I and Sp5C (n=4 mice) (Figure 4.7) at the level of caudal NA. Sometimes, there are scattered GFP+ neurons in the Sp5I and oral part of the Sp5 (Sp5O) at the level of caudal 7N (n=3 mice). There are some labelled neurons in the reticular formation (n=4 mice) throughout the medulla which assembling in the ipsilateral IRt (Figure 4.7), especially at the level of the injection (preBötC). A small fraction of the GFP+ neurons in the IRt also express ChAT signals (n=4 mice). Interestingly, we identified few GFP+ neurons in the area dorsal medial to the NA at the BötC level which matches the recently proposed post-inspiratory rhythm generator (PiCo)(Toor et al., 2019) (n=4 mice), while only in one case we found labelled neurons in PiCo expressing ChAT (Figure 4.7).

Only one or two neurons were labelled in 12N area (n=2 mice), and we found one expressing ChAT signal (n=1 mice). Some labeled neurons surrounding the 12N were identified (n=4 mice), especially in the nucleus of Roller (Ro) region (Figure 4.7), and scattered in the dorsal paragigantocellular nucleus (DPGi) region (n=4 mice). We identified several neurons in 10N (n=4 mice) but none of them were cholinergic. Furthermore, we identified GFP+ neurons in and surrounding the ipsilateral, caudal region of the 10N (n=4 mice) which occasionally expressed light ChAT signals (n=2 mice) (Figure 4.7). A few neurons were also identified in NTS (n=4 mice), a fraction of which coexpressed ChAT signals (n=3 mice) (Figure 4.7).

In the dorsal middle medulla, a small number of GFP+ neurons were found in the Pr especially at the dorsal edge (Figure 4.7) (n=4 mice), and occasionally, the labelled neurons express ChAT signals (n=1 mice). There were also several neurons in the dorsal marginal layer (n=3 mice) and some express ChAT signals (n=2 mice). We found scattered GFP+ neurons in the Ve (n=4 mice) throughout its rostro-caudal extend, sometimes the labelled neurons were ChAT+ (n=2 mice). Interestingly, in most cases (n=3 mice), GFP+ neurons were identified in the medial vestibular nucleus, parvicellular part (MVePC) (n=3 mice) at the abducens nucleus (6N) level (Figure 4.7). In addition, we found small number of labeled neurons in locus coeruleus (LC) (n=4 mice) bilaterally (n=3 mice), with prevalence in the ipsilateral side of the brain (Figure 4.7). These GFP+ neurons in MVePC and LC possibly corresponding to the dorsal medial population that show respiratory-related local field potentials (LPFs) in previous study(Dhingra et al., 2019). Furthermore, some GFP+ neurons surround the genu of the facial nerve (g7) at the same level (n=3 mice) (Figure 4.7).

Bregma -7.56 mm

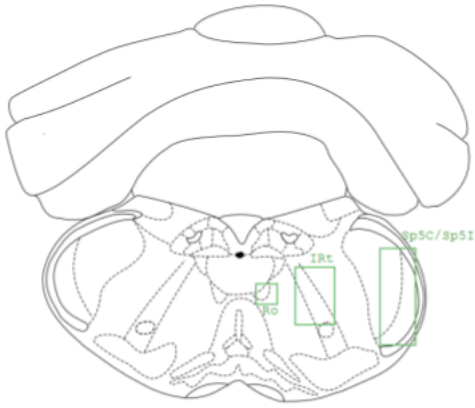

Bregma -6.64 mm (BötC)

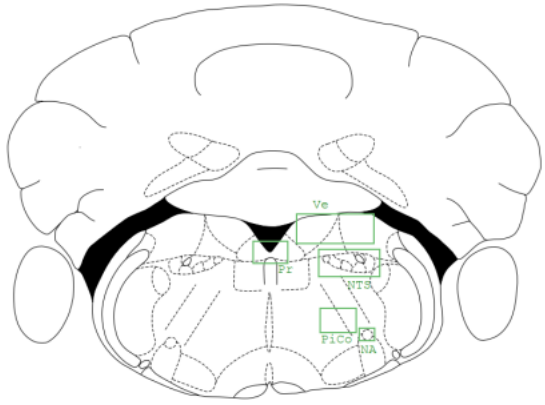

Bregma -6.36 mm

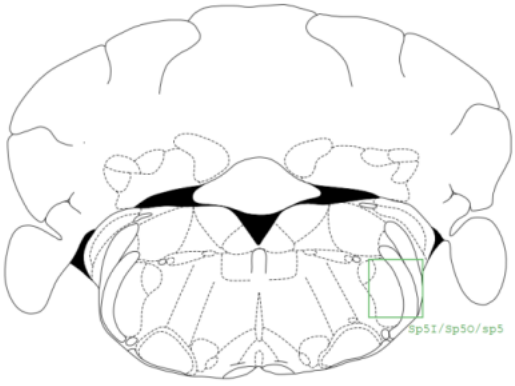

Bregma -5.80 mm

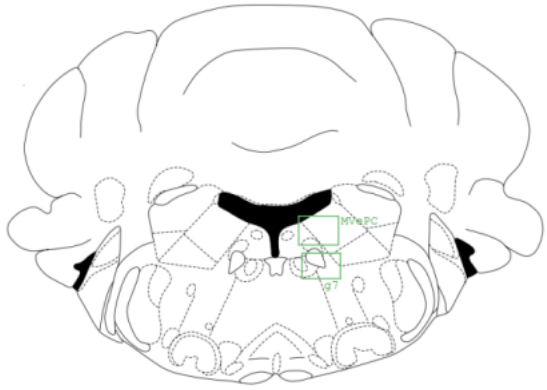

Retrogradely labeled neurons in dorsal and middle medulla

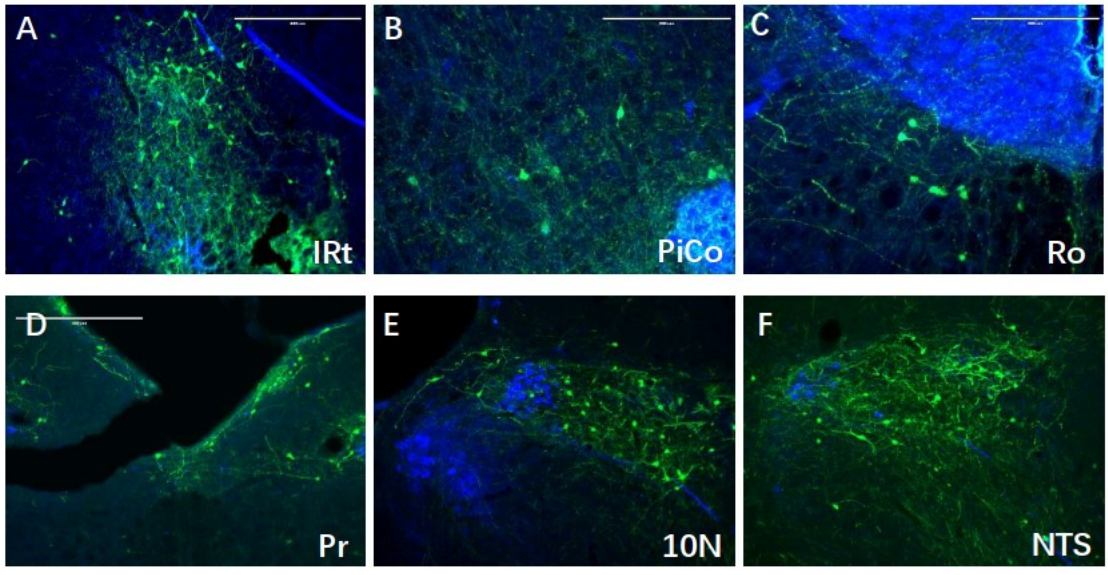

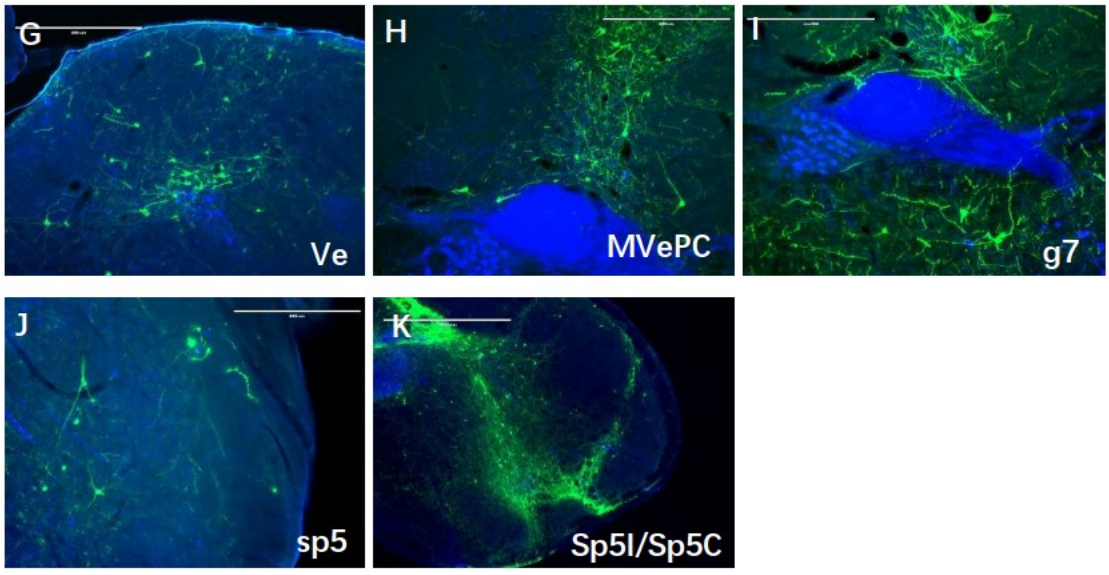

Figure 4. 7 | HSV retrogradely labeled neurons in dorsal and middle medulla.

We found labeled neurons in the IRt (A), PiCo (B), Ro (C), Pr (D), 10N (E), NTS (F), Ve (G), MVePC (H), around g7 (I), sp5 (J), Sp5I/Sp5C (K). Blue-ChAT; Green-GFP. Blue-ChAT; Green-GFP. Panel B, C scale bar=200μm; Panel K scale bar=1000μm; Rest scale bar=400μm.

4.3.2 Pontine projections to the preBötC

There are a fairly large number of labeled neurons in the PB (n=4 mice) particularly in the lateral subdivision (LPB) of the ipsilateral side (Figure 4.8), while some of them expressing ChAT signals (n=3 mice). Additionally, some GFP+ neurons were identified in the ipsilateral KF (n=4 mice) with sparse neurons in the contralateral KF, some of which were ChAT+ (n=4 mice) (Figure 4.8). We observed a few GFP+ neurons in the regions around the 5N, such as the supratrigeminal nucleus (Su5) (n=4 mice), the subcoeruleus nucleus (SubC) (n=4 mice) especially the ventral part (SubCV), and the PCRt below 5N (n=4 mice) (Figure 4.8). However, only one or two labeled neurons surrounding the 5N express ChAT signals (n=3 mice). In addition, we found labelled neurons in the areas around 5TT/m5, and occasionally found labelled ChAT+ neurons (n=3 mice). The number

of labeled neurons in the PAG (n=4 mice) is remarkable (Figure 4.8), but none was ChAT+. Surprisingly, we found sparse labeled neurons in bilateral PPT and LDT in all four injected mice, and we only identified one labelled neuron expressing ChAT in the ipsilateral LDT (Figure 4.8). There were only one or two labelled neurons in the dorsomedial tegmental area (DMTg) (n=3 mice) region below the LDT and none was ChAT+. We also found sparse GFP+ neurons in the pontine reticular nucleus (n=4 mice), while one or two of them were ChAT+ (n=2 mice) (Figure 4.8). Notably, the labelled neurons were seldom found to be cholinergic and we did not find any labelled cholinergic neurons in the cholinergic nuclei including the PPT, the 5N, the 4N, and the PBG (n=4 mice).

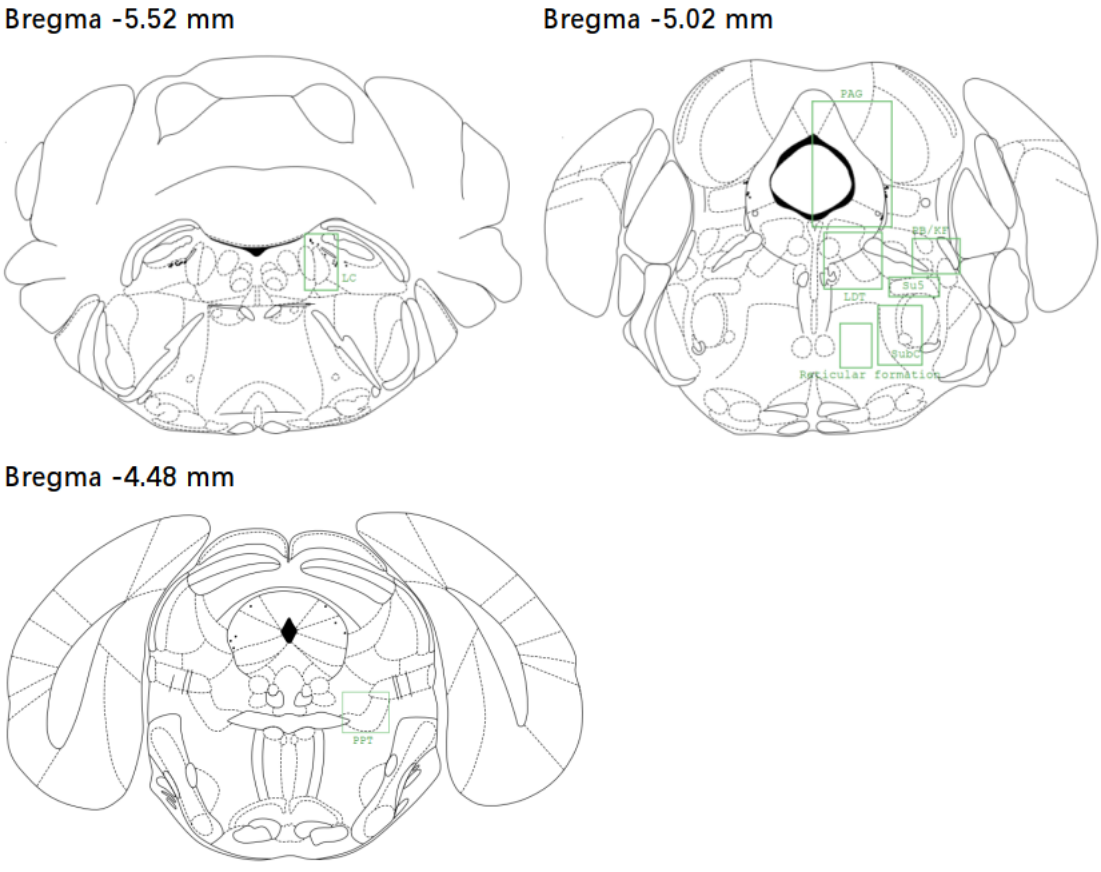

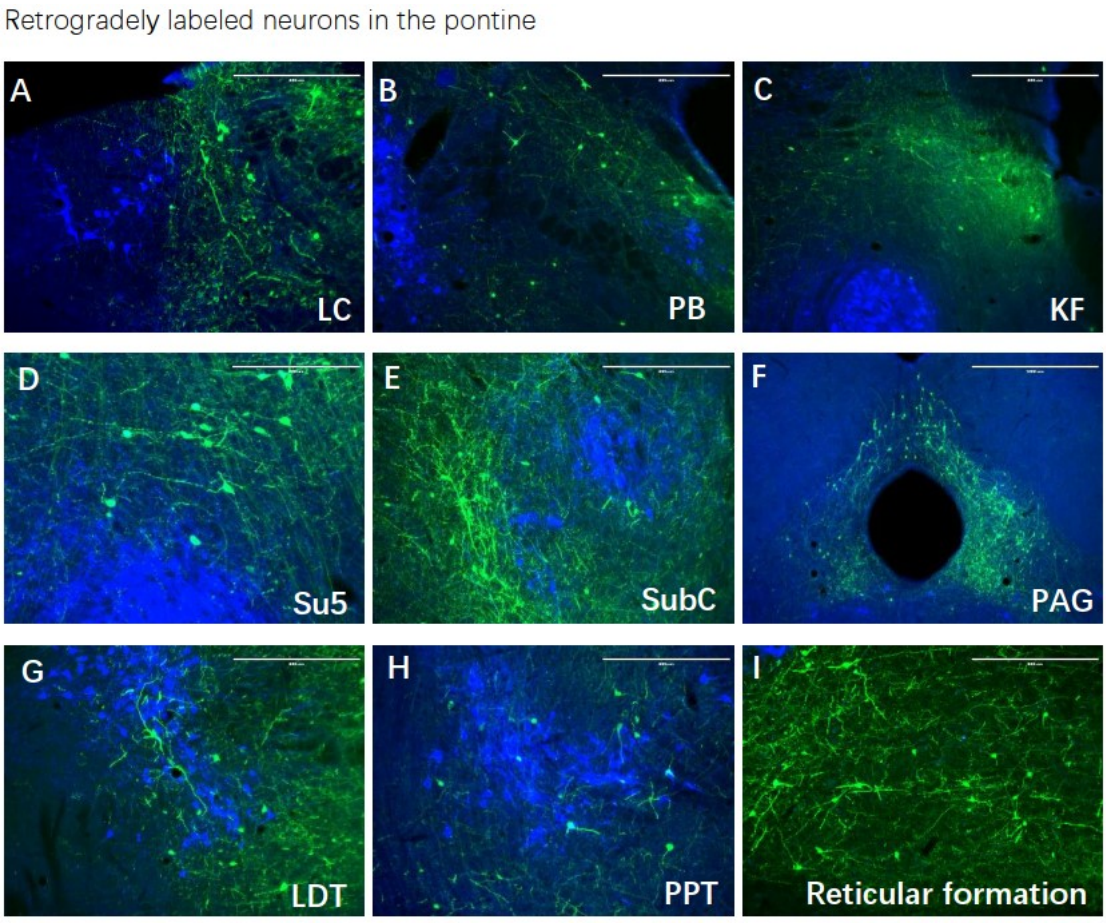

Figure 4. 8 | HSV retrogradely labeled neurons in pontine structures.

We found labeled neurons in the LC (A), PB (B), KF (C), Su5 (D), SubC (E), PAG (F), LDT (G), PPT (H), and pontine reticular formation (I). Blue-ChAT; Green-GFP. Panel D scale bar=200μm; Panel F scale bar=1000μm; Rest scale bar=400μm.

Despite our confirmation of the location of the injection site, the distribution of GFP+ neurons were slightly different between mice. We summarized the region of interest and the average density of labelled neurons, and found most significant distribution of GFP cells in the region between Sp5I and Sp5C, VRG, paraNA, LPGi, GiV/GiA, IRt, NTS, RTN, PB/KF, PAG, the regions around 5TT/5m, and the regions around 5N. Of note, although the HSV retrogradely labelled plentiful neurons throughout the brainstem, only a small fraction of them expressed ChAT signals (Table 4.1, Table 4.2).

Table 4. 1 HSV labeling in the major cholinergic nuclei

	Average density of GFP+ neurons	GFP+ cases (mice#)	GFP+/ChAT+ cases (mice#)
Medulla			
6N	-	0	0
7N	+	3	0
NA	+	4	1
10N	+	4	0
12N	+	2	1
Pons			
5N	-	0	0
4N/3N	-	0	0
PPT	+	4	0
LDT	+	4	1
PBG	-	0	0

Table 4. 2 HSV labeling in other regions

		Average density of GFP+ neurons	GFP+ cases (mice#)	GFP+/ChAT+ cases (mice#)
Medulla				
VRG	cVRG/rVRG	+	2	0
	preBotC	++	4	0
	BotC	++	4	0
lateral to rostral VRG		+	4	1

between Sp5I and Sp5C		++	4	0
paraNA		++	4	3
LPGi		++	4	1
GiV/GiA		++	4	3
para7N	RTN	++	4	2
	pFRG	+	4	0
para10N		+	4	2
NTS		++	4	3
para12N		+	4	0
Raphe nucleus		+	4	2
Reticular formation	IRt	++	4	4
	PiCo	+	4	1
Ve		+	4	2
dorsal marginal layer		+	3	2
Pr		+	4	1
Sp5I and Sp5O		+	3	0
around g7		+	3	0
Pons				
LC		+	4	0
PB/KF		++	4	4
PAG		++	4	0
DMTg		+	3	0
PnO		+	4	2
around 5N (SubC/SubCV/PCRtA)		++	4	3
around 5TT/5m		++	4	3

(+): There are sparse and occasionally labeled neurons in that region.

(++): There are relatively dense labeled neurons in that region.

4.4 Cre-dependent retrograde tracing

Because the HSV targeted projections in a non-Cre dependent fashion, we decided to use a Cre-DIO system with the retrograde labeling approach in ChAT-Cre mice to better identify the origins of cholinergic inputs to the preBötC.

Three kinds of Cre-dependent retrograde AAVs (AAV2-retro-EF1a-DIO-mCherry, AAV2-retro-hSyn-DIO-EGFP, and AAV9-EF1a-DIO-EYFP) were injected into the right preBötC of ChAT-Cre mice (Table 3.1). Histological analysis 3-6 weeks following viral injection confirmed that the injection site was centered in the preBötC and depicted the cholinergic transmission map. Because of the Cre-dependent expression, the number of the AAVs retrogradely labeled neurons was much smaller than the number of neurons labelled by the HSV. Additionally, most retrogradely labeled neurons were distributed in the ipsilateral side to the injection and occasionally in the contralateral side, while most of the GFP/mCherry expressing neurons displayed strong ChAT signal. However, we observed a limited fractions of mCherry+/GFP+ neurons expressing light and occasionally no detectable ChAT signals.

Overall, we identified dense labeled ChAT+ neurons in the NA and LPGi in all 11 cases. There were fewer labeled cholinergic neurons in the RTN (n=6 mice), the dorsal part of 7N (n=7 mice), the reticular formation (n=10 mice), the NTS (n=9 mice), the dorsal marginal layer of medulla (n=8 mice), and the Pr (n=9 mice). In addition, we found sparse cholinergic neurons in the region lateral to the rostral VRG (n=7 mice), the Ve (n=7 mice), the para12N (n=6 mice), the Rob (n=6 mice), and the regions around 5TT/m5 (n=10 mice).

Furthermore, we occasionally (n<5 out of 11 mice) identified several cholinergic neurons in the 5N (n=1 mice), the 6N (n=1 mice), the 12N (n=1 mice), the PPT (n=1 mice), the LDT (n=3 mice), the SubCV (n=4 mice), and the pFRG (n=1 mice). These results are summarized in the table 4.3 and figures below.

Table 4. 3 Brainstem regions with retrogradely labeled cholinergic neurons.

	Average Neuronal Density	**AAV-mCherry (n=4 mice)**	**AAV-hSyn (n=4 mice)**	**AAV9 (n=3 mice)**	**Total (n=11 mice)**
Medulla					
NA	+++	4/4	4/4	3/3	11/11
LPGi	+++	4/4	4/4	3/3	11/11
lateral to rostral VRG	+	3/4	3/4	1/3	7/11
RTN/pFv	++	2/4	2/4	2/3	6/11
pFRG	+	0/4	1/4	0/3	1/11
7N (dorsal part)	++	0/4	4/4	3/3	7/11
reticular formation	++	4/4	3/4	3/3	10/11
NTS	++	4/4	2/4	3/3	9/11
Ve	+	2/4	3/4	2/3	7/11
medulla dorsal marginal layer	++	3/4	3/4	2/3	8/11
Pr	++	4/4	4/4	1/3	9/11
para12N	+	2/4	2/4	2/3	6/11
Rob	+	3/4	2/4	1/3	6/11

Pons					
LDT	+	0/4	2/4	1/3	3/11
PPT	+	0/4	1/4	0/3	1/11
around 5TT/m5	+	3/4	4/4	3/3	10/11
Sub CV	+	0/4	3/4	1/3	4/11
5N	+	0/4	1/4	0/3	1/11
6N	+	0/4	1/4	0/3	1/11
12N	+	0/4	0/4	1/3	1/11

Initially, we injected the pAAV-EF1a-double floxed-hChR2(H134R)-mCherry-WPRE-HGHpA (AAV2-retro-EF1a-DIO-mCherry)(Lazaridis et al., 2019) into the right preBötC (n=4 mice). The injections were centered and mostly limited to the preBötC (Figure 4.9). Surprisingly, we identified no direct input from PPT and LDT to the preBötC with this viral approach. However, we found a fair number of double labeled (GFP+/ChAT+) neurons in LPGi (n=4 mice), NA (n=4 mice), IRt (n=4 mice), and NTS (n=4 mice) in all mice that were correctly injected into the preBotC and analyzed. Additionally, we identified fewer labelled cholinergic neurons in the Pr (n=4 mice) and the contiguous dorsal marginal layer (n=3 mice). Sometimes, sparse cholinergic neurons were labeled in the region lateral to the rostral VRG (especially at the level of preBötC and BötC) (n=3 mice), in the parafacial region (n=2 mice), in the Ve (n=2 mice), in the Rob (n=3 mice), and in the para12N (n=3 mice) (Figure 4.10). In addition, we identified only a small number of labelled cholinergic neurons in the pons (n=3 mice), mainly in the middle lateral area. In most cases (n=3 mice), these neurons were in the middle and dorsal to the m5/5TT at the level just rostral to the end of 5N, and at the level of caudal PPT. We found few labelled cholinergic neurons in para5N only in 1 mouse (Figure 4.10).

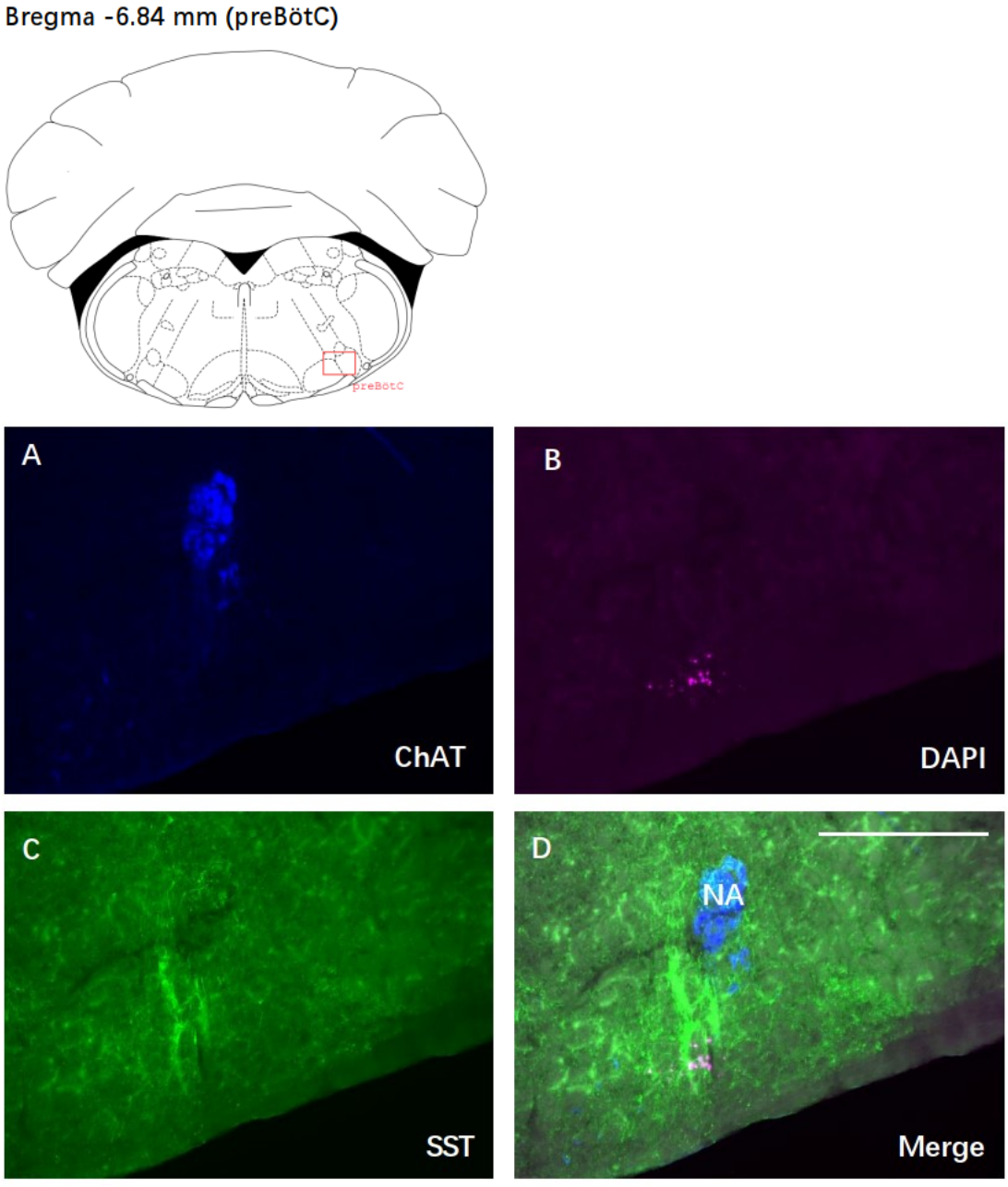

Figure 4. 9 | Stereotaxic injection of AAV2-retro-EF1a-DIO-mCherry into the right preBötC of the ChAT-Cre mouse.

Immunofluorescence staining of brain sections at the level of preBötC following infection with AAV2-retro-EF1a-DIO-mCherry and fluorobeads. Blue-ChAT (A); Purple-DAPI (B); Green-SST (C), and the merged image (D). Scale bar=400μm.

Bregma -6.84 mm (preBötC)

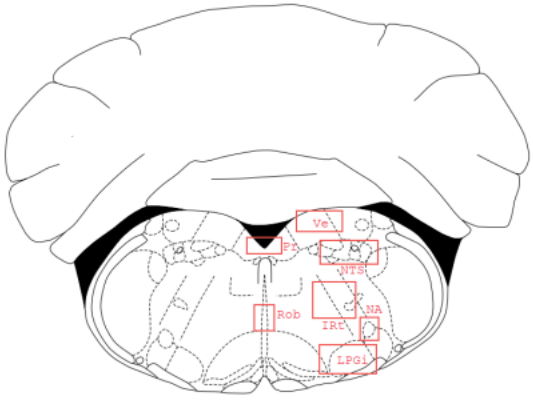

Bregma -6.36 mm

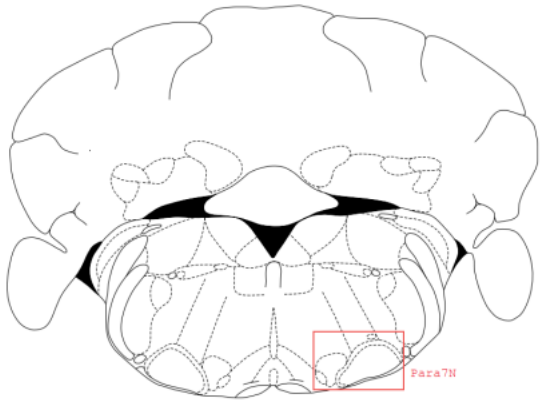

Bregma -5.02 mm

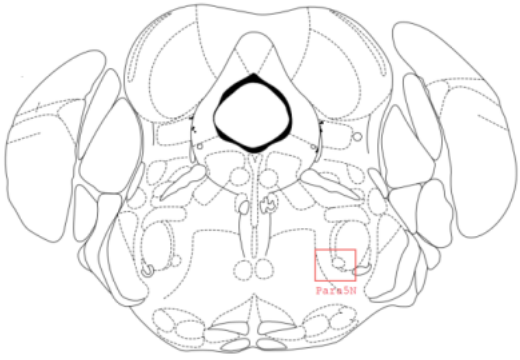

Bregma -4.84 mm

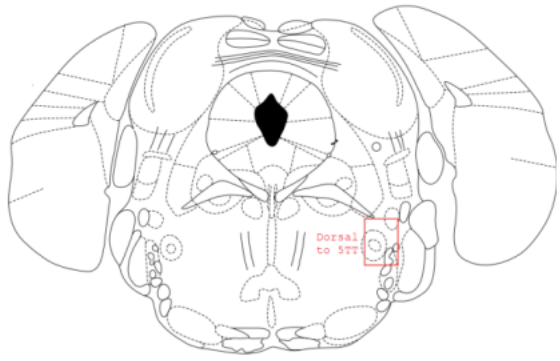

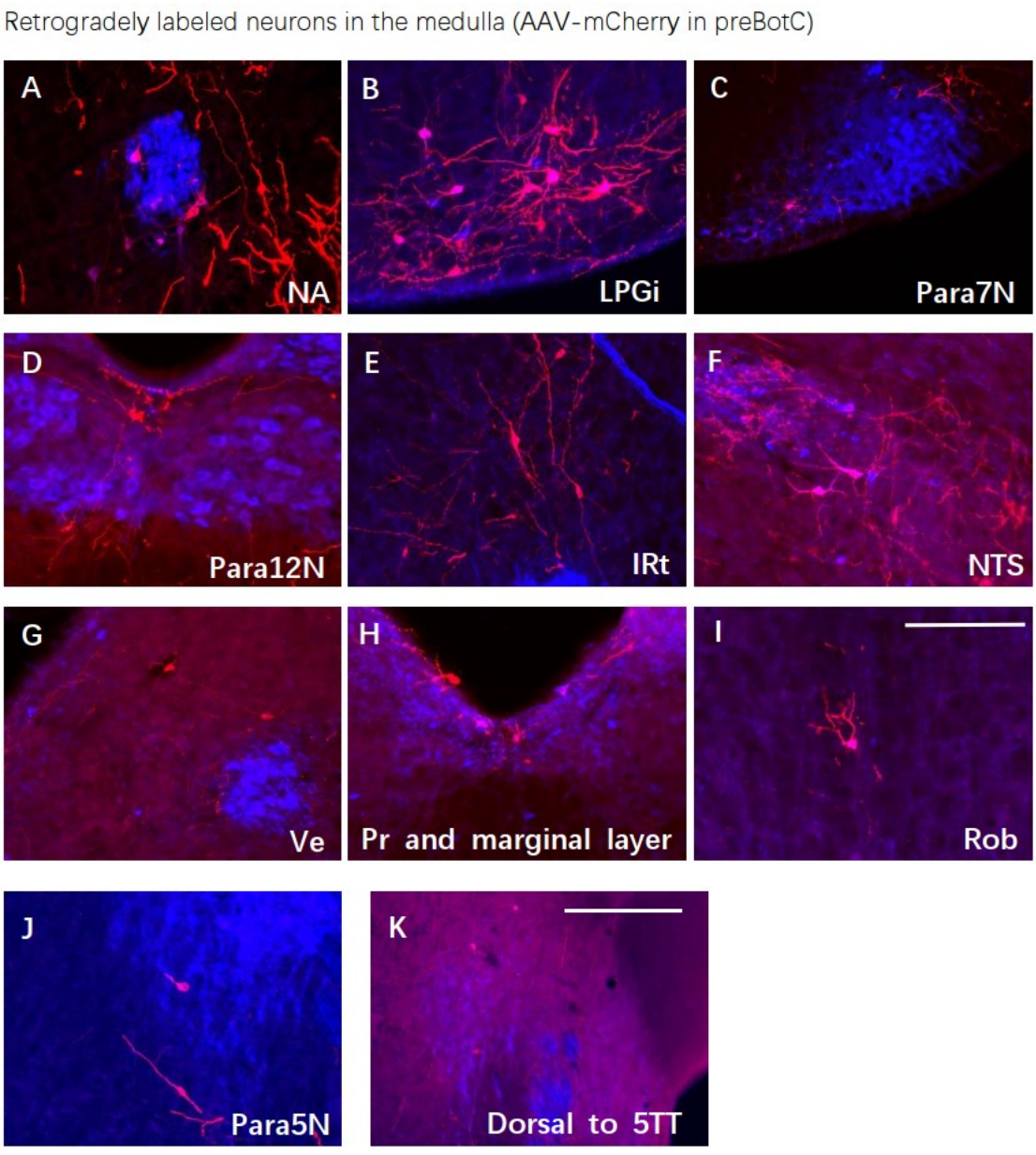

Figure 4. 10 | Retrogradely labeled neurons in brainstem (AAV2-retro-EF1a-DIO-mCherry).

In medulla, we found labeled cholinergic neurons in the NA (A), LPGi (B), para7N (C), para12N (D), IRt (E), NTS (F), Ve (G), Pr and dorsal marginal layer of medulla (H), and Rob (I). In pons, we found labeled cholinergic neurons in the para5N (J), and the regions around 5TT/m5 (K). Blue-ChAT; Red-mCherry. Panel C, K scale bar=400μm (in panel K); Rest scale bar=200μm (in panel I).

Based on the location of the most strongly retrogradely labeled cholinergic neurons, we analyzed neurons in the regions of the NA and the LPGi. These results were obtained from ten 50μm thick brain sections (200μm interval) collected rostrocaudally from Bregma-7.68 mm to Bregma-6.68, in 4 mice (Table 4.4). Among the 6 level, the most rostral level represents the number of neurons at the BötC level, and the two levels before represent that at the preBötC level. Overall, 89.02% of labeled neurons in the LPGi express ChAT signals, and 96.36% of the labeled neurons in the NA are ChAT+ (Table 4.4). Their rostrocaudal distribution is illustrated in figure 4.11.

Table 4. 4 AAV2-retro-EF1a-DIO-mCherry retrogradely labeled neurons in LPGi and NA

AAV-mCherry	**NA-Labeled neurons #**			**LPGi-Labeled neurons #**		
Animal #	GFP+	GFP+/ChAT+	Percentage	GFP+	GFP+/ChAT+	Percentage
mCherry-0306-5	6	6	100.00%	10	7	70.00%
mCherry-0417-1	15	14	93.33%	25	24	96.00%
mCherry-0417-5	12	11	91.67%	31	29	93.55%
mCherry-0417-6	22	22	100.00%	16	13	81.25%
Average	13.75	13.25	96.25%	20.5	18.25	85.20%
Total	55	53	96.36%	82	73	89.02%

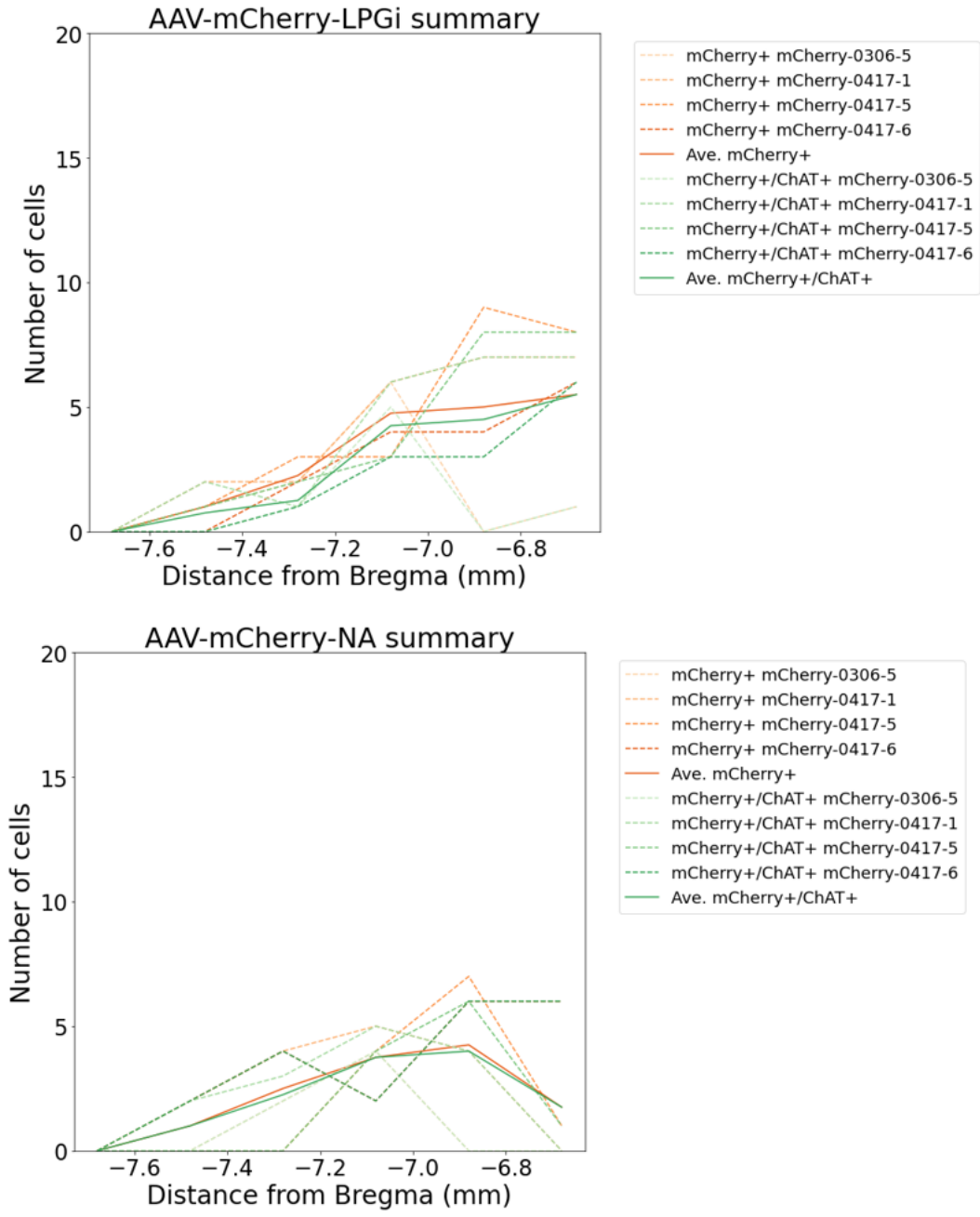

Figure 4. 11 | The distribution of AAV2-retro-EF1a-DIO-mCherry retrogradely labeled cholinergic neurons in the LPGi and NA.

The line graphs illustrate the distribution of labeled (mCherry+) neurons and the colabeled cholinergic (mCherry+/ChAT+) neurons in the LPGi and the NA along rostral caudal axis. The solid line represents the average data, and the dash lines represent the data of individual mice. The yellow lines represent the mCherry+ neurons, while the green lines

represent the mCherry+/ChAT+ neurons.

Because of the unexpected lack of expression of the reporter protein (mCherry) in the PPT and the LDT, we tested additional viruses with retrograde properties: the pAAV-hSyn-DIO-EGFP(Bittar et al., 2021; Krishnan et al., 2017; Okunomiya et al., 2020) (AAV2-retro-hSyn-DIO-EGFP) with a different promoter (human synapsin), and the AAV9-EF1a-DIO-EYFP which has a different AAV serotype with known retrograde properties (Chokshi et al., 2019; D. Wang et al., 2015).

The AAV2-retro-hSyn-DIO-EGFP was injected into the right preBötC of four ChAT-Cre mice (Figure 4.12), and labeled cholinergic neurons were identified in the LPGi (n=4 mice) and the pF_V region (n=2 mice), in the compact NA (n=4 mice) in the BötC, in the NTS (n=2 mice), and in the IRt (n=3 mice), similar to the original Cre-dependent virus used. Likewise, we identified fewer labeled cholinergic neurons lateral to the BötC (n=3 mice), the Ve (n=3 mice), the Pr (n=4 mice), the dorsal marginal layer (n=3 mice), and the Rob (n=2 mice). In addition, we identified labeled ChAT+ neurons in the caudal 7N (n=4 mice), and occasionally in the pFRG (n=1 mice). Compared to the number of labeled neurons in medulla, we observed fewer GFP+ neurons in the pons, most of which only expressed weak ChAT signal and sometimes lacked detectable ChAT expression. Neurons were observed in the region surrounding m5/5TT (n=4 mice) at the level of rostral end of 5N, most of them are ChAT- (n=2 mice). Additionally, there were several labeled ChAT+ neurons in P5 (n=2 mice) and SubCV (n=2 mice) (Figure 4.13)

Interestingly, we found only one or two GFP+/ChAT+ neurons in the LDT (n=2 mice), and some non-cholinergic neurons labelled in the DMTg region below the LDT (n=4 mice). Sporadically, we identified labeled cholinergic motor neurons in PPT, 6N and 5N in only 1 mouse (Figure 4.13).

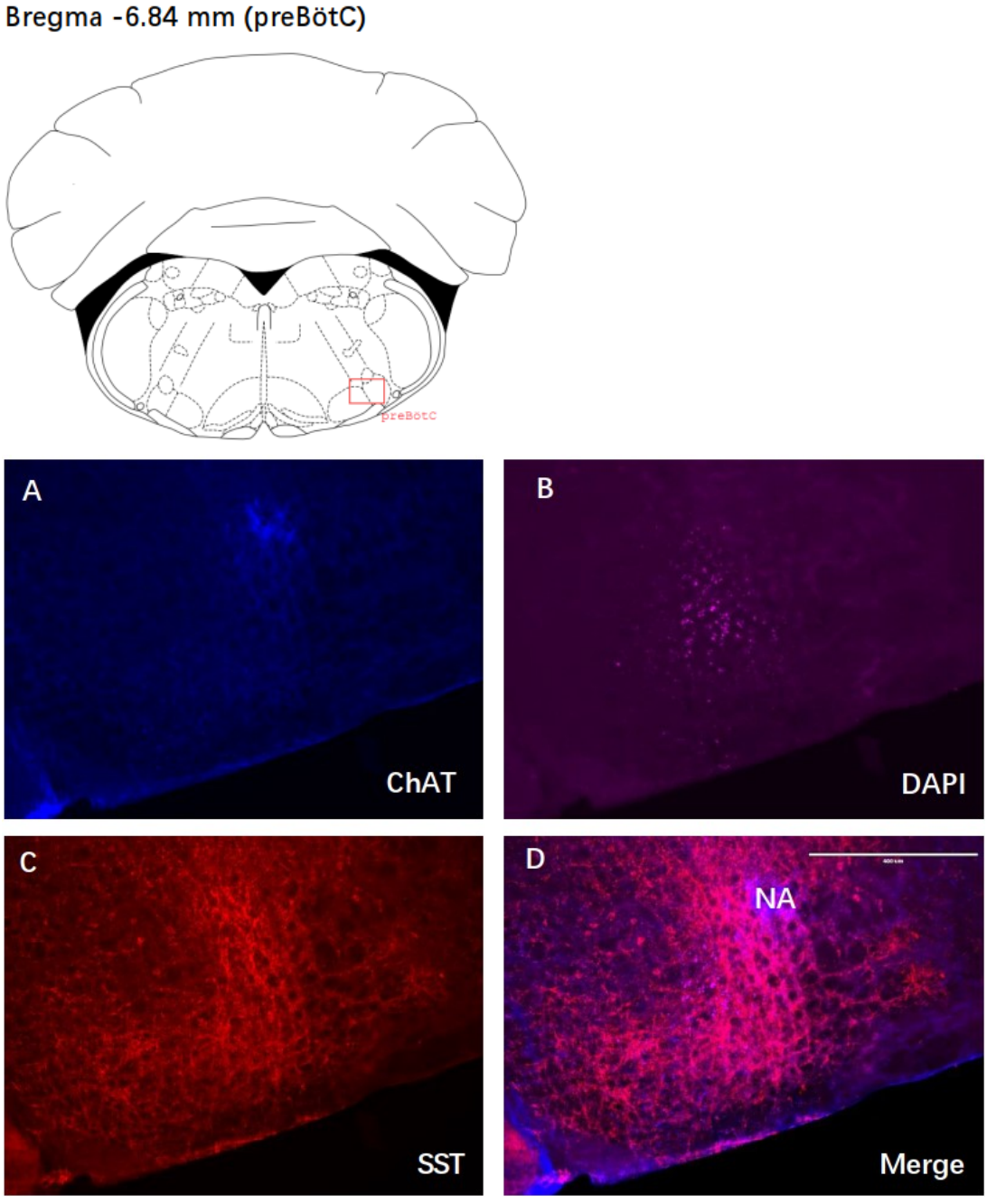

Figure 4. 12 | The injection site in one of the mice used with AAV2-retro-hSyn-DIO-EGFP.

The Immunofluorescence staining images of brain sections show the right preBötC, identified by SST staining (red) and the injection site, labelled with fluorobeads (purple). Blue-ChAT (A); Purple-DAPI (B); Red-SST (C), and the merged image (D). Scale

bar=400μm.

Bregma -6.84 mm (preBötC)

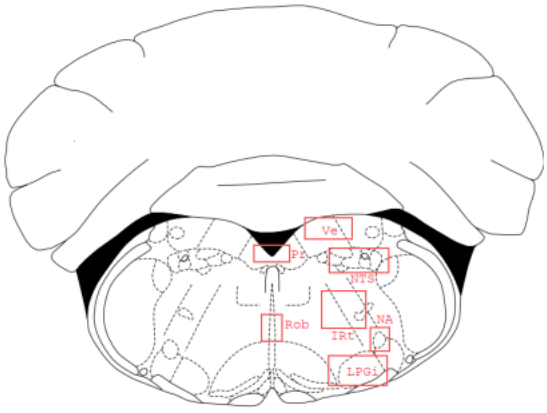

Bregma -6.36 mm

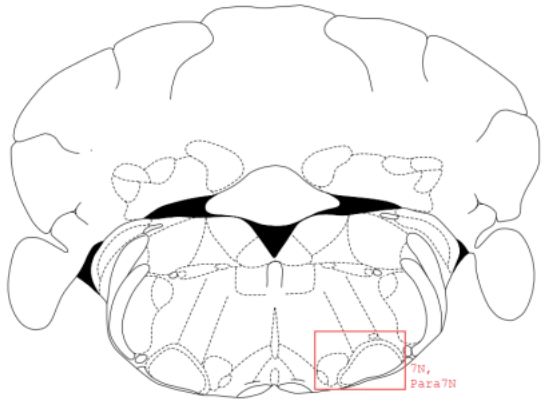

Bregma -5.80 mm

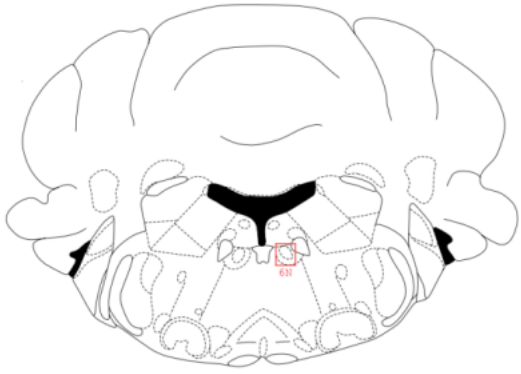

Bregma -5.02 mm

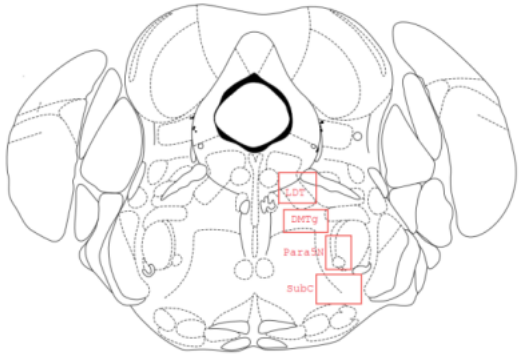

Bregma -4.84 mm

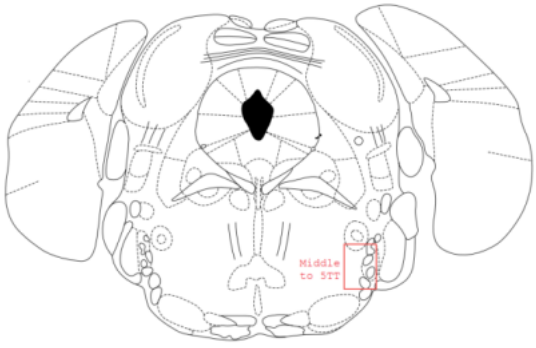

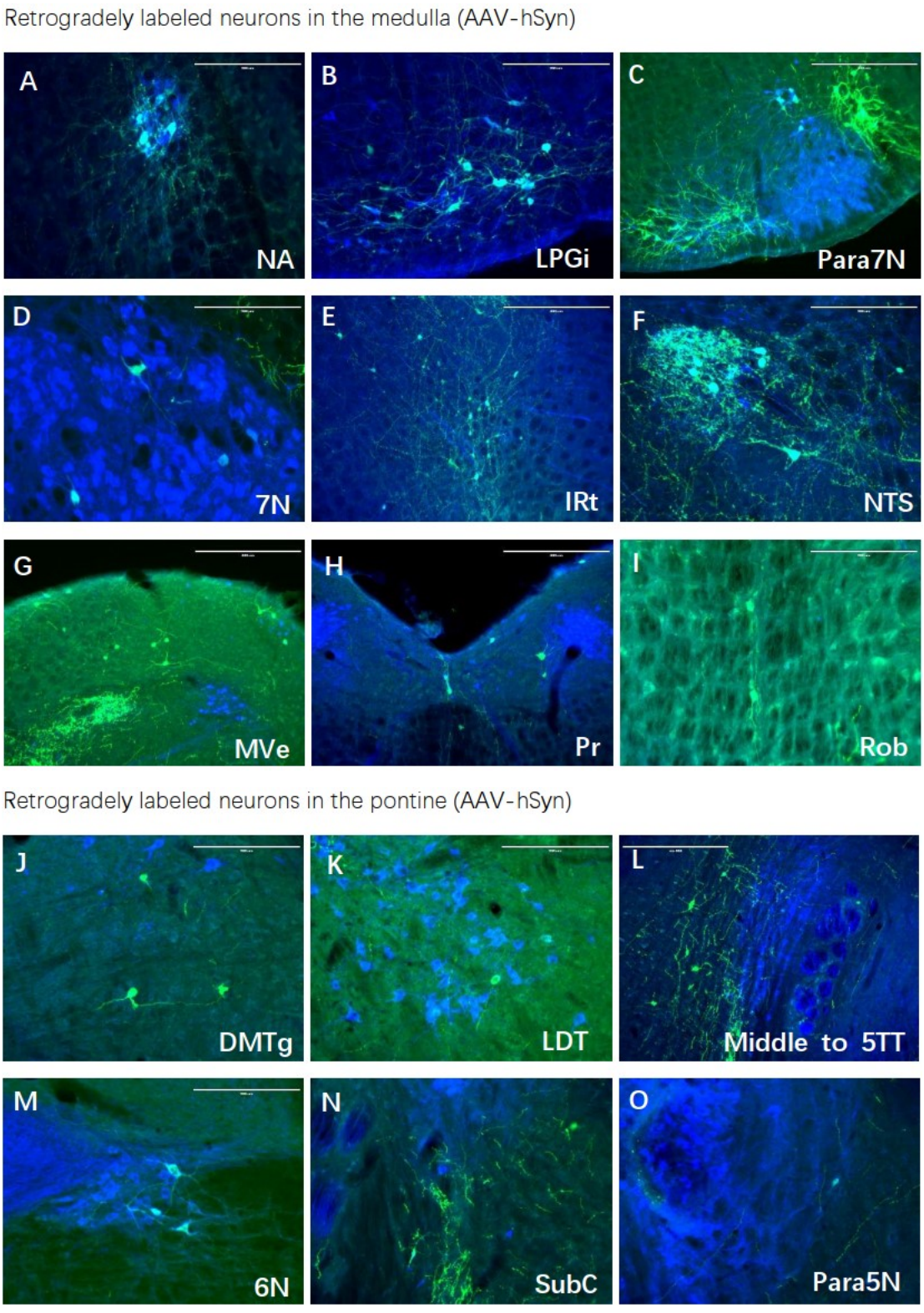

Figure 4. 13 | Retrogradely labeled neurons in brainstem (AAV-retro-hSyn-DIO-EGFP).

In medulla, we found labeled cholinergic neurons in the NA (A), LPGi (B), para7N (C), 7N (D), reticular formation (E), NTS (F), MVe (G), Pr and dorsal marginal layer of medulla (H), and Rob (I). In the pons, we found labeled neurons in the DMTg (ChAT-) (J), the LDT (K), the regions around 5TT/m5 (L), 6N (M), Sub C (N) and para5N (O). Blue-ChAT; Green-GFP. Panel C, E, G, H, L, O scale bar=400μm; Rest scale bar=200μm.

Likewise, we analyzed the distribution of labeled cholinergic neurons in the LPGi and NA of the mice which received AAV-retro-hSyn-DIO-EGFP (Table 4.5; Figure 4.14). Overall, 83.44% and 95.18% of labeled neurons are ChAT+ in the LPGi and in the NA, respectively. Overall, the AAV2-retro-hSyn-DIO-EGFP virus labeled more neurons in the LPGi than the AAV2-retro-EF1a-DIO-mCherry, with a similar rostrocaudal distribution.

Table 4. 5 AAV2-retro-hSyn-DIO-EGFP retrogradely labeled neurons in LPGi and NA

AAV-hSyn	**NA (number of neurons)**			**LPGi (number of neurons)**		
name	GFP+	GFP+/ChAT+	Percentage	GFP+	GFP+/ChAT+	Percentage
hSyn0304-1	24	22	91.67%	12	9	75.00%
hSyn0719-1	45	44	97.78%	77	64	83.12%
hSyn0806-2	6	6	100.00%	15	11	73.33%
hSyn1211-3	8	7	87.50%	47	42	89.36%
Average	20.75	19.75	94.24%	37.75	31.5	80.20%
Total	83	79	95.18%	151	126	83.44%

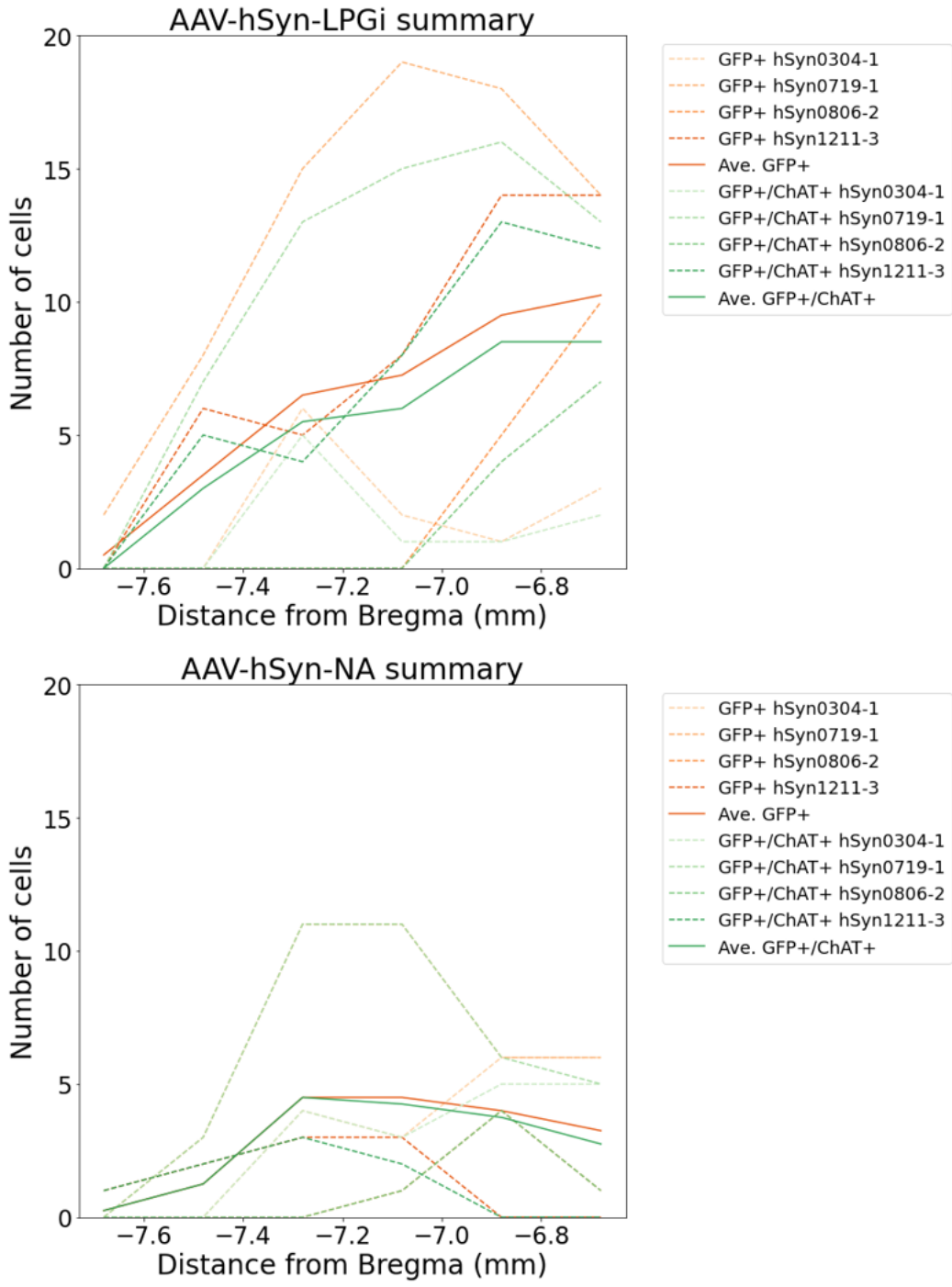

Figure 4. 14 | The graphs illustrate distribution of AAV-retro-hSyn-DIO-EGFP retrogradely labeled cholinergic neurons in the LPGi and NA.

The line graphs demonstrate the distribution of labeled (GFP+) neurons and the labeled cholinergic (GFP+/ChAT+) neurons in the LPGi and the NA along rostral caudal axis. The

solid line represents the average data, and the dash lines represent the data of individual mice. The yellow lines represent the GFP+ neurons, while the green lines represent the GFP+/ChAT+ neurons.

In order to determine whether the lack of GFP/mCherry expression in cholinergic neurons was due to the inability of the viruses used (AAV2-retro stereotype) to infect cholinergic neurons, we verified the results with a different viral serotype that may present a different tropism (AAV9 serotype, pAAV-EF1a-double floxed-hChR2(H134R)-EYFP-WPRE-HGHpA; AAV9-EF1a-DIO-EYFP) as well (n=3 mice) (Figure 4.15). In this case, we barely identified direct cholinergic input from the PPT (n=0 mice) and the LDT (n=1 mice) to the preBötC. Instead, we found the majority of double labeled (GFP+/ChAT+) neurons again in the LPGi (n=3 mice), the NA (n=3 mice), the IRt (n=3 mice), and the NTS (n=3 mice). Some cholinergic neurons in the RTN/pFv (n=2 mice) and dorsal part of 7N (n=3 mice) were also labelled. In addition, we observed sparse labelled cholinergic neurons in the rostral para12N (n=2 mice), the caudal Pr (n=1 mice), the dorsal marginal layer (n=2 mice), the region lateral to the VRG (n=1 mice), the Ve (n=2 mice), and the Rob (n=1 mice) (Figure 4.16). In the pons, we identified few labelled cholinergic neurons in the region dorsal to 5TT (n=3 mice) at the level of caudal PPT. In one case, we identified one or two GFP+/ChAT+ neurons in the para5N (n=1 mice) and SubC (n=1 mice) as well (Figure 4.16).

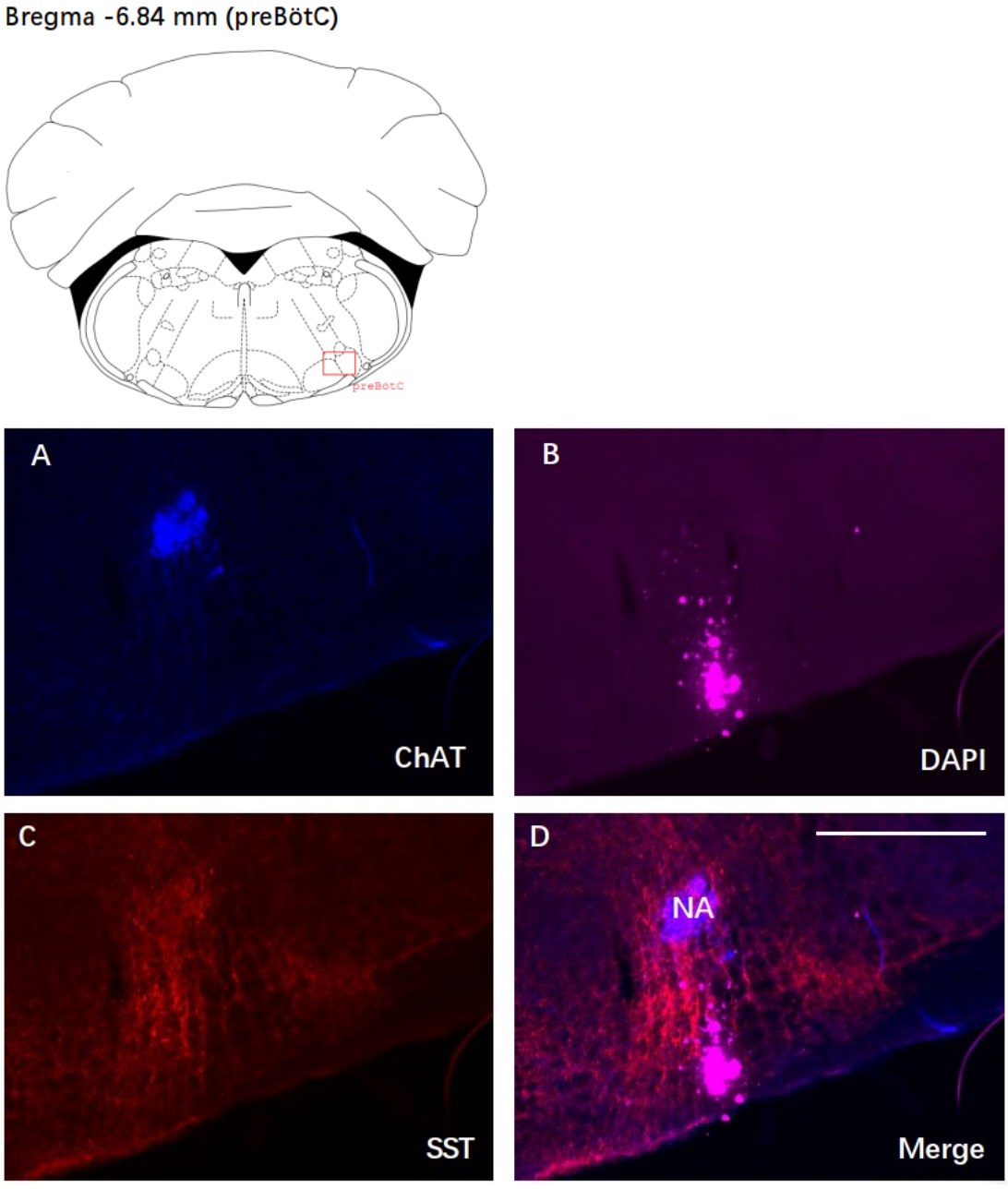

Figure 4. 15 | The injection site of AAV9-EF1a-DIO-EYFP.

The Immunofluorescence staining images of brain sections show the right preBötC, identified by SST staining (red) and the injection site, labelled with fluorobeads (purple). Blue-ChAT (A); Purple-DAPI (B); Red-SST (C), and the merged image (D). Scale bar=400μm.

Bregma -6.84 mm (preBötC)

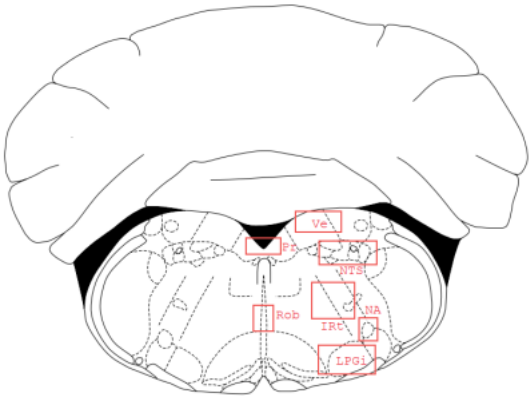

Bregma -6.64 mm (BötC)

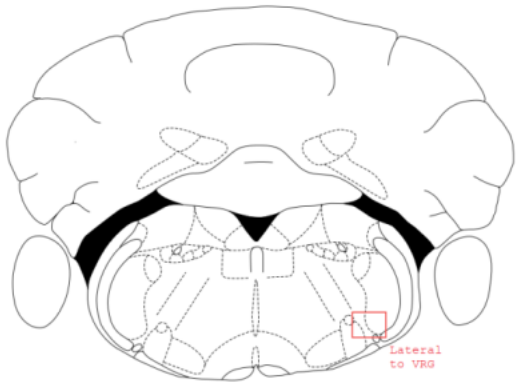

Bregma -6.36 mm

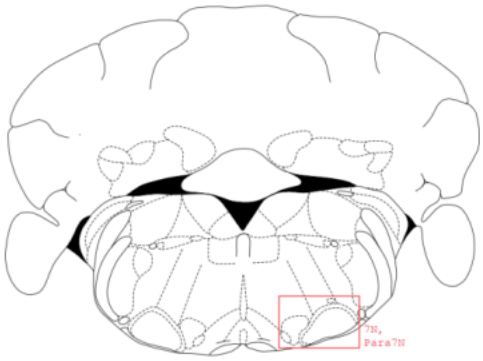

Bregma -5.02 mm

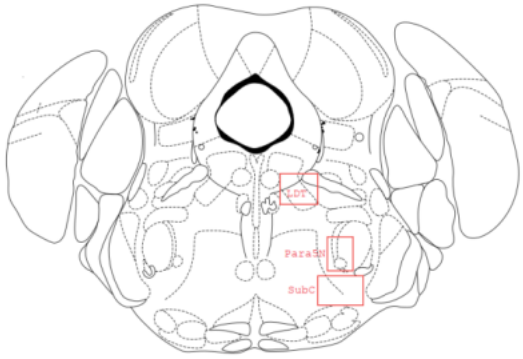

Bregma -4.84 mm

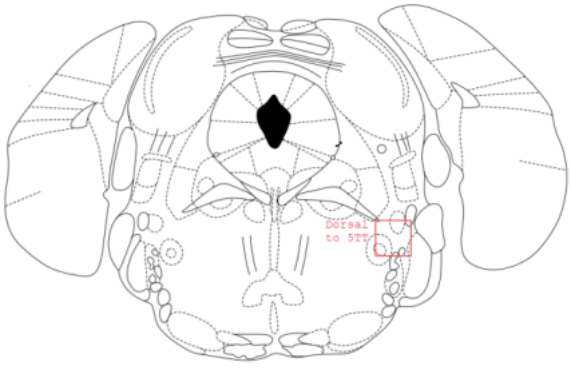

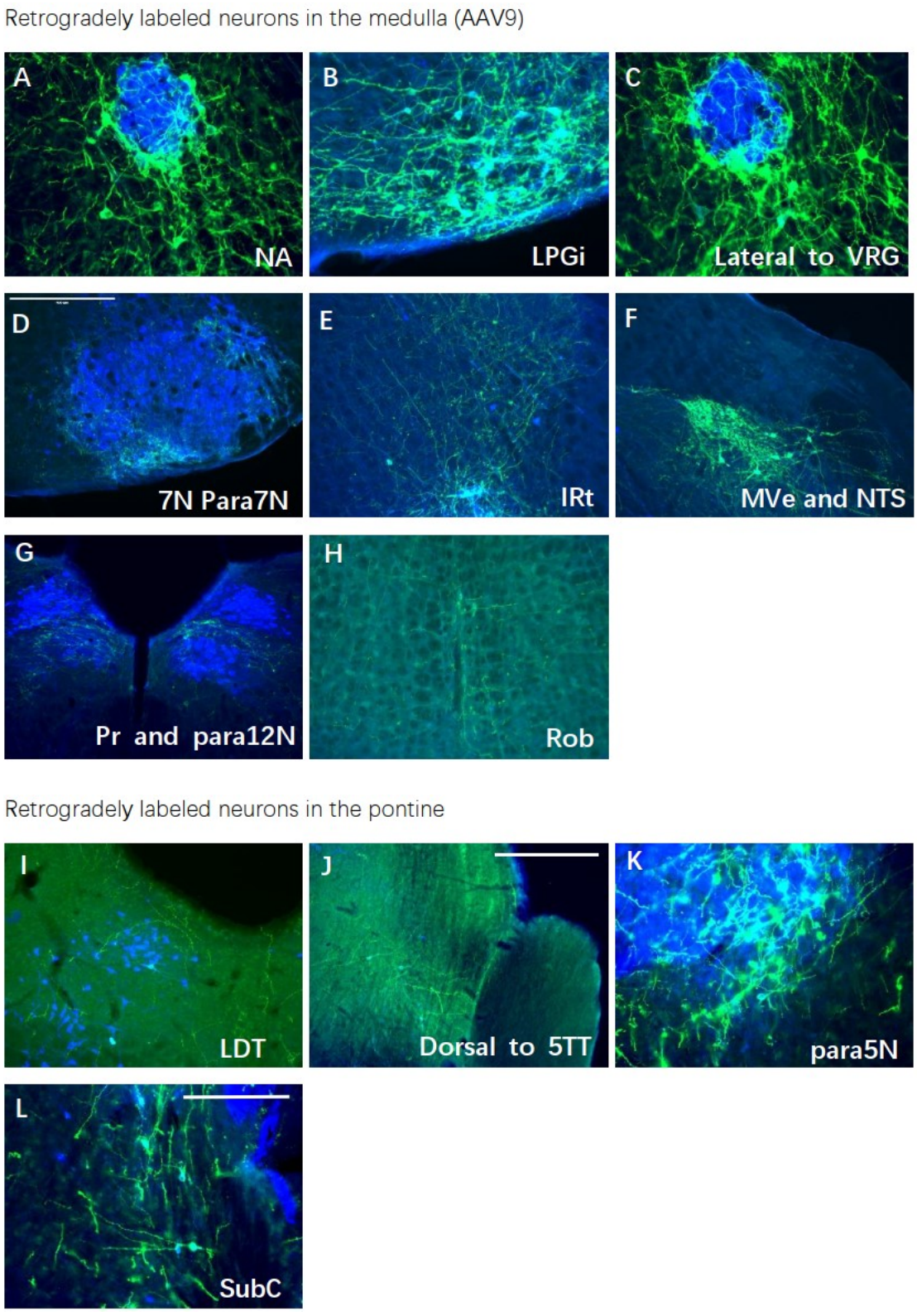

Figure 4. 16 | Retrogradely labeled neurons in brainstem (AAV9-EF1a-DIO-EYFP).

In medulla, cholinergic neurons were identified in the NA (A), LPGi (B), in the region lateral to VRG (C), 7N and para7N (D), reticular formation (E), NTS and MVe (F), Pr and para12N (G), and Rob (H). In pons, labeled cholinergic neurons were observed in the LDT (I), the regions around 5TT (J), para5N (K), Sub C (L). Blue-ChAT; Green-GFP. Panel D-J scale bar=400μm (in panel J); Rest scale bar=200μm (in panel L).

Again, we analyzed the distribution of labeled cholinergic neurons in the LPGi and NA which received AAV9-EF1a-DIO-EYFP (Table 4.6). Overall, 73.74% of labeled neurons in the LPGi expressed ChAT signals, and 90.10% of the labeled neurons in NA were ChAT+. As shown in the line graph (Figure 4.17), the labeled neurons in the LPGi had similar rostrocaudal distribution as the previous virus used.

Table 4. 6 AAV9-EF1a-DIO-EYFP retrogradely labeled neurons in LPGi and NA

AAV9	**NA**			**LPGi**		
	GFP+	GFP+/ChAT+	Percentage	GFP+	GFP+/ChAT+	Percentage
AAV9-1008-1	42	39	92.86%	44	35	79.55%
AAV9-0904-3	25	24	96.00%	19	12	63.16%
AAV9-0904-2	34	28	82.35%	36	26	72.22%
Average	33.67	30.33	90.40%	33	24.33	71.64%
Total	101	91	90.10%	99	73	73.74%

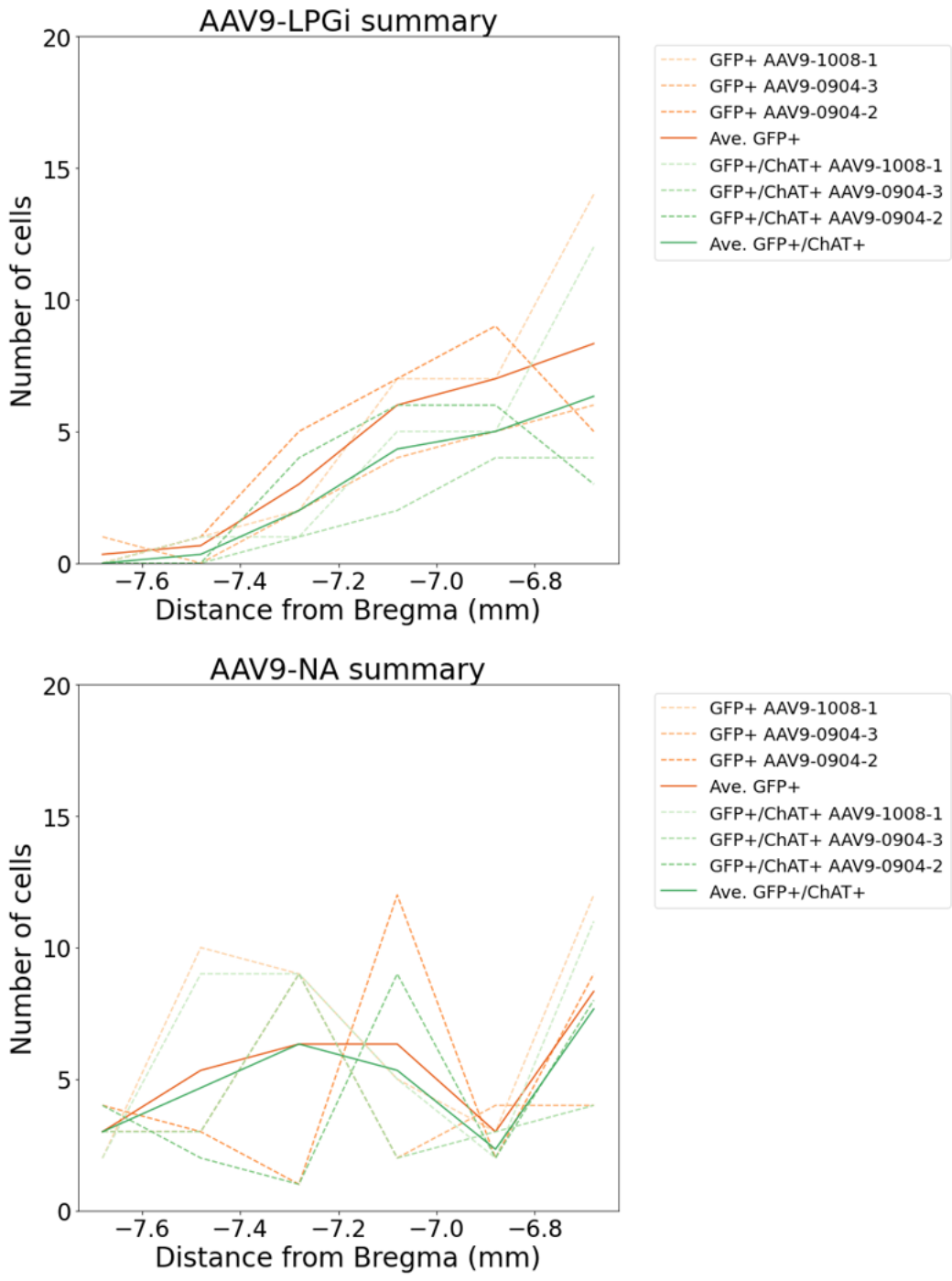

Figure 4. 17 | The distribution of AAV9-EF1a-DIO-EYFP retrogradely labeled cholinergic neurons in the LPGi and NA.

The line graphs illustrate the distribution of labeled (GFP+, orange) neurons and the labeled cholinergic (GFP+/ChAT+, green) neurons in the LPGi and the NA along rostral

caudal axis. The solid line represents the average data, and the dash lines represent the data of individual mice.

4.5 Cre dependent anterograde tracing

Because we identified scarcely any cholinergic inputs from PPT/LDT to the preBötC with the retrograde tracing approaches, we chose to use anterograde tracers to verify the retrograde results. Primarily, we used the Cre-dependent anterograde virus rAAV2/Ef1a-DIO-hchR2(H134R)-EYFP (rAAV2-EF1a-DIO-EYFP) together with the ChAT-Cre mice to determine the neuronal projections of cholinergic neurons from the PPT/LDT to the preBötC.

Recombinant AAV2-EF1a-DIO-EYFP virus was injected either unilaterally (n=6 mice) or bilaterally into the PPT and LDT (n=4 mice). Afterwards, we performed the immunofluorescence staining and analyzed the results in 50 μm thick sections (200 μm interval, Figure 4.18). By definition, the PPT/LDT is depicted by a continuum of cholinergic neurons starting from the substantia nigra pars reticulate (SNR) and end at the lateral central gray matter in the periventricular area(Mena-Segovia, 2016). Because there is no definite separation between PPT and LDT(Mena-Segovia, 2016), for the convenience of data analysis, we define the cholinergic neurons rostral to Bregma-4.9mm as the PPT neurons, and the caudal cholinergic groups as to LDT based on their relative position along the rostra-caudal axis (Paxinos mouse brain atlas)(Franklin et al., 2008).

A

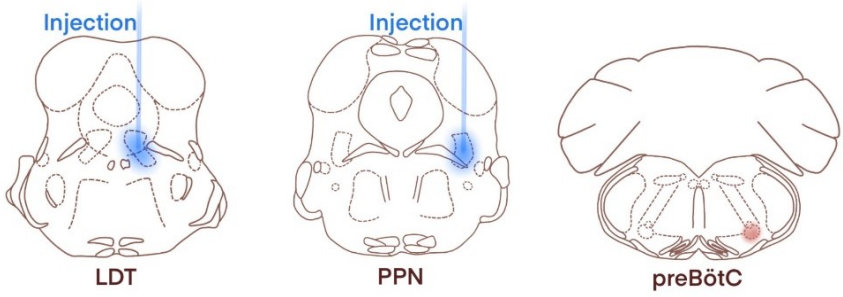

B LDT **C** PPT

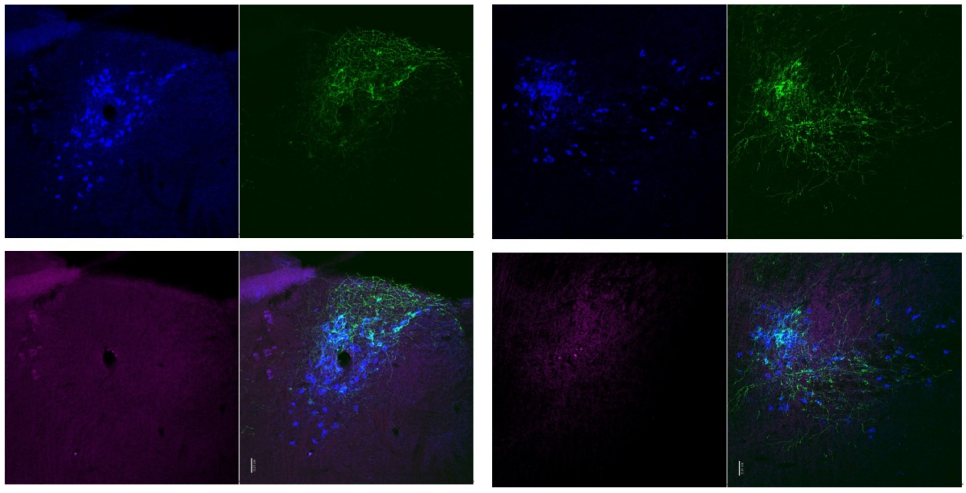

Figure 4. 18 | Anterograde tracing with rAAV2-EF1a-DIO-EYFP.

The schematic shows the anterograde tracing approach (A). The Immunofluorescence staining images show the LDT (B) and the PPT (C) as well as the injection site labelled with purple fluorospheres. Blue-ChAT; Purple-DAPI; Green-EGFP. Left-lateral; Right-middle; Up-dorsal; Down-ventral. Scale bar=100μm (left corner).

In all cases (n=10 mice), the virus successfully labeled cholinergic neurons in the PPT and LDT, whereas few (17.40%) labeled neurons display undetectable ChAT signals. (Table 4.7, 4.8). Because our injection volume was limited to reduce spread to other areas, the overall infection rate was low, from 6.21% to 16.10% (unilateral), and 7.04% to 21.21% (bilateral) of the total number of cholinergic cells. The distribution of the cholinergic neurons, labeled neurons and labelled cholinergic neurons are shown in the line graphs

(Figure 4.19). In some cases, some additional cholinergic neurons in parabigeminal nucleus (PBG) (n=5 mice), trochlear nucleus (4N) and oculomotor nucleus (3N) (n=2 mice), and caudal PB/KF (n=2 mice) were infected.

Table 4. 7 AAV2-EF1a-DIO-EYFP anterogradely labelled neurons in PPT and LDT - Unilateral injections

bilateral injections	ChAT+	GFP+	ChAT+/GFP+	labelled%	double labelled%	labelled fibers in preBötC?
AAV-E2	938	78.00	66	8.32%	7.04%	N
AAV0724	924	238.00	196	25.76%	21.21%	sparse
AAV1028-2	914	164.00	131	17.94%	14.33%	sparse
AAV1028-3	772	95.00	71	12.31%	9.20%	sparse
average	887.00	143.75	116.00	16.08%	12.94%	
Total	3548.00	575.00	464.00	16.21%	13.08%	

Table 4. 8 AAV2-EF1a-DIO-EYFP anterogradely labeled neurons in PPT and LDT - Bilateral injections

unilateral injections (right side)	ChAT+	GFP+	ChAT+/GFP+	labelled%	double labelled%	labelled fibers in preBötC?
AAV0128-3	467	33.00	29	7.07%	6.21%	N
AAV0128-4	405	33.00	32	8.15%	7.90%	only 1 fiber
AAV0128-5	473	55.00	50	11.63%	10.57%	N
rAAV1212-1	539	69.00	52	12.80%	9.65%	sparse
rAAV1212-2	441	83.00	71	18.82%	16.10%	sparse
rAAV1212-3	510	59.00	40	11.57%	7.84%	sparse

Average	472.50	55.33	45.67	11.67%	9.71%	
Total	2835.00	332.00	274.00	11.71%	9.66%	

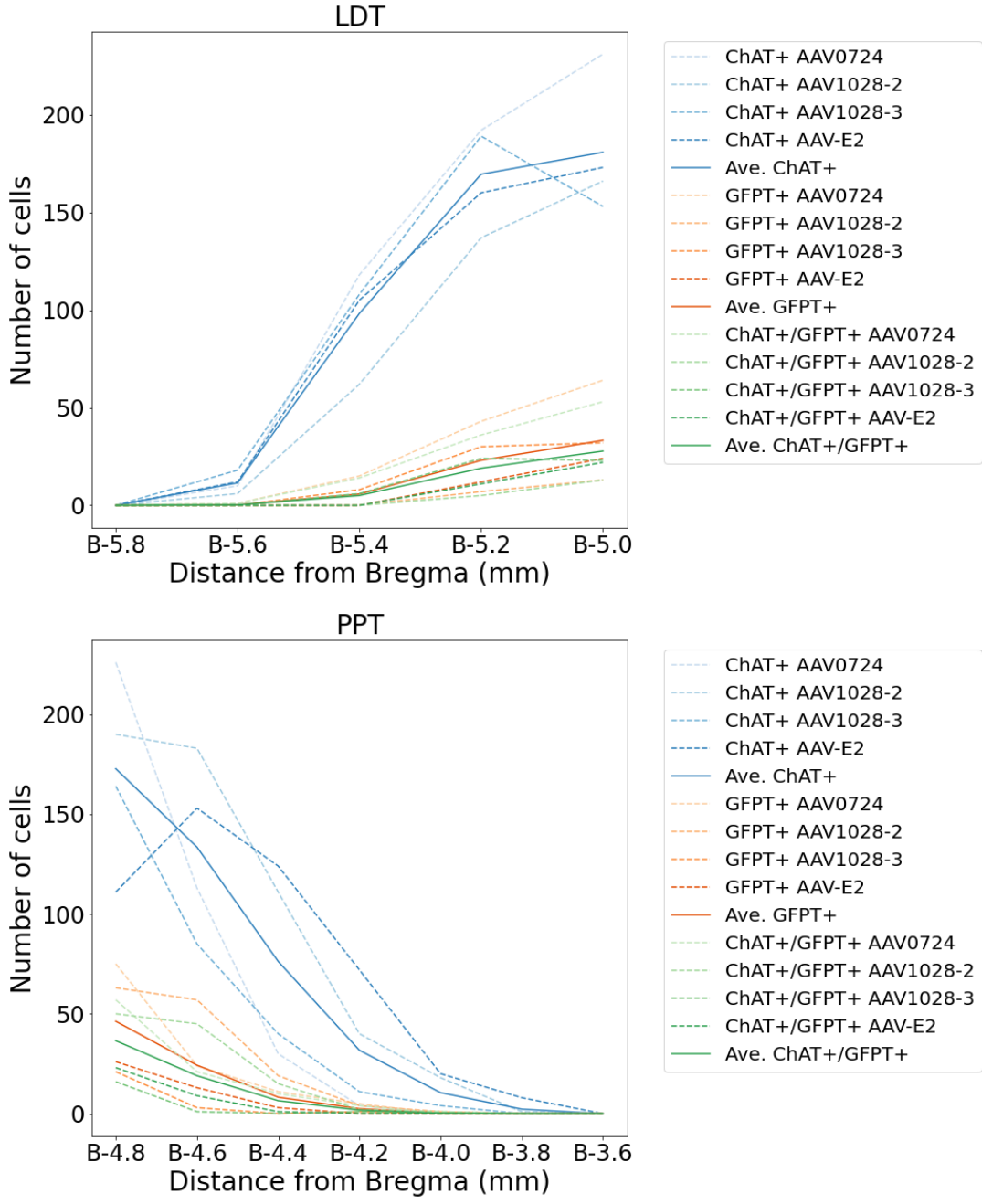

Figure 4. 19 | The distribution of rAAV2-EF1a-DIO-EYFP anterogradely labeled cholinergic neurons in the bilateral LDT and PPT.

The line graphs demonstrate the distribution of cholinergic (ChAT+, blue) neurons, rAAV2-EF1a-DIO-EYFP labeled (GFP+, orange) neurons, and the labeled cholinergic (GFP+/ChAT+, green) neurons in the LDT (A) and the PPT (B) along rostral caudal axis. The solid line represents the average data, and the dash lines represent the data of individual mice.

As reported in the previously literature(Mena-Segovia & Bolam, 2017), we identified labelled cholinergic neuronal axons in medullary reticular formation (most in the IRt) and pontine reticular formation (most in the PnO) (n=10 mice). Which indicates that the AAV2-EF1a-DIO-EYFP is capable to infect the PPT/LDT cholinergic neurons and label their axons which extend as far as caudal medulla. Nevertheless, when we looked at the expression of GFP axons at the level of preBötC, we observed sparse fibers within this area (n=7 mice) (Figure 4.20), confirming limited cholinergic inputs from the PPT and LDT to the preBötC.

A preBötC

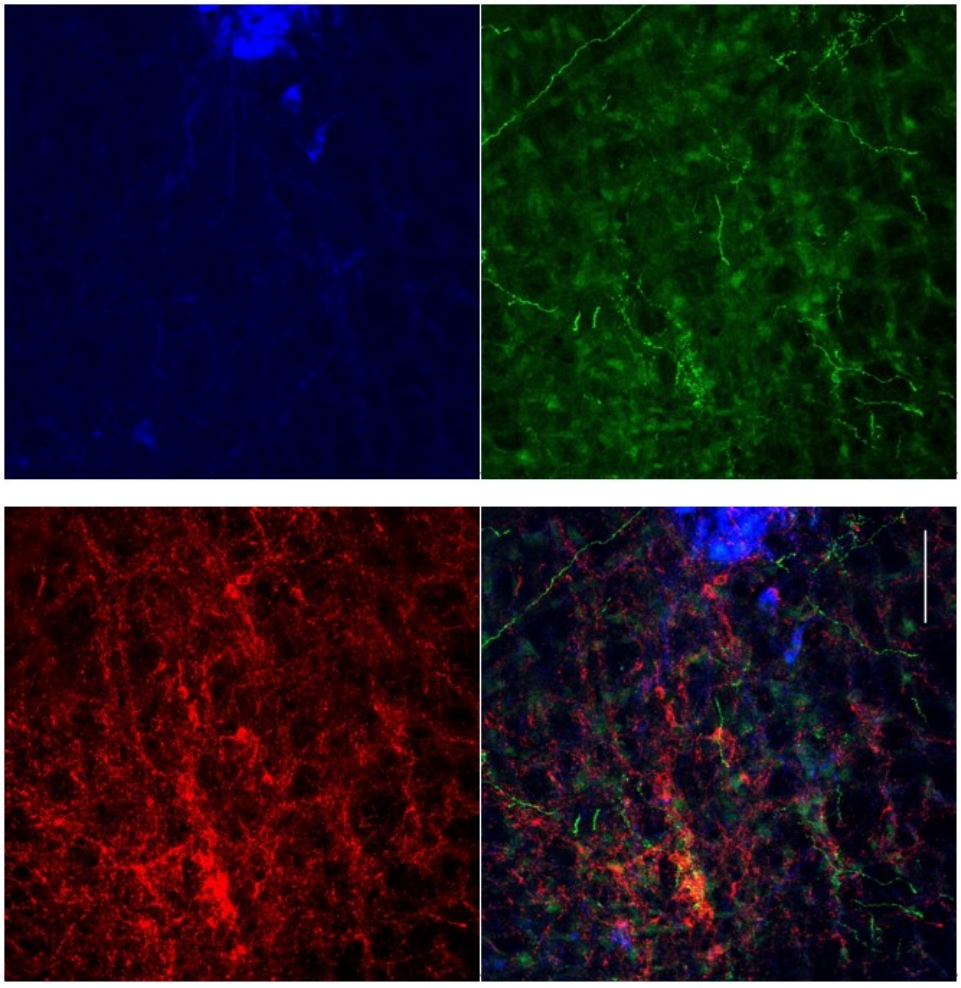

B IRt

C PnO

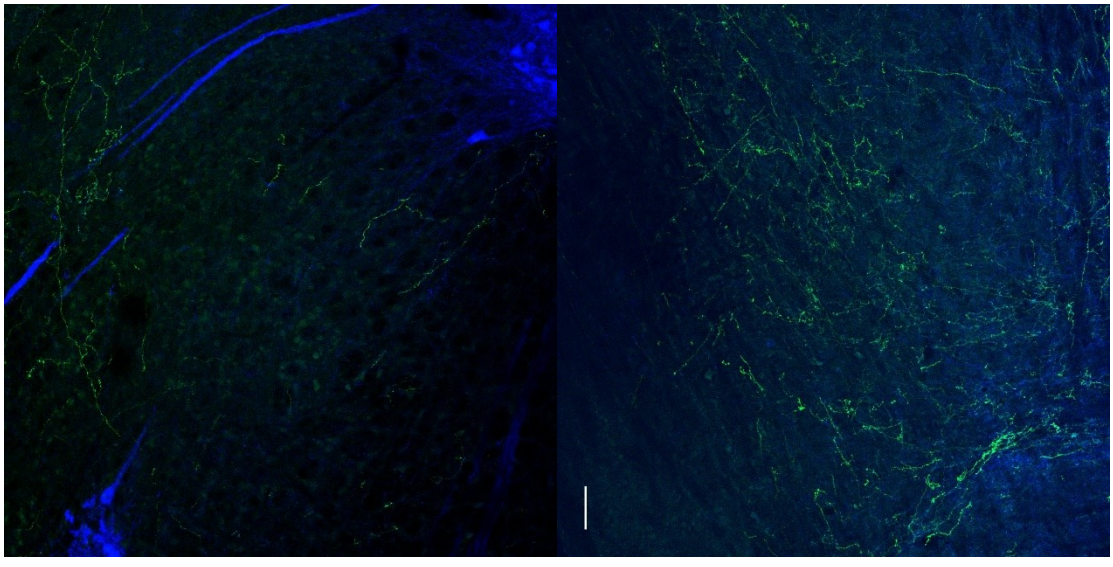

Figure 4. 20 | Retrogradely labeled axons in brainstem (rAAV2-EF1a-DIO-EYFP).

We found sparse EYFP labeled axons in the preBötC (A), IRt (B) and PnO (C). Blue-ChAT; Green-GFP; Red-SST. Scale bar=100μm.

To further verify these projections (or lack thereof), we used additional Cre-dependent anterograde viruses, which included the rAAV2/Ef1a-DIO-hChR2-(E123T/T159C)-p2A-mCherry-WPRE (rAAV2-EF1a-DIO-p2A-mCherry) (n=4 mice), AAV2/hSyn-DIO-mCherry (AAV2-hSyn-DIO-mCherry) (n=2 mice), and rAAV5/Ef1a-DIO-hchR2(H134R)-mCherry (AAV5-EF1a-DIO-mCherry) (n=1 mice) (Table 4.9). We selected these additional viruses with different characteristics because the expression level of reporter protein could depend on factors like the gene itself, the serotype of viral vector, viral titer, methods of application, etc.(Tang et al., 2009). For example, the rAAV2-EF1a-DIO-p2A-mCherry has the p2A sequence that helps to increase the translation and expression efficiency of proteins(Tang et al., 2009), the hSyn (human synapsin) is another promoter which confers highly selective neuron-specific transgene expression(Nieuwenhuis et al., 2021), while the AAV5-EF1a-DIO-mCherry is a different serotype of AAV which has been used to transfect other cholinergic neurons in the ChAT-Cre system(Threlfell et al., 2012).

Similar to the injections with the initial virus, we obtained an infection rate of around 10%~20% in the PPT and LDT and observed a similar pattern of immunofluorescent fibers in the medullary and pontine reticular formation (n=7 mice), and a few to none axons labelled in the preBötC area (Figure 4.21).

Table 4. 9 The tracing results of the additional anterograde AAVs

Virus and injection site	**Animal #**	**labelled cholinergic neurons in PPT/LDT?**	**labelled axons in PnO/IRt?**	**labelled axons in preBötC?**
rAAV2-EF1a-DIO-p2A-mCherry				
-Bilateral PPT&LDT				
	p2A0521-1	Y	Y	sparse
	p2A0521-2	Y	Y	1 axon
-Unilateral PPT&LDT				
	AAV0319-1	Y	Y	N
	AAV0319-2	Y	Y	sparse
AAV2-hSyn-DIO-mCherry				
-Unilateral PPT&LDT				
	AAV0319-3	Y	Y	sparse
	AAV0319-4	Y	Y	1 axon
AAV5-EF1a-DIO-mCherry				
-Bilateral PPT&LDT				
	AAV0630	Y	Y	sparse

A PPT **B** LDT

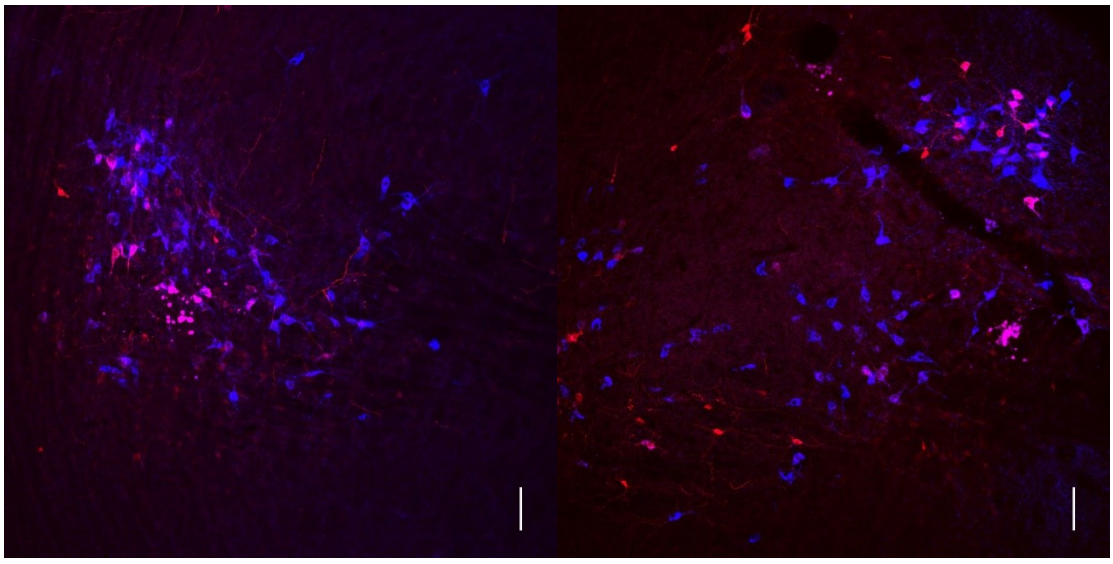

C preBötC

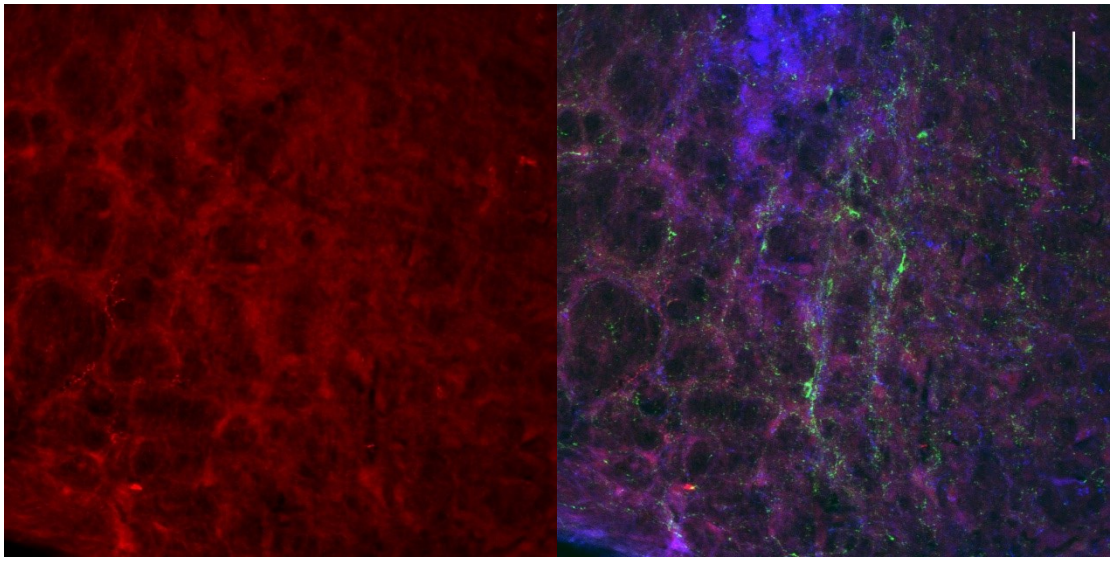

Figure 4. 21 | Anterograde tracing with and retrogradely labeled axons in brainstem (rAAV2-EF1a-DIO-p2A-mCherry).

We found labeled cholinergic neurons in PPT(A) and LDT (B), and labeled axons in preBötC (C, D). Blue-ChAT; Red-mCherry; Green-SST. Scale bar=100μm.

Chapter 5 Discussion

In this MSc thesis project, we investigated the source of cholinergic inputs that may influence the function of the preBötC. We initially mapped the neurons that have a direct projection to the preBötC neurons by using the retrograde virus HSV, independent of their phenotype. We observed HSV-labelled neurons in multiple brainstem structures, consistent with previous reports(Gang et al., 1995; Schwarzacher et al., 1995; Yang et al., 2019), and interestingly, in additional regions.

Based on these results, we further investigated the regions with cholinergic projections to the preBötC neurons with the use of Cre-dependent retrograde AAVs in ChAT-Cre transgenic mice. Finally, we used a Cre-dependent anterograde viral approach to verify whether cholinergic connections exist between the preBötC and the PPT/LDT. Our findings indicate that the cholinergic connections between PPT/LDT and the preBötC are few, and the majority of neurons projecting to the preBötC from PPT/LDT have instead other phenotypes. Our data suggest that the source of cholinergic inputs to the preBötC is instead originating mainly from neighboring regions in the ventral medulla, including the LPGi and NA.

5.1 Technical considerations

The AAV and HSV systems are a powerful tool for the study the neuronal circuits. In our study, we selected a group of AAVs with various serotypes, promoter and reporter proteins because the rate of infection and the expression level of reporter proteins may depend on factors like the gene itself, the serotype of viral vector, etc.(Tang et al., 2009). Thus, trials with different AAVs provided more evidence to support our unexpected findings. For example, we selected two types of AAVs with different promoter, EF1a and hSyn, because

different type of promoters can modulate the expression of the transgene as they provide different binding sites for cellular machinery to transduce viral constructs(Nieuwenhuis et al., 2021).

Moreover, the transduction of AAV depends on the interactions between the AAV capsid and the surface proteins of the target cell(Haery et al., 2019; Srivastava, 2016; Sun et al., 2019; Yao et al., 2018). Consequently, different serotypes (defined by the specific serological profiles of each primate AAV capsid sequences) of AAVs may have distinct tropism (i.e., the ability of a virus to infect a specific type of cell or tissue) with respect to various cholinergic neurons(Castle et al., 2014; Haery et al., 2019; Schultz & Chamberlain, 2008). According to previous studies which used the AAVs together with the ChAT-Cre mice, we selected AAV vectors of serotype AAV2-retro(Song et al., 2020; Y. Wang et al., 2020), AAV2(Stornetta et al., 2013; Warner-Schmidt et al., 2012; Witten et al., 2010), AAV5(Helseth et al., 2021; Moehle et al., 2017; Zhang et al., 2018), and AAV9(Case et al., 2017; Helseth et al., 2021; Rothermel et al., 2013; Song et al., 2020; Zhang et al., 2018) to study the cholinergic connections in ChAT-Cre mice.

We initially selected the AAV2-retro serotype, then tested AAV9 to verify the results obtained in our retrograde study. The retro-AAV2 was initially selected since it was developed to offer efficient retrograde transport in addition to its ability to infect somas at the exposure site(Haery et al., 2019; Tervo et al., 2016). However, the unexpected results of AAV2-retro labelling led us to test the AAV9, another vector which exhibits natural retrograde trafficking activity at high doses(Haery et al., 2019; Masamizu et al., 2011). Previous study used Slc6a4 (SERT)-Cre mice and proved the retrograde property of AAV9 in serotonergic neurons(Rothermel et al., 2013). Of note, we found that AAV9 was also used for anterograde transport in most studies(Case et al., 2017; Herman et al., 2016; Zhang et al., 2018). For example, one study used the same pAAV-EF1a-double floxed-

hChR2(H134R)-EYFP-WPRE-HGHpA (AAV9, Addgene, #20297, 60nl) with ChAT-Cre mice (Jackson Laboratory, #028861), and delivered ChR2 onto cholinergic medial septum (MS) neurons at the site of injection(Zhang et al., 2018). Another study applied AAV9 to label projections of the horizontal diagonal band of Broca (HDB) cholinergic neurons in ChAT-Cre mice(Case et al., 2017) although their injection volume [0.75–1 μL (750nl-1000nl)] was much larger than our protocols (50nl-100nl). These studies thus indicate the ability of AAV9 to travel retrogradely and to infect cholinergic neurons in ChAT-Cre mice.

Although we kept the concentration of each virus fixed, and attempted to control the injection volume (50nl~100nl(Tervo et al., 2016)) to make the viruses work in their optimal conditions (neither too small volume, which may decrease the transduction efficiency, nor too large, which may lead to the virus spreading to other brain structures or cause toxicity because of high doses(Haery et al., 2019)), the actual expression of virus injected into the preBötC varied. This could depend on the levels of diffusion and backflow of the virus at the time of injection, causing infection of affected neighboring regions like the rVRG, the BötC, the IRt, and the NTS to some extents (as verified by the fluorobeads visualization)(Ai et al., 2007; Gang et al., 1995; Yang et al., 2019), and possibly resulting in various levels of gene expression and somewhat different tracing outcomes.

5.2 Cholinergic inputs to preBötC

The cholinergic modulation of preBötC is facilitated by the nAChRs and mAChRs(X. Shao & Feldman, 2000; X. M. Shao & Feldman, 2005, 2009). Increasing the ACh within the preBotC accelerates the respiratory rhythm, induces tonic activity in respiratory neurons, stabilizes respiratory activity, enhances the amplitude and duration of 12N bursts(X. M. Shao & Feldman, 2005). Specifically, nicotine depolarizes the preBotC inspiratory neurons via promoting excitatory glutamatergic input(X. M. Shao & Feldman,

2007), while muscarine depolarized inspiratory neurons(X. Shao & Feldman, 2000) but decreases the firing rate of most “burst like” spiking glycinergic neurons in the preBötC(Zheng et al., 2020).

Our initial hypothesis that the PPT/LDT structures sent cholinergic inputs to the preBötC was based on the current literature on cholinergic modulation of preBötC neurons(X. M. Shao & Feldman, 2009) and previous anatomical evidence which suggested that the PPT/LDT provided cholinergic inputs to the brainstem reticular formation(Jones, 1990; Woolf, 1991).

However, results from our study indicate that only sparse neurons in the LDT were labelled by HSV (n=4/4 mice), and only a few of them expressed light ChAT signals (n=1/4 mice). Similarly, only one or two cholinergic neurons were occasionally labelled by the use of retrograde Cre-dependent AAVs (n=3/11 mice: 2/4 with AAV-hSyn and 1/3 with AAV9), supporting the results obtained with the non-phenotype specific targeting.

As for the anterograde tracing, although we had a low efficiency in viral infection, and found some mCherry+/GFP+ fibers in the medullary reticular formation, there were only a few labelled axons in the preBötC. In brief, both the anterograde and retrograde tracing results indicate the presence of minimal inputs from the PPT/LDT to the preBötC.

Results from the retrograde viral tracing approach suggest the presence of very limited cholinergic inputs originating from the major cholinergic nuclei (e.g., brainstem motor nuclei, PPT/LDT, PBG(X. Li et al., 2018)) with the exception of the NA. Rather, we identified a fair number of projecting cholinergic neurons distributed in several structures in the medulla (e.g., IRt, LPGi, NTS). Despite the evidence that transduction efficiency of retrograde AAV is highly circuit-dependent(Haery et al., 2019), our results indicates that

the retrogradely labelled cholinergic neurons are mostly located in close proximity to the injection sites, suggesting that either local short range cholinergic neurons are modulating preBötC neurons, or that AAVs are capable of infecting neurons in a very close range to the injection site.

A comparison between results with the various AAVs indicate that all the AAV used resulted in infecting LPGi neurons with variable results (likely depending on small variations in injected volume) in addition to cholinergic neurons within the IRt (n=10 mice) and the NTS (n=9 mice) in most cases. Furthermore, we also identified sparse cholinergic neurons in the Pr (n=9 mice), the dorsal marginal layer of medulla (n=8 mice), and the region around 5TT/5m (n=10 mice) with all AAVs investigated. One point of concern is that retrograde AAVs (AAV2-retro and AAV9) can label cells at the injection site as well as the neurons that project to the injection site(J. Wang & Zhang, 2021; Weiss et al., 2020), thus, the robust expression of the reporter gene in the LPGi and NA, in particular, which are either adjacent to the injection site, may result from the diffusion and ectopic local expression of the AAVs.

Overall, our study indicates that the cholinergic neurons in the LPGi and NA are the most likely source of Ach to preBotC, in addition to scattered non-motor neurons in the IRT and NTS.

The lateral paragigantocellular nucleus (LPGi), also known as the rostral ventrolateral medulla (RVLM), is a sympathoexcitatory site which participates in regulating blood pressure and REM sleep(Sirieix et al., 2012). Previous studies suggest that the respiratory (rostral) division of VRG (corresponding to the area of the preBötC in later studies) has reciprocal connections with LPGi(H. Ellenberger & Feldman, 1990). In addition, a group of cholinergic neurons lying in the medial aspect of the RVLM (mRVLM-ChAT neurons)(D. A. Ruggiero et al., 1990b) form a continuum that extends lateral to the

pyramidal tract starting from the caudal end of the 7N to the level of Obex (caudal end of the fourth ventricle)(D. A. Ruggiero et al., 1990a; Stornetta et al., 2013). The mRVLM-ChAT neurons primarily regulate the somatosensory information, and they send cholinergic projections to the dorsal column nuclei, the central gray, the inferior colliculus, the cochlear nuclei, the superior olivary complex, the spinal trigeminal nucleus, the dorsal horn of the spinal cord, etc.(Kamiya et al., 1988; Stornetta et al., 2013). Of note, the mRVLM-ChAT neurons also send sparse projections to the adjacent ventrolateral medulla(Stornetta et al., 2013), which may include the preBötC based on their contiguity, and that by definition the preBötC is part of the RVLM as well(J. Smith et al., 1991).

Likewise, the NA cholinergic motor neurons could provide inputs to the preBötC considering their close proximity, whereas the sparse motoneurons of ventral NA intermingle with the rostral VRG neurons (primarily at the level of BötC). Based on the cytoarchitecture and projections, NA can be divided into four parts: the rostral esophagomotor compact formation, the intermediate pharyngomotor semi-compact formation, the caudal laryngomotor loose formation, and the general visceromotor external formation(Altschuler et al., 1991; Bieger & Hopkins, 1987). Considering its heterogenous structure, the retrograde AAVs labelled cholinergic neurons lateral to the BötC may belong to the NA (external formation) as well(H. H. Ellenberger, 1999). In addition, the NA motor neurons, especially the pharyngeal and laryngeal motoneurons, are involved in swallowing, respiration and vocalization, with axons and dendrites widely distributed within VLM which contains the preBötC(Rekling & Feldman, 1997; Saxon et al., 1996) and could help integrating the orofacial behavior and upper airway activity with breathing rhythms.

ChAT immunoreactive neurons have been identified within the IRt of both mouse and rat(Toor et al., 2019; Volgin et al., 2008). In particular, a group of cholinergic neurons medial and dorsal to NA was proposed to be the generator of the postinspiratory

activity(Toor et al., 2019). Interestingly, instead of PiCo, we found sparse labeled cholinergic neurons in the IRt dorsal to the NA at the preBötC injection level. NTS is another essential site for the coordination of chemoreflex, baroreflex, cardiorespiratory response(Furuya et al., 2020). Only a few NTS neurons are cholinergic and their function is yet to be clarified(Garfield et al., 2012; Maley, 1996).

It is important to note though that although we observed quite a few mRVLM-ChAT and NA cholinergic neurons labeled by retrograde AAVs (n=11 out of 11 mice) the HSV injections barely labelled cholinergic neurons in the LPGi and NA (n=1 mice out of 4 mice). Multiple explanations should be considered: the first one is that HSV may have some toxic effect at the injection site(Jacobs et al., 1999): preliminary data from our laboratory in fact indicate that HSV injected rats in the preBötC had a reduced survival rate during anesthesia, suggesting potential toxic effect at the injection site.

The second one is that HSV may not be the optimal approach to target cholinergic neurons due to a potential lack of tropism(Duarte et al., 2019). In fact, we observed several GFP+ non-cholinergic neurons adjacent to the injection site including the LPGi, NA, and the paraNA, which indicated the capability of HSV to infect nearby neurons.

However, it is important to consider that HSV was initially used for the ability of target presynaptic terminals without infecting neurons at the injection site and therefore further anterograde studies will be necessary to verify the projections of LPGi and NA neurons to the preBotC.

5.3 Future Directions

Our study provided the anatomical evidence for the source of cholinergic inputs within the

preBötC. We discovered that the cholinergic neurons in the NA and LPGi send cholinergic inputs to the preBötC. However, the roles of these neurons in respiratory modulation, especially the mRVLM-ChAT neurons, have not yet been investigated. Future studies aimed at manipulating activity of mRVLM-ChAT neurons will help researchers to understand the significance of these neurons in the modulation of breathing.

In contrast to our initial hypothesis, we identified only few cholinergic connections between the PPT/LDT and the preBötC. However, the low infection rate in the anterograde study may result in false negative results. Thus, a larger injection volume or a better tracer which specifically infects the majority of PPT/LDT cholinergic neurons can confirm our findings.

Even if modest projections are still identified with larger injection, it is possible that sparse projections from the PPT/LDT to the preBötC can still serve an important function in respiratory control. Thus, future studies aiming at stimulating (pharmachologically or optogenetically) these axon terminals in the preBötC could identify their physiological role in the control of respiration. In complementary experiments, it was observed that glutamatergic and GABAergic neurons in the PPT/LDT project to the preBötC. It will be important to determine whether these inputs are of relevance for respiratory control and state dependent modulation of respiratory activity.

5.4 Conclusion

Cholinergic neurotransmission modulates several aspects of breathing: respiratory rate and motor output, state-dependent modulation of multiple functions, post-inspiratory activity, active expiration, central and peripheral chemosensitivity. Researchers continues to make progress in the understanding of cholinergic modulation of the preBötC, which is the kernel of breathing control system. Genetically engineered Cre knock-in mice and Cre

dependent viruses provide powerful tools for analyzing the connectome of the preBötC and the respiratory networks. The findings of our studies indicate that the origins of ACh in the preBötC are unlikely from the major cholinergic nuclei PPT/LDT. Instead, these cholinergic inputs appear to originate from cholinergic neurons in neighboring regions of the ventral medulla, including the LPGi and NA. Insight into cholinergic connections of the preBötC will provide an anatomical basis for analyzing the functional roles of these related nuclei in the regulation of respiration.

Reference

Ahmed, N. Y., Knowles, R., & Dehorter, N. (2019). New Insights Into Cholinergic Neuron Diversity. *Frontiers in Molecular Neuroscience*, *12*, 204. https://doi.org/10.3389/fnmol.2019.00204

Ai, J., Epstein, P. N., Gozal, D., Yang, B., Wurster, R., & Cheng, Z. J. (2007). Morphology and topography of nucleus ambiguus projections to cardiac ganglia in rats and mice. *Neuroscience*, *149*(4), 845–860. https://doi.org/10.1016/j.neuroscience.2007.07.062

Allaway, K. C., & Machold, R. (2017). Developmental specification of forebrain cholinergic neurons. *Developmental Biology*, *421*(1), 1–7.

Alsahafi, Z., Dickson, C. T., & Pagliardini, S. (2015). Optogenetic excitation of preBötzinger complex neurons potently drives inspiratory activity *in vivo*: PreBötzinger complex optostimulation. *The Journal of Physiology*, *593*(16), 3673–3692. https://doi.org/10.1113/JP270471

Altschuler, S. M., Bao, X., & Miselis, R. R. (1991). Dendritic architecture of nucleus ambiguus motoneurons projecting to the upper alimentary tract in the rat. *The Journal of Comparative Neurology*, *309*(3), 402–414. https://doi.org/10.1002/cne.903090309

Anderson, T. M., Garcia, A. J., Baertsch, N. A., Pollak, J., Bloom, J. C., Wei, A. D., Rai, K. G., & Ramirez, J.-M. (2016). A novel excitatory network for the control of breathing. *Nature*, *536*(7614), 76–80. https://doi.org/10.1038/nature18944

Aserinsky, E. (1965). Periodic respiratory pattern occurring in conjunction with eye movements during sleep. *Science*, *150*(3697), 763–766.

Ashhad, S., & Feldman, J. L. (2019). *Network synchronization and synchrony propagation: Emergent elements of inspiration* [Preprint]. Neuroscience. https://doi.org/10.1101/664946

Ashhad, S., & Feldman, J. L. (2020). Emergent Elements of Inspiratory Rhythmogenesis:

Network Synchronization and Synchrony Propagation. *Neuron*, *106*(3), 482-497.e4. https://doi.org/10.1016/j.neuron.2020.02.005

Ausborn, J., Koizumi, H., Barnett, W. H., John, T. T., Zhang, R., Molkov, Y. I., Smith, J. C., & Rybak, I. A. (2018). Organization of the core respiratory network: Insights from optogenetic and modeling studies. *PLoS Computational Biology*, *14*(4), e1006148.

Baertsch, N. A., Baertsch, H. C., & Ramirez, J. M. (2018). The interdependence of excitation and inhibition for the control of dynamic breathing rhythms. *Nature Communications*, *9*(1), 843. https://doi.org/10.1038/s41467-018-03223-x

Baertsch, N. A., & Ramirez, J.-M. (2019). Insights into the dynamic control of breathing revealed through cell-type-specific responses to substance P. *ELife*, *8*, e51350. https://doi.org/10.7554/eLife.51350

Baertsch, N. A., Severs, L. J., Anderson, T. M., & Ramirez, J.-M. (2019). A spatially dynamic network underlies the generation of inspiratory behaviors. *Proceedings of the National Academy of Sciences*, *116*(15), 7493–7502. https://doi.org/10.1073/pnas.1900523116

Ballantyne, D., & Richter, D. (1984). Post-synaptic inhibition of bulbar inspiratory neurones in the cat. *The Journal of Physiology*, *348*(1), 67–87.

Ballinger, E. C., Ananth, M., Talmage, D. A., & Role, L. W. (2016). Basal forebrain cholinergic circuits and signaling in cognition and cognitive decline. *Neuron*, *91*(6), 1199–1218.

Barmack, N., Baughman, R., & Eckenstein, F. (1992). Cholinergic innervation of the cerebellum of rat, rabbit, cat, and monkey as revealed by choline acetyltransferase activity and immunohistochemistry. *Journal of Comparative Neurology*, *317*(3), 233–249.

Bearer, E., Breakefield, X., Schuback, D., Reese, T., & LaVail, J. (2000). Retrograde axonal transport of herpes simplex virus: Evidence for a single mechanism and a

role for tegument. *Proceedings of the National Academy of Sciences*, *97*(14), 8146–8150.

Bellingham, M. C., & Funk, G. D. (2000). Cholinergic modulation of respiratory brainstem neurons and its function in sleep–wake state determination. *Clinical and Experimental Pharmacology and Physiology*, *27*(1–2), 132–137.

Bellingham, M. C., & Ireland, M. F. (2002). Contribution of cholinergic systems to state-dependent modulation of respiratory control. *Respiratory Physiology & Neurobiology*, *131*(1–2), 135–144. https://doi.org/10.1016/S1569-9048(02)00043-5

Benagiano, V., Virgintino, D., Flace, P., Girolamo, F., Errede, M., & Roncali, L. (2003). Choline acetyltransferase-containing neurons in the human parietal neocortex. *European Journal of Histochemistry*, *47*(3), 253–256.

Biancardi, V., Saini, J., Pageni, A., Prashaad M., H., Funk, G. D., & Pagliardini, S. (2020). Mapping of the excitatory, inhibitory, and modulatory afferent projections to the anatomically defined active expiratory oscillator in adult male rats. *Journal of Comparative Neurology*, cne.24984. https://doi.org/10.1002/cne.24984

Bieger, D., & Hopkins, D. A. (1987). Viscerotopic representation of the upper alimentary tract in the medulla oblongata in the rat: The nucleus ambiguus. *The Journal of Comparative Neurology*, *262*(4), 546–562. https://doi.org/10.1002/cne.902620408

Bittar, T. P., Pelaez, M. C., Silva, J. C. H., Quessy, F., Lavigne, A.-A., Morency, D., Blanchette, L.-J., Arsenault, E., Cherasse, Y., Seigneur, J., & others. (2021). Chronic Stress Induces Sex-Specific Functional and Morphological Alterations in Corticoaccumbal and Corticotegmental Pathways. *Biological Psychiatry*.

Bonis, J. M., Neumueller, S. E., Krause, K. L., Kiner, T., Smith, A., Marshall, B. D., Qian, B., Pan, L. G., & Forster, H. V. (2010). A role for the Kölliker-Fuse nucleus in cholinergic modulation of breathing at night during wakefulness and NREM sleep. *Journal of Applied Physiology*, *109*(1), 159–170.

https://doi.org/10.1152/japplphysiol.00933.2009

Bonsi, P., Cuomo, D., Martella, G., Madeo, G., Schirinzi, T., Puglisi, F., Ponterio, G., & Pisani, A. (2011). Centrality of striatal cholinergic transmission in basal ganglia function. *Frontiers in Neuroanatomy*, *5*, 6.

Boskovic, Z., Milne, M. R., Qian, L., Clifton, H. D., McGovern, A. E., Turnbull, M. T., Mazzone, S. B., & Coulson, E. J. (2018). Cholinergic basal forebrain neurons regulate fear extinction consolidation through p75 neurotrophin receptor signaling. *Translational Psychiatry*, *8*(1), 199. https://doi.org/10.1038/s41398-018-0248-x

Boutin, R. C., Alsahafi, Z., & Pagliardini, S. (2017). Cholinergic modulation of the parafacial respiratory group. *The Journal of Physiology*, *595*(4), 1377–1392.

Boutin, R. C. T., Alsahafi, Z., & Pagliardini, S. (2017). Cholinergic modulation of the parafacial respiratory group: Cholinergic modulation of active expiration. *The Journal of Physiology*, *595*(4), 1377–1392. https://doi.org/10.1113/JP273012

Brinkman, J. E., & Sharma, S. (2019). Physiology, respiratory drive. *StatPearls [Internet]*.

Burke, P. G. R., Kanbar, R., Basting, T. M., Hodges, W. M., Viar, K. E., Stornetta, R. L., & Guyenet, P. G. (2015). State-dependent control of breathing by the retrotrapezoid nucleus: RTN, breathing and sleep. *The Journal of Physiology*, *593*(13), 2909–2926. https://doi.org/10.1113/JP270053

Burton, M. D., Johnson, D. C., & Kazemi, H. (1997). The central respiratory effects of acetylcholine vary with CSF pH. *Journal of the Autonomic Nervous System*, *62*(1–2), 27–32. https://doi.org/10.1016/S0165-1838(96)00104-X

Burton, M. D., Nouri, M., & Kazemi, H. (1995). Acetylcholine and central respiratory control: Perturbations of acetylcholine synthesis in the isolated brainstem of the neonatal rat. *Brain Research*, *670*(1), 39–47. https://doi.org/10.1016/0006-8993(94)01249-H

Burton, M., Nouri, K., Baichoo, S., Samuels-Toyloy, N., & Kazemi, H. (1994). Ventilatory output and acetylcholine: Perturbations in release and muscarinic receptor

activation. *Journal of Applied Physiology*, *77*(5), 2275–2284.

Carlson, A. B., & Kraus, G. P. (2018). *Physiology, cholinergic receptors*.

Carroll, M. S., & Ramirez, J.-M. (2013). Cycle-by-cycle assembly of respiratory network activity is dynamic and stochastic. *Journal of Neurophysiology*, *109*(2), 296–305. https://doi.org/10.1152/jn.00830.2011

Case, D. T., Burton, S. D., Gedeon, J. Y., Williams, S.-P. G., Urban, N. N., & Seal, R. P. (2017). Layer- and cell type-selective co-transmission by a basal forebrain cholinergic projection to the olfactory bulb. *Nature Communications*, *8*(1), 652. https://doi.org/10.1038/s41467-017-00765-4

Castle, M. J., Gershenson, Z. T., Giles, A. R., Holzbaur, E. L. F., & Wolfe, J. H. (2014). Adeno-Associated Virus Serotypes 1, 8, and 9 Share Conserved Mechanisms for Anterograde and Retrograde Axonal Transport. *Human Gene Therapy*, *25*(8), 705–720. https://doi.org/10.1089/hum.2013.189

Caulfield, M. P. (1993). Muscarinic receptors—Characterization, coupling and function. *Pharmacology & Therapeutics*, *58*(3), 319–379.

Chokshi, V., Gao, M., Grier, B. D., Owens, A., Wang, H., Worley, P. F., & Lee, H.-K. (2019). Input-specific metaplasticity in the visual cortex requires Homer1a-mediated mGluR5 signaling. *Neuron*, *104*(4), 736–748.

Coddou, C., Bravo, E., & Eugenín, J. (2009). Alterations in cholinergic sensitivity of respiratory neurons induced by pre-natal nicotine: A mechanism for respiratory dysfunction in neonatal mice. *Philosophical Transactions of the Royal Society B: Biological Sciences*, *364*(1529), 2527–2535. https://doi.org/10.1098/rstb.2009.0078

Cui, Y., Kam, K., Sherman, D., Janczewski, W. A., Zheng, Y., & Feldman, J. L. (2016). Defining preBötzinger Complex Rhythm- and Pattern-Generating Neural Microcircuits In Vivo. *Neuron*, *91*(3), 602–614. https://doi.org/10.1016/j.neuron.2016.07.003

Dani, J. A., & Bertrand, D. (2007). Nicotinic acetylcholine receptors and nicotinic cholinergic mechanisms of the central nervous system. *Annu. Rev. Pharmacol. Toxicol.*, *47*, 699–729.

Datta, S. (2009). Cholinergic Brainstem. In M. D. Binder, N. Hirokawa, & U. Windhorst (Eds.), *Encyclopedia of Neuroscience* (pp. 705–708). Springer Berlin Heidelberg. https://doi.org/10.1007/978-3-540-29678-2_1002

Dautan, D., Hacioğlu Bay, H., Bolam, J. P., Gerdjikov, T. V., & Mena-Segovia, J. (2016). Extrinsic sources of cholinergic innervation of the striatal complex: A whole-brain mapping analysis. *Frontiers in Neuroanatomy*, *10*, 1.

de Sousa Abreu, R. P., Bondarenko, E., & Feldman, J. L. (2021). Phase-and State-Dependent Modulation of Breathing Pattern by preBötzinger Complex Somatostatin Expressing Neurons. *BioRxiv*.

Dehkordi, O., Haxhiu, M. A., Millis, R. M., Dennis, G. C., Kc, P., Jafri, A., Khajavi, M., Trouth, C. O., & Zaidi, S. I. (2004). Expression of α-7 nAChRs on spinal cord–brainstem neurons controlling inspiratory drive to the diaphragm. *Respiratory Physiology & Neurobiology*, *141*(1), 21–34.

Del Negro, C. A., Funk, G. D., & Feldman, J. L. (2018). Breathing matters. *Nature Reviews Neuroscience*, *19*(6), 351–367. https://doi.org/10.1038/s41583-018-0003-6

Del Negro, C. A., Morgado-Valle, C., Hayes, J. A., Mackay, D. D., Pace, R. W., Crowder, E. A., & Feldman, J. L. (2005). Sodium and calcium current-mediated pacemaker neurons and respiratory rhythm generation. *Journal of Neuroscience*, *25*(2), 446–453.

del Toro, E. D., Juiz, J. M., Peng, X., Lindstrom, J., & Criado, M. (1994). Immunocytochemical localization of the α7 subunit of the nicotinic acetylcholine receptor in the rat central nervous system. *Journal of Comparative Neurology*, *349*(3), 325–342.

Dhingra, R. R., Furuya, W. I., Bautista, T. G., Dick, T. E., Galán, R. F., & Dutschmann, M.

(2019). Increasing Local Excitability of Brainstem Respiratory Nuclei Reveals a Distributed Network Underlying Respiratory Motor Pattern Formation. *Frontiers in Physiology*, *10*, 887. https://doi.org/10.3389/fphys.2019.00887

Dhingra, R. R., Furuya, W. I., Dick, T. E., & Dutschmann, M. (2021). Response to: The post-inspiratory complex (PiCo), what is the evidence? *The Journal of Physiology*, *599*(1), 361–362.

Dick, T. E., Oku, Y., Romaniuk, J. R., & Cherniack, N. (1993). Interaction between central pattern generators for breathing and swallowing in the cat. *The Journal of Physiology*, *465*(1), 715–730.

Douglas, N. J. (2005). Respiratory physiology: Control of ventilation. In *Principles and practice of sleep medicine* (pp. 224–231). Elsevier.

Dringenberg, H. C., & Vanderwolf, C. (1998). Involvement of direct and indirect pathways in electrocorticographic activation. *Neuroscience & Biobehavioral Reviews*, *22*(2), 243–257.

Duarte, L. F., Farías, M. A., Álvarez, D. M., Bueno, S. M., Riedel, C. A., & González, P. A. (2019). Herpes simplex virus type 1 infection of the central nervous system: Insights into proposed interrelationships with neurodegenerative disorders. *Frontiers in Cellular Neuroscience*, *13*, 46.

Dutschmann, M., & Herbert, H. (2006). The Kölliker-Fuse nucleus gates the postinspiratory phase of the respiratory cycle to control inspiratory off-switch and upper airway resistance in rat. *European Journal of Neuroscience*, *24*(4), 1071–1084. https://doi.org/10.1111/j.1460-9568.2006.04981.x

Eger, E. I., Zhang, Y., Laster, M., Flood, P., Kendig, J. J., & Sonner, J. M. (2002). Acetylcholine receptors do not mediate the immobilization produced by inhaled anesthetics. *Anesthesia & Analgesia*, *94*(6), 1500–1504.

Ellenberger, H., & Feldman, J. (1990). Brainstem connections of the rostral ventral respiratory group of the rat. *Brain Research*, *513*(1), 35–42.

Ellenberger, H. H. (1999). Nucleus ambiguus and bulbospinal ventral respiratory group neurons in the neonatal rat. *Brain Research Bulletin*, *50*(1), 1–13.

Eugenín, J., & Nicholls, J. G. (1997). Chemosensory and cholinergic stimulation of fictive respiration in isolated cns of neonatal opossum. *The Journal of Physiology*, *501*(2), 425–437. https://doi.org/10.1111/j.1469-7793.1997.425bn.x

Feldman, J. L., Del Negro, C. A., & Gray, P. A. (2013). Understanding the rhythm of breathing: So near, yet so far. *Annual Review of Physiology*, *75*, 423–452.

Feldman, J. L., & Kam, K. (2015). Facing the challenge of mammalian neural microcircuits: Taking a few breaths may help: Principles of mammalian microcircuits controlling breathing. *The Journal of Physiology*, *593*(1), 3–23. https://doi.org/10.1113/jphysiol.2014.277632

Fleming, P. J., Cade, D., Bryan, M. H., & Bryan, A. C. (1980). Congenital central hypoventilation and sleep state. *Pediatrics*, *66*(3), 425–428.

Franklin, K. B., Paxinos, G., & others. (2008). *The mouse brain in stereotaxic coordinates*.

French, I. T., & Muthusamy, K. A. (2018). A review of the pedunculopontine nucleus in Parkinson's disease. *Frontiers in Aging Neuroscience*, *10*, 99.

Fukuda, Y., & Loeschcke, H. H. (1979). A cholinergic mechanism involved in the neuronal excitation by H+ in the respiratory chemosensitive structures of the ventral medulla oblongata of rats in vitro. *Pflügers Archiv*, *379*(2), 125–135.

Fuller, P. M., Saper, C. B., & Lu, J. (2007). The pontine REM switch: Past and present. *The Journal of Physiology*, *584*(3), 735–741.

Furuya, W. I., Bassi, M., Menani, J. V., Colombari, E., Zoccal, D. B., & Colombari, D. S. A. (2020). Modulation of hypercapnic respiratory response by cholinergic transmission in the commissural nucleus of the solitary tract. *Pflügers Archiv - European Journal of Physiology*, *472*(1), 49–60. https://doi.org/10.1007/s00424-019-02341-9

Gang, S., Sato, Y., Kohama, I., & Aoki, M. (1995). Afferent projections to the Bötzinger

complex from the upper cervical cord and other respiratory related structures in the brainstem in cats: Retrograde WGA-HRP tracing. *Journal of the Autonomic Nervous System*, *56*(1–2), 1–7.

Garfield, A. S., Patterson, C., Skora, S., Gribble, F. M., Reimann, F., Evans, M. L., Myers, M. G., & Heisler, L. K. (2012). Neurochemical Characterization of Body Weight-Regulating Leptin Receptor Neurons in the Nucleus of the Solitary Tract. *Endocrinology*, *153*(10), 4600–4607. https://doi.org/10.1210/en.2012-1282

Gilbert, K. A., & Lydic, R. (1990). Parabrachial neuron discharge in the cat is altered during the carbachol-induced REM sleep-like state (DCarb). *Neuroscience Letters*, *120*(2), 241–244.

Gilbert, K. A., & Lydic, R. (1994). Pontine cholinergic reticular mechanisms cause state-dependent changes in the discharge of parabrachial neurons. *American Journal of Physiology-Regulatory, Integrative and Comparative Physiology*, *266*(1), R136–R150.

Goridis, C., Dubreuil, V., Thoby-Brisson, M., Fortin, G., & Brunet, J.-F. (2010). Phox2b, congenital central hypoventilation syndrome and the control of respiration. *Seminars in Cell & Developmental Biology*, *21*(8), 814–822.

Grace, K. P., Hughes, S. W., & Horner, R. L. (2013). Identification of the mechanism mediating genioglossus muscle suppression in REM sleep. *American Journal of Respiratory and Critical Care Medicine*, *187*(3), 311–319.

Grace, K. P., Hughes, S. W., & Horner, R. L. (2014). Identification of a pharmacological target for genioglossus reactivation throughout sleep. *Sleep*, *37*(1), 41–50.

Gray, P. A., Hayes, J. A., Ling, G. Y., Llona, I., Tupal, S., Picardo, M. C. D., Ross, S. E., Hirata, T., Corbin, J. G., Eugenin, J., & Del Negro, C. A. (2010). Developmental Origin of PreBotzinger Complex Respiratory Neurons. *Journal of Neuroscience*, *30*(44), 14883–14895. https://doi.org/10.1523/JNEUROSCI.4031-10.2010

Gray, P. A., Janczewski, W. A., Mellen, N., McCrimmon, D. R., & Feldman, J. L. (2001).

Normal breathing requires preBötzinger complex neurokinin-1 receptor-expressing neurons. *Nature Neuroscience*, *4*(9), 927–930.

Greer, J., Smith, J., & Feldman, J. (1991). Role of excitatory amino acids in the generation and transmission of respiratory drive in neonatal rat. *The Journal of Physiology*, *437*(1), 727–749.

Gremel, C. M., Chancey, J. H., Atwood, B. K., Luo, G., Neve, R., Ramakrishnan, C., Deisseroth, K., Lovinger, D. M., & Costa, R. M. (2016). Endocannabinoid Modulation of Orbitostriatal Circuits Gates Habit Formation. *Neuron*, *90*(6), 1312–1324. https://doi.org/10.1016/j.neuron.2016.04.043

Gut, N. K. (2016). The pedunculopontine tegmental nucleus—A functional hypothesis from the comparative literature. *Movement Disorders*, *31*(5), 10.

Guthrie, S. (2007). Patterning and axon guidance of cranial motor neurons. *Nature Reviews Neuroscience*, *8*(11), 859–871.

Guyenet, P. G. (2005). Regulation of Ventral Surface Chemoreceptors by the Central Respiratory Pattern Generator. *Journal of Neuroscience*, *25*(39), 8938–8947. https://doi.org/10.1523/JNEUROSCI.2415-05.2005

Haery, L., Deverman, B. E., Matho, K. S., Cetin, A., Woodard, K., Cepko, C., Guerin, K. I., Rego, M. A., Ersing, I., Bachle, S. M., Kamens, J., & Fan, M. (2019). Adeno-Associated Virus Technologies and Methods for Targeted Neuronal Manipulation. *Frontiers in Neuroanatomy*, *13*, 93. https://doi.org/10.3389/fnana.2019.00093

Harris, K. D., Dashevskiy, T., Mendoza, J., Garcia III, A. J., Ramirez, J.-M., & Shea-Brown, E. (2017). Different roles for inhibition in the rhythm-generating respiratory network. *Journal of Neurophysiology*, *118*(4), 2070–2088.

Hasselmo, M. E., & McGaughy, J. (2004). High acetylcholine levels set circuit dynamics for attention and encoding and low acetylcholine levels set dynamics for consolidation. *Progress in Brain Research*, *145*, 207–231.

Haxhiu, M. A., Van Lunteren, E., Van De Graaff, W. B., Strohl, K. P., Bruce, E. N., Mitra,

J., & Cherniack, N. S. (1984). Action of nicotine on the respiratory activity of the diaphragm and genioglossus muscles and the nerves that innervate them. *Respiration Physiology*, *57*(2), 153–169.

Heijden, M. E., & Zoghbi, H. Y. (2020). Development of the brainstem respiratory circuit. *WIREs Developmental Biology*, *9*(3). https://doi.org/10.1002/wdev.366

Helseth, A. R., Hernandez-Martinez, R., Hall, V. L., Oliver, M. L., Turner, B. D., Caffall, Z. F., Rittiner, J. E., Shipman, M. K., King, C. S., Gradinaru, V., & others. (2021). Cholinergic neurons engage the integrated stress response for dopamine modulation and skill learning. *Science (New York, NY)*, *372*(6540).

Herman, A. M., Ortiz-Guzman, J., Kochukov, M., Herman, I., Quast, K. B., Patel, J. M., Tepe, B., Carlson, J. C., Ung, K., Selever, J., Tong, Q., & Arenkiel, B. R. (2016). A cholinergic basal forebrain feeding circuit modulates appetite suppression. *Nature*, *538*(7624), 253–256. https://doi.org/10.1038/nature19789

Horner, R. L. (2008a). Neuromodulation of hypoglossal motoneurons during sleep. *Respiratory Physiology & Neurobiology*, *164*(1–2), 179–196.

Horner, R. L. (2008b). Pathophysiology of obstructive sleep apnea. *Journal of Cardiopulmonary Rehabilitation and Prevention*, *28*(5), 289–298.

Hülsmann, S. (2021). The post-inspiratory complex (PiCo), what is the evidence? *The Journal of Physiology*, *599*(1), 357–359.

Jacobs, A., Breakefield, X. O., & Fraefel, C. (1999). HSV-1-based vectors for gene therapy of neurological diseases and brain tumors: Part II. Vector systems and applications. *Neoplasia*, *1*(5), 402–416.

Janczewski, W. A., Tashima, A., Hsu, P., Cui, Y., & Feldman, J. L. (2013). Role of inhibition in respiratory pattern generation. *Journal of Neuroscience*, *33*(13), 5454–5465.

Jones, B. E. (1990). Immunohistochemical study of choline acetyltransferase-immunoreactive processes and cells innervating the pontomedullary reticular

formation in the rat. *Journal of Comparative Neurology*, *295*(3), 485–514.

Kallurkar, P. S., Grover, C., Picardo, M. C. D., & Del Negro, C. A. (2020). Evaluating the burstlet theory of inspiratory rhythm and pattern generation. *Eneuro*, *7*(1).

Kallurkar, P. S., Picardo, M. C. D., Sugimura, Y. K., Saha, M. S., Smith, G. D. C., & Del Negro, C. A. (2021). *Transcriptomes of Electrophysiologically Recorded Dbx1-derived Inspiratory Neurons of the preBötzinger Complex in Neonatal Mice* [Preprint]. Neuroscience. https://doi.org/10.1101/2021.08.01.454659

Kam, K., Worrell, J. W., Janczewski, W. A., Cui, Y., & Feldman, J. L. (2013). Distinct inspiratory rhythm and pattern generating mechanisms in the preBötzinger complex. *Journal of Neuroscience*, *33*(22), 9235–9245.

Kamiya, H., Itoh, K., Yasui, Y., Ino, T., & Mizuno, N. (1988). Somatosensory and auditory relay nucleus in the rostral part of the ventrolateral medulla: A morphological study in the cat. *Journal of Comparative Neurology*, *273*(3), 421–435.

Kinney, H. C., Filiano, J. J., Sleeper, L. A., Mandell, F., Valdes-Dapena, M., & White, W. F. (1995). Decreased muscarinic receptor binding in the arcuate nucleus in sudden infant death syndrome. *Science*, *269*(5229), 1446–1450.

Koizumi, H., Mosher, B., Tariq, M. F., Zhang, R., Koshiya, N., & Smith, J. C. (2016). Voltage-Dependent Rhythmogenic Property of Respiratory Pre-Bötzinger Complex Glutamatergic, Dbx1-Derived, and Somatostatin-Expressing Neuron Populations Revealed by Graded Optogenetic Inhibition. *Eneuro*, *3*(3), ENEURO.0081-16.2016. https://doi.org/10.1523/ENEURO.0081-16.2016

Krishnan, V., Stoppel, D. C., Nong, Y., Johnson, M. A., Nadler, M. J., Ozkaynak, E., Teng, B. L., Nagakura, I., Mohammad, F., Silva, M. A., & others. (2017). Autism gene Ube3a and seizures impair sociability by repressing VTA Cbln1. *Nature*, *543*(7646), 507–512.

Kubin, L. (2001). Carbachol models of REM sleep: Recent developments and new directions. *Archives Italiennes de Biologie*, *139*(1), 147–168.

Kubin, L., & Fenik, V. (2004). Pontine cholinergic mechanisms and their impact on respiratory regulation. *Respiratory Physiology & Neurobiology*, *143*(2–3), 235–249. https://doi.org/10.1016/j.resp.2004.04.017

Lai, J., Shao, X. M., Pan, R. W., Dy, E., Huang, C. H., & Feldman, J. L. (2001). RT-PCR reveals muscarinic acetylcholine receptor mRNA in the pre-Bötzinger complex. *American Journal of Physiology-Lung Cellular and Molecular Physiology*, *281*(6), L1420–L1424. https://doi.org/10.1152/ajplung.2001.281.6.L1420

Lazaridis, I., Tzortzi, O., Weglage, M., Märtin, A., Xuan, Y., Parent, M., Johansson, Y., Fuzik, J., Fürth, D., Fenno, L. E., & others. (2019). A hypothalamus-habenula circuit controls aversion. *Molecular Psychiatry*, *24*(9), 1351–1368.

Levy, J., Facchinetti, P., Jan, C., Achour, M., Bouvier, C., Brunet, J., Delzescaux, T., & Giuliano, F. (2019). Tridimensional mapping of Phox2b expressing neurons in the brainstem of adult *Macaca fascicularis* and identification of the retrotrapezoid nucleus. *Journal of Comparative Neurology*, cne.24713. https://doi.org/10.1002/cne.24713

Li, F., Jiang, H., Shen, X., Yang, W., Guo, C., Wang, Z., Xiao, M., Cui, L., Luo, W., Kim, B. S., & others. (2021). Sneezing reflex is mediated by a peptidergic pathway from nose to brainstem. *Cell*.

Li, P., Janczewski, W. A., Yackle, K., Kam, K., Pagliardini, S., Krasnow, M. A., & Feldman, J. L. (2016). The peptidergic control circuit for sighing. *Nature*, *530*(7590), 293–297. https://doi.org/10.1038/nature16964

Li, X., Yu, B., Sun, Q., Zhang, Y., Ren, M., Zhang, X., Li, A., Yuan, J., Madisen, L., Luo, Q., Zeng, H., Gong, H., & Qiu, Z. (2018). Generation of a whole-brain atlas for the cholinergic system and mesoscopic projectome analysis of basal forebrain cholinergic neurons. *Proceedings of the National Academy of Sciences*, *115*(2), 415–420. https://doi.org/10.1073/pnas.1703601115

Lim, S. A. O., Kang, U. J., & McGehee, D. S. (2014). Striatal cholinergic interneuron

regulation and circuit effects. *Frontiers in Synaptic Neuroscience*, *6*, 22.

Lydic, R., & Baghdoyan, H. A. (1993). Pedunculopontine stimulation alters respiration and increases ACh release in the pontine reticular formation. *American Journal of Physiology-Regulatory, Integrative and Comparative Physiology*, *264*(3), R544–R554.

Magalhães, K. S., da Silva, M. P., Mecawi, A. S., Paton, J. F., Machado, B. H., & Moraes, D. J. (2021). Intrinsic and synaptic mechanisms controlling the expiratory activity of excitatory lateral parafacial neurones of rats. *The Journal of Physiology*.

Maley, B. E. (1996). Immunohistochemical Lòcalization of Neuropeptides and Neurotransmitters in the Nucleus Solitarius. *Chemical Senses*, *21*(3), 367–376. https://doi.org/10.1093/chemse/21.3.367

Mallard, C., Tolcos, M., Leditschke, J., Campbell, P., & Rees, S. (1999). Reduction in choline acetyltransferase immunoreactivity but not muscarinic-m2 receptor immunoreactivity in the brainstem of SIDS infants. *Journal of Neuropathology and Experimental Neurology*, *58*(3), 255–264.

Marcus, C. L. (2001). Sleep-disordered breathing in children. *American Journal of Respiratory and Critical Care Medicine*, *164*(1), 16–30.

Masamizu, Y., Okada, T., Kawasaki, K., Ishibashi, H., Yuasa, S., Takeda, S., Hasegawa, I., & Nakahara, K. (2011). Local and retrograde gene transfer into primate neuronal pathways via adeno-associated virus serotype 8 and 9. *Neuroscience*, *193*, 249–258. https://doi.org/10.1016/j.neuroscience.2011.06.080

McKay, L. C., Janczewski, W. A., & Feldman, J. L. (2005). Sleep-disordered breathing after targeted ablation of preBötzinger complex neurons. *Nature Neuroscience*, *8*(9), 1142–1144.

Mena-Segovia, J. (2016). Structural and functional considerations of the cholinergic brainstem. *Journal of Neural Transmission*, *123*(7), 731–736. https://doi.org/10.1007/s00702-016-1530-9

Mena-Segovia, J., & Bolam, J. P. (2017). Rethinking the Pedunculopontine Nucleus: From Cellular Organization to Function. *Neuron*, *94*(1), 7–18. https://doi.org/10.1016/j.neuron.2017.02.027

Meredith, G., Blank, B., & Groenewegen, H. (1989). The distribution and compartmental organization of the cholinergic neurons in nucleus accumbens of the rat. *Neuroscience*, *31*(2), 327–345.

Mesulam, M., Mufson, E., Wainer, B., & Levey, A. (1983). Central cholinergic pathways in the rat: An overview based on an alternative nomenclature (Ch1–Ch6). *Neuroscience*, *10*(4), 1185–1201.

Metz, B. (1966). Hypercapnia and acetylcholine release from the cerebral cortex and medulla. *The Journal of Physiology*, *186*(2), 321–332.

Minces, V., Pinto, L., Dan, Y., & Chiba, A. A. (2017). Cholinergic shaping of neural correlations. *Proceedings of the National Academy of Sciences*, *114*(22), 5725–5730.

Mitchell, R., Loeschcke, H., Severinghaus, J., Richardson, B., & Massion, W. (1963). Regions of respiratory chemosensitivity on the surface of the medulla. *Annals of the New York Academy of Sciences*, *109*(2), 661–681.

Moehle, M. S., Pancani, T., Byun, N., Yohn, S. E., Wilson, G. H., Dickerson, J. W., Remke, D. H., Xiang, Z., Niswender, C. M., Wess, J., Jones, C. K., Lindsley, C. W., Rook, J. M., & Conn, P. J. (2017). Cholinergic Projections to the Substantia Nigra Pars Reticulata Inhibit Dopamine Modulation of Basal Ganglia through the M4 Muscarinic Receptor. *Neuron*, *96*(6), 1358-1372.e4. https://doi.org/10.1016/j.neuron.2017.12.008

Montandon, G., Liu, H., & Horner, R. L. (2016). Contribution of the respiratory network to rhythm and motor output revealed by modulation of GIRK channels, somatostatin and neurokinin-1 receptors. *Scientific Reports*, *6*(1), 1–15.

Monteau, R., Morin, D., & Hilaire, G. (1990). Acetylcholine and central chemosensitivity:

In vitro study in the newborn rat. *Respiration Physiology*, *81*(2), 241–253. https://doi.org/10.1016/0034-5687(90)90049-5

Moore, J. D., Deschênes, M., Furuta, T., Huber, D., Smear, M. C., Demers, M., & Kleinfeld, D. (2013). Hierarchy of orofacial rhythms revealed through whisking and breathing. *Nature*, *497*(7448), 205–210.

Moore, J. D., Kleinfeld, D., & Wang, F. (2014). How the brainstem controls orofacial behaviors comprised of rhythmic actions. *Trends in Neurosciences*, *37*(7), 370–380.

Morgado-Valle, C., Fernandez-Ruiz, J., Lopez-Meraz, L., & Beltran-Parrazal, L. (2015). Substitution of extracellular Ca2+ by Sr2+ prolongs inspiratory burst in pre-Bötzinger complex inspiratory neurons. *Journal of Neurophysiology*, *113*(4), 1175–1183.

Moser, N., Mechawar, N., Jones, I., Gochberg-Sarver, A., Orr-Urtreger, A., Plomann, M., Salas, R., Molles, B., Marubio, L., Roth, U., & others. (2007). Evaluating the suitability of nicotinic acetylcholine receptor antibodies for standard immunodetection procedures. *Journal of Neurochemistry*, *102*(2), 479–492.

Muñoz-Manchado, A. B., Gonzales, C. B., Zeisel, A., Munguba, H., Bekkouche, B., Skene, N. G., Lönnerberg, P., Ryge, J., Harris, K. D., Linnarsson, S., & others. (2018). Diversity of interneurons in the dorsal striatum revealed by single-cell RNA sequencing and PatchSeq. *Cell Reports*, *24*(8), 2179–2190.

Muñoz-Ortiz, J., Muñoz-Ortiz, E., López-Meraz, L., Beltran-Parrazal, L., & Morgado-Valle, C. (2019). The pre-Bötzinger complex: Generation and modulation of respiratory rhythm. *Neurología (English Edition)*, *34*(7), 461–468. https://doi.org/10.1016/j.nrleng.2018.05.006

Murakoshi, T., Suzue, T., & Tamai, S. (1985). A pharmacological study on respiratory rhythm in the isolated brainstem-spinal cord preparation of the newborn rat. *British Journal of Pharmacology*, *86*(1), 95–104.

Nattie, E. E., & Li, A. (1990). Ventral medulla sites of muscarinic receptor subtypes

involved in cardiorespiratory control. *Journal of Applied Physiology*, *69*(1), 33–41.

Nattie, E., & Li, A. (2010). Central chemoreception in wakefulness and sleep: Evidence for a distributed network and a role for orexin. *Journal of Applied Physiology*, *108*(5), 1417–1424.

Nattie, E., & Li, A. (2011). Central chemoreceptors: Locations and functions. *Comprehensive Physiology*, *2*(1), 221–254.

Nattie, E., Wood, J., Mega, A., & Goritski, W. (1989). Rostral ventrolateral medulla muscarinic receptor involvement in central ventilatory chemosensitivity. *Journal of Applied Physiology*, *66*(3), 1462–1470.

Nectow, A. R., & Nestler, E. J. (2020). Viral tools for neuroscience. *Nature Reviews Neuroscience*, *21*(12), 669–681. https://doi.org/10.1038/s41583-020-00382-z

Newman, E. L., Gupta, K., Climer, J. R., Monaghan, C. K., & Hasselmo, M. E. (2012). Cholinergic modulation of cognitive processing: Insights drawn from computational models. *Frontiers in Behavioral Neuroscience*, *6*, 24.

Nieuwenhuis, B., Haenzi, B., Hilton, S., Carnicer-Lombarte, A., Hobo, B., Verhaagen, J., & Fawcett, J. W. (2021). Optimization of adeno-associated viral vector-mediated transduction of the corticospinal tract: Comparison of four promoters. *Gene Therapy*, *28*(1–2), 56–74. https://doi.org/10.1038/s41434-020-0169-1

Nurse, C. A. (2010). Neurotransmitter and neuromodulatory mechanisms at peripheral arterial chemoreceptors. *Experimental Physiology*, *95*(6), 657–667.

Oke, Y., Miwakeichi, F., Oku, Y., Hirrlinger, J., & Hülsmann, S. (2018). Cell type-dependent activation sequence during rhythmic bursting in the preBötzinger complex in respiratory rhythmic slices from mice. *Frontiers in Physiology*, *9*, 1219.

Okunomiya, T., Hioki, H., Nishimura, C., Yawata, S., Imayoshi, I., Kageyama, R., Takahashi, R., & Watanabe, D. (2020). Generation of a MOR-CreER knock-in mouse line to study cells and neural circuits involved in mu opioid receptor signaling. *Genesis*, *58*(1), e23341.

Onimaru, H., & Homma, I. (2003). A Novel Functional Neuron Group for Respiratory Rhythm Generation in the Ventral Medulla. *The Journal of Neuroscience*, *23*(4), 1478–1486. https://doi.org/10.1523/JNEUROSCI.23-04-01478.2003

Onimaru, H., Ikeda, K., & Kawakami, K. (2008). CO2-sensitive preinspiratory neurons of the parafacial respiratory group express Phox2b in the neonatal rat. *Journal of Neuroscience*, *28*(48), 12845–12850.

Pagliardini, S., Greer, J. J., Funk, G. D., & Dickson, C. T. (2012). State-Dependent Modulation of Breathing in Urethane-Anesthetized Rats. *Journal of Neuroscience*, *32*(33), 11259–11270. https://doi.org/10.1523/JNEUROSCI.0948-12.2012

Pagliardini, S., Janczewski, W. A., Tan, W., Dickson, C. T., Deisseroth, K., & Feldman, J. L. (2011). Active Expiration Induced by Excitation of Ventral Medulla in Adult Anesthetized Rats. *Journal of Neuroscience*, *31*(8), 2895–2905. https://doi.org/10.1523/JNEUROSCI.5338-10.2011

Pagliardini, S., Ren, J., & Greer, J. J. (2003). Ontogeny of the Pre-Bötzinger Complex in Perinatal Rats. *The Journal of Neuroscience*, *23*(29), 9575–9584. https://doi.org/10.1523/JNEUROSCI.23-29-09575.2003

Peng, C., Yan, Y., Kim, V. J., Engle, S. E., Berry, J. N., McIntosh, J. M., Neve, R. L., & Drenan, R. M. (2019). Gene editing vectors for studying nicotinic acetylcholine receptors in cholinergic transmission. *European Journal of Neuroscience*, *50*(3), 2224–2238. https://doi.org/10.1111/ejn.13957

Picardo, M. C. D., Weragalaarachchi, K. T., Akins, V. T., & Del Negro, C. A. (2013). Physiological and morphological properties of Dbx1-derived respiratory neurons in the pre-Bötzinger complex of neonatal mice. *The Journal of Physiology*, *591*(10), 2687–2703.

Picciotto, M. R., Higley, M. J., & Mineur, Y. S. (2012). Acetylcholine as a Neuromodulator: Cholinergic Signaling Shapes Nervous System Function and Behavior. *Neuron*, *76*(1), 116–129. https://doi.org/10.1016/j.neuron.2012.08.036

Poppi, L. A., Holt, J. C., Lim, R., & Brichta, A. M. (2020). A review of efferent cholinergic synaptic transmission in the vestibular periphery and its functional implications. *Journal of Neurophysiology*, *123*(2), 608–629.

Ramirez, J.-M., & Baertsch, N. (2018a). Defining the rhythmogenic elements of mammalian breathing. *Physiology*, *33*(5), 302–316.

Ramirez, J.-M., & Baertsch, N. A. (2018b). The Dynamic Basis of Respiratory Rhythm Generation: One Breath at a Time. *Annual Review of Neuroscience*, *41*(1), 475–499. https://doi.org/10.1146/annurev-neuro-080317-061756

Rekling, J. C., & Feldman, J. L. (1997). Bidirectional Electrical Coupling Between Inspiratory Motoneurons in the Newborn Mouse Nucleus Ambiguus. *Journal of Neurophysiology*, *78*(6), 3508–3510. https://doi.org/10.1152/jn.1997.78.6.3508

Ren, J., Qin, C., Hu, F., Tan, J., Qiu, L., Zhao, S., Feng, G., & Luo, M. (2011). Habenula "cholinergic" neurons corelease glutamate and acetylcholine and activate postsynaptic neurons via distinct transmission modes. *Neuron*, *69*(3), 445–452.

Richter, D. W., & Smith, J. C. (2014). Respiratory rhythm generation in vivo. *Physiology*, *29*(1), 58–71.

Rossi, J., Balthasar, N., Olson, D., Scott, M., Berglund, E., Lee, C. E., Choi, M. J., Lauzon, D., Lowell, B. B., & Elmquist, J. K. (2011). Melanocortin-4 Receptors Expressed by Cholinergic Neurons Regulate Energy Balance and Glucose Homeostasis. *Cell Metabolism*, *13*(2), 195–204. https://doi.org/10.1016/j.cmet.2011.01.010

Rothermel, M., Brunert, D., Zabawa, C., Diaz-Quesada, M., & Wachowiak, M. (2013). Transgene Expression in Target-Defined Neuron Populations Mediated by Retrograde Infection with Adeno-Associated Viral Vectors. *Journal of Neuroscience*, *33*(38), 15195–15206. https://doi.org/10.1523/JNEUROSCI.1618-13.2013

Ruggiero, D. A., Giuliano, R., Anwar, M., Stornetta, R., & Reis, D. J. (1990a). Anatomical substrates of cholinergic-autonomic regulation in the rat. *Journal of Comparative*

Neurology, *292*(1), 1–53.

Ruggiero, D. A., Giuliano, R., Anwar, M., Stornetta, R., & Reis, D. J. (1990b). Anatomical substrates of cholinergic-autonomic regulation in the rat. *Journal of Comparative Neurology*, *292*(1), 1–53.

Ruggiero, D., Pickel, V., Milner, T., Anwar, M., Otake, K., Mtui, E., & Park, D. (2019). Viscerosensory processing in nucleus tractus solitarii: Structural and neurochemical substrates. In *Nucleus of the solitary tract* (pp. 3–34). CRC Press.

Rybak, I. A. (n.d.). *Rhythmic Bursting in the Pre-Bötzinger Complex: Mechanisms and Models*. 23.

Saunders, A., & Sabatini, B. L. (2015). Cre Activated and Inactivated Recombinant Adeno-Associated Viral Vectors for Neuronal Anatomical Tracing or Activity Manipulation. *Current Protocols in Neuroscience*, *72*(1). https://doi.org/10.1002/0471142301.ns0124s72

Saxon, D. W., Robertson, G. N., & Hopkins, D. A. (1996). Ultrastructure and synaptology of the nucleus ambiguus in the rat: The semicompact and loose formations. *The Journal of Comparative Neurology*, *375*(1), 109–127. https://doi.org/10.1002/(SICI)1096-9861(19961104)375:1<109::AID-CNE7>3.0.CO;2-7

Schäfer, M. K.-H., Eiden, L. E., & Weihe, E. (1998). Cholinergic neurons and terminal fields revealed by immunohistochemistry for the vesicular acetylcholine transporter. I. Central nervous system. *Neuroscience*, *84*(2), 331–359. https://doi.org/10.1016/S0306-4522(97)00516-2

Schultz, B. R., & Chamberlain, J. S. (2008). Recombinant Adeno-associated Virus Transduction and Integration. *Molecular Therapy*, *16*(7), 1189–1199. https://doi.org/10.1038/mt.2008.103

Schwarzacher, S. W., Smith, J. C., & Richter, D. W. (1995). Pre-Botzinger complex in the cat. *Journal of Neurophysiology*, *73*(4), 1452–1461.

https://doi.org/10.1152/jn.1995.73.4.1452

Shao, X., & Feldman, J. (2000). Acetylcholine modulates respiratory pattern: Effects mediated by M3-like receptors in preBotzinger complex inspiratory neurons. *Journal of Neurophysiology*, *83*(3), 1243–1252.

Shao, X. M., & Feldman, J. L. (2001). Mechanisms underlying regulation of respiratory pattern by nicotine in preBotzinger complex. *Journal of Neurophysiology*, *85*(6), 2461–2467.

Shao, X. M., & Feldman, J. L. (2005). Cholinergic neurotransmission in the preBÖtzinger Complex modulates excitability of inspiratory neurons and regulates respiratory rhythm. *Neuroscience*, *130*(4), 1069–1081. https://doi.org/10.1016/j.neuroscience.2004.10.028

Shao, X. M., & Feldman, J. L. (2007). Efficient measurement of endogenous neurotransmitters in small localized regions of central nervous systems in vitro with HPLC. *Journal of Neuroscience Methods*, *160*(2), 256–263.

Shao, X. M., & Feldman, J. L. (2009). Central cholinergic regulation of respiration: Nicotinic receptors. *Acta Pharmacologica Sinica*, *30*(6), 761–770. https://doi.org/10.1038/aps.2009.88

Sherman, D., Worrell, J. W., Cui, Y., & Feldman, J. L. (2015). Optogenetic perturbation of preBötzinger complex inhibitory neurons modulates respiratory pattern. *Nature Neuroscience*, *18*(3), 408–414. https://doi.org/10.1038/nn.3938

Silva, J. N., Oliveira, L. M., Souza, F. C., Moreira, T. S., & Takakura, A. C. (2019). Distinct pathways to the parafacial respiratory group to trigger active expiration in adult rats. *American Journal of Physiology-Lung Cellular and Molecular Physiology*, ajplung.00467.2018. https://doi.org/10.1152/ajplung.00467.2018

Simmons, D. D., Bertolotto, C., Typpo, K., Clay, A., & Wu, M. (n.d.). *Differential development of cholinergic-like neurons in the superior olive: A light microscopic study*. 11.

Sirieix, C., Gervasoni, D., Luppi, P.-H., & Léger, L. (2012). Role of the Lateral Paragigantocellular Nucleus in the Network of Paradoxical (REM) Sleep: An Electrophysiological and Anatomical Study in the Rat. *PLoS ONE*, *7*(1), e28724. https://doi.org/10.1371/journal.pone.0028724

Smith, J. C., Abdala, A. P. L., Borgmann, A., Rybak, I. A., & Paton, J. F. R. (2013). Brainstem respiratory networks: Building blocks and microcircuits. *Trends in Neurosciences*, *36*(3), 152–162. https://doi.org/10.1016/j.tins.2012.11.004

Smith, J. C., Abdala, A. P. L., Rybak, I. A., & Paton, J. F. R. (2009). Structural and functional architecture of respiratory networks in the mammalian brainstem. *Philosophical Transactions of the Royal Society B: Biological Sciences*, *364*(1529), 2577–2587. https://doi.org/10.1098/rstb.2009.0081

Smith, J., Ellenberger, H., Ballanyi, K., Richter, D., & Feldman, J. (1991). Pre-Botzinger complex: A brainstem region that may generate respiratory rhythm in mammals. *Science*, *254*(5032), 726–729. https://doi.org/10.1126/science.1683005

Sobrinho, C. R., Kuo, F.-S., Barna, B. F., Moreira, T. S., & Mulkey, D. K. (2016). Cholinergic control of ventral surface chemoreceptors involves Gq/inositol 1,4,5-trisphosphate-mediated inhibition of KCNQ channels: Cholinergic modulation of ventral surface chemoreceptors. *The Journal of Physiology*, *594*(2), 407–419. https://doi.org/10.1113/JP271761

Song, D., Wang, D., Yang, Q., Yan, T., Wang, Z., Yan, Y., Zhao, J., Xie, Z., Liu, Y., Ke, Z., Qazi, T. J., Li, Y., Wu, Y., Shi, Q., Lang, Y., Zhang, H., Huang, T., Wang, C., Quan, Z., & Qing, H. (2020). The lateralization of left hippocampal CA3 during the retrieval of spatial working memory. *Nature Communications*, *11*(1), 2901. https://doi.org/10.1038/s41467-020-16698-4

Souza, G. M. P. R., Kanbar, R., Stornetta, D. S., Abbott, S. B. G., Stornetta, R. L., & Guyenet, P. G. (2018). Breathing regulation and blood gas homeostasis after near complete lesions of the retrotrapezoid nucleus in adult rats: Retrotrapezoid nucleus,

breathing and PCO2 homeostasis. *The Journal of Physiology*, *596*(13), 2521–2545. https://doi.org/10.1113/JP275866

Spann, BryanM., & Grofova, I. (1992). Cholinergic and non-cholinergic neurons in the rat pedunculopontine tegmental nucleus. *Anatomy and Embryology*, *186*(3). https://doi.org/10.1007/BF00174143

Srivastava, A. (2016). In vivo tissue-tropism of adeno-associated viral vectors. *Current Opinion in Virology*, *21*, 75–80. https://doi.org/10.1016/j.coviro.2016.08.003

STEWART, W. C., & ANDERSON, E. A. (1968). Effect of a cholinesterase inhibitor when injected into the medulla of the rabbit. *Journal of Pharmacology and Experimental Therapeutics*, *162*(2), 309–318.

Stornetta, R. L., Macon, C. J., Nguyen, T. M., Coates, M. B., & Guyenet, P. G. (2013). Cholinergic neurons in the mouse rostral ventrolateral medulla target sensory afferent areas. *Brain Structure and Function*, *218*(2), 455–475. https://doi.org/10.1007/s00429-012-0408-3

Stornetta, R. L., Rosin, D. L., Wang, H., Sevigny, C. P., Weston, M. C., & Guyenet, P. G. (2003). A group of glutamatergic interneurons expressing high levels of both neurokinin-1 receptors and somatostatin identifies the region of the pre-Bötzinger complex: Somatostatin in the Pre-BötC. *Journal of Comparative Neurology*, *455*(4), 499–512. https://doi.org/10.1002/cne.10504

Sugimura, T., & Saito, Y. (2021). Distinct proportions of cholinergic neurons in the rat prepositus hypoglossi nucleus according to their cerebellar projection targets. *Journal of Comparative Neurology*, *529*(7), 1541–1552.

Sun, L., Tang, Y., Yan, K., Yu, J., Zou, Y., Xu, W., Xiao, K., Zhang, Z., Li, W., Wu, B., Hu, Z., Chen, K., Fu, Z. F., Dai, J., & Cao, G. (2019). Differences in neurotropism and neurotoxicity among retrograde viral tracers. *Molecular Neurodegeneration*, *14*(1), 8. https://doi.org/10.1186/s13024-019-0308-6

Takakura, A. C., Barna, B. F., Cruz, J. C., Colombari, E., & Moreira, T. S. (2014). Phox2b-

expressing retrotrapezoid neurons and the integration of central and peripheral chemosensory control of breathing in conscious rats. *Experimental Physiology*, *99*(3), 571–585.

Takeshita, S., Sasa, M., Ishihara, K., Matsubayashi, H., Yajin, K., Okada, M., Izumi, R., Arita, K., & Kurisu, K. (1999). Cholinergic and glutamatergic transmission in medial vestibular nucleus neurons responding to lateral roll tilt in rats. *Brain Research*, *840*(1–2), 99–105.

Tan, W., Janczewski, W. A., Yang, P., Shao, X. M., Callaway, E. M., & Feldman, J. L. (2008). Silencing preBötzinger complex somatostatin-expressing neurons induces persistent apnea in awake rat. *Nature Neuroscience*, *11*(5), 538–540.

Tan, W., Pagliardini, S., Yang, P., Janczewski, W. A., & Feldman, J. L. (2010). Projections of preBötzinger Complex neurons in adult rats. *The Journal of Comparative Neurology*, *518*(10), 1862–1878. https://doi.org/10.1002/cne.22308

Tang, W., Ehrlich, I., Wolff, S. B. E., Michalski, A.-M., Wolfl, S., Hasan, M. T., Luthi, A., & Sprengel, R. (2009). Faithful Expression of Multiple Proteins via 2A-Peptide Self-Processing: A Versatile and Reliable Method for Manipulating Brain Circuits. *Journal of Neuroscience*, *29*(27), 8621–8629. https://doi.org/10.1523/JNEUROSCI.0359-09.2009

Teppema, L. J., & Baby, S. (2011). Anesthetics and control of breathing. *Respiratory Physiology & Neurobiology*, *177*(2), 80–92. https://doi.org/10.1016/j.resp.2011.04.006

Tervo, D. G. R., Hwang, B.-Y., Viswanathan, S., Gaj, T., Lavzin, M., Ritola, K. D., Lindo, S., Michael, S., Kuleshova, E., Ojala, D., Huang, C.-C., Gerfen, C. R., Schiller, J., Dudman, J. T., Hantman, A. W., Looger, L. L., Schaffer, D. V., & Karpova, A. Y. (2016). A Designer AAV Variant Permits Efficient Retrograde Access to Projection Neurons. *Neuron*, *92*(2), 372–382. https://doi.org/10.1016/j.neuron.2016.09.021

Thoby-Brisson, M. (2005). Emergence of the Pre-Botzinger Respiratory Rhythm

Generator in the Mouse Embryo. *Journal of Neuroscience*, *25*(17), 4307–4318. https://doi.org/10.1523/JNEUROSCI.0551-05.2005

Threlfell, S., Lalic, T., Platt, N. J., Jennings, K. A., Deisseroth, K., & Cragg, S. J. (2012). Striatal Dopamine Release Is Triggered by Synchronized Activity in Cholinergic Interneurons. *Neuron*, *75*(1), 58–64. https://doi.org/10.1016/j.neuron.2012.04.038

Tokumaru, T. (1968). The nature of toxins of herpes simplex virus. *Archiv Für Die Gesamte Virusforschung*, *24*(1–2), 104–122.

Toor, R. U. A. S., Sun, Q.-J., Kumar, N. N., Le, S., Hildreth, C. M., Phillips, J. K., & McMullan, S. (2019). Neurons in the Intermediate Reticular Nucleus Coordinate Postinspiratory Activity, Swallowing, and Respiratory-Sympathetic Coupling in the Rat. *The Journal of Neuroscience*, *39*(49), 9757–9766. https://doi.org/10.1523/JNEUROSCI.0502-19.2019

Tupal, S., Rieger, M. A., Ling, G.-Y., Park, T. J., Dougherty, J. D., Goodchild, A. K., & Gray, P. A. (2014). Testing the role of preBötzinger Complex somatostatin neurons in respiratory and vocal behaviors. *European Journal of Neuroscience*, *40*(7), 3067–3077. https://doi.org/10.1111/ejn.12669

Ugolini, G., Kuypers, H., & Simmons, A. (1987). Retrograde transneuronal transfer of herpes simplex virus type 1 (HSV 1) from motoneurones. *Brain Research*, *422*(2), 242–256.

Van Dort, C. J., Zachs, D. P., Kenny, J. D., Zheng, S., Goldblum, R. R., Gelwan, N. A., Ramos, D. M., Nolan, M. A., Wang, K., Weng, F.-J., Lin, Y., Wilson, M. A., & Brown, E. N. (2015). Optogenetic activation of cholinergic neurons in the PPT or LDT induces REM sleep. *Proceedings of the National Academy of Sciences*, *112*(2), 584–589. https://doi.org/10.1073/pnas.1423136112

Varga, A. G., Maletz, S. N., Bateman, J. T., Reid, B. T., & Levitt, E. S. (2021). Neurochemistry of the Kölliker-Fuse nucleus from a respiratory perspective. *Journal of Neurochemistry*, *156*(1), 16–37. https://doi.org/10.1111/jnc.15041

Volgin, D. V., Rukhadze, I., & Kubin, L. (2008). Hypoglossal premotor neurons of the intermediate medullary reticular region express cholinergic markers. *Journal of Applied Physiology*, *105*(5), 1576–1584.

Von Engelhardt, J., Eliava, M., Meyer, A. H., Rozov, A., & Monyer, H. (2007). Functional characterization of intrinsic cholinergic interneurons in the cortex. *Journal of Neuroscience*, *27*(21), 5633–5642.

WADA, E. (1989). Distribution of alpha 2. Alpha 3. Alpha 4 and beta 2 neuronal nicotinic receptor subunit hybridization histochemical study in the rat. *J. Comp. Neurol*, *284*, 314–335.

Wada, E., McKinnon, D., Heinemann, S., Patrick, J., & Swanson, L. W. (1990). The distribution of mRNA encoded by a new member of the neuronal nicotinic acetylcholine receptor gene family (α5) in the rat central nervous system. *Brain Research*, *526*(1), 45–53.

Wallén-Mackenzie, \AAsa, Wootz, H., & Englund, H. (2010). Genetic inactivation of the vesicular glutamate transporter 2 (VGLUT2) in the mouse: What have we learnt about functional glutamatergic neurotransmission? *Upsala Journal of Medical Sciences*, *115*(1), 11–20.

Wang, D., He, X., Zhao, Z., Feng, Q., Lin, R., Sun, Y., Ding, T., Xu, F., Luo, M., & Zhan, C. (2015). Whole-brain mapping of the direct inputs and axonal projections of POMC and AgRP neurons. *Frontiers in Neuroanatomy*, *9*, 40.

Wang, H.-L., & Morales, M. (2009). Pedunculopontine and laterodorsal tegmental nuclei contain distinct populations of cholinergic, glutamatergic and GABAergic neurons in the rat. *European Journal of Neuroscience*, *29*(2), 340–358. https://doi.org/10.1111/j.1460-9568.2008.06576.x

Wang, J., & Zhang, L. (2021). Retrograde axonal transport property of adeno-associated virus and its possible application in future. *Microbes and Infection*, *23*(8), 104829. https://doi.org/10.1016/j.micinf.2021.104829

Wang, Y., Sanghvi, M., Gribizis, A., Zhang, Y., Song, L., Morley, B., Barson, D., Santos-Sacchi, J., Navaratnam, D. S., & Crair, M. (2020). Efferent feedback enforces bilateral coupling of spontaneous activity in the developing auditory system. *BioRxiv*.

Warner-Schmidt, J. L., Schmidt, E. F., Marshall, J. J., Rubin, A. J., Arango-Lievano, M., Kaplitt, M. G., Ibañez-Tallon, I., Heintz, N., & Greengard, P. (2012). Cholinergic interneurons in the nucleus accumbens regulate depression-like behavior. *Proceedings of the National Academy of Sciences*, *109*(28), 11360–11365.

Weiss, A. R., Liguore, W. A., Domire, J. S., Button, D., & McBride, J. L. (2020). Intra-striatal AAV2.retro administration leads to extensive retrograde transport in the rhesus macaque brain: Implications for disease modeling and therapeutic development. *Scientific Reports*, *10*(1), 6970. https://doi.org/10.1038/s41598-020-63559-7

Wessler, I., & Kirkpatrick, C. (2008). Acetylcholine beyond neurons: The non-neuronal cholinergic system in humans. *British Journal of Pharmacology*, *154*(8), 1558–1571.

Weston, M. C., Stornetta, R. L., & Guyenet, P. G. (2004). Glutamatergic neuronal projections from the marginal layer of the rostral ventral medulla to the respiratory centers in rats. *Journal of Comparative Neurology*, *473*(1), 73–85.

Winter, S. M., Fresemann, J., Schnell, C., Oku, Y., Hirrlinger, J., & Hülsmann, S. (2009). Glycinergic interneurons are functionally integrated into the inspiratory network of mouse medullary slices. *Pflügers Archiv-European Journal of Physiology*, *458*(3), 459–469.

Witten, I. B., Lin, S.-C., Brodsky, M., Prakash, R., Diester, I., Anikeeva, P., Gradinaru, V., Ramakrishnan, C., & Deisseroth, K. (2010). Cholinergic interneurons control local circuit activity and cocaine conditioning. *Science*, *330*(6011), 1677–1681.

Woolf, N. J. (1991). Cholinergic systems in mammalian brain and spinal cord. *Progress in*

Neurobiology, *37*(6), 475–524.

Xu, M., Chung, S., Zhang, S., Zhong, P., Ma, C., Chang, W.-C., Weissbourd, B., Sakai, N., Luo, L., Nishino, S., & others. (2015). Basal forebrain circuit for sleep-wake control. *Nature Neuroscience*, *18*(11), 1641–1647.

Yang, C. F., & Feldman, J. L. (2018). Efferent projections of excitatory and inhibitory preBötzinger Complex neurons. *Journal of Comparative Neurology*, *526*(8), 1389–1402. https://doi.org/10.1002/cne.24415

Yang, C. F., Kim, E. J., Callaway, E. M., & Feldman, J. L. (2019). Monosynaptic projections to excitatory and inhibitory preBötzinger Complex neurons. *BioRxiv*, 694711. https://doi.org/10.1101/694711

Yao, F., Zhang, E., Gao, Z., Ji, H., Marmouri, M., & Xia, X. (2018). Did you choose appropriate tracer for retrograde tracing of retinal ganglion cells? The differences between cholera toxin subunit B and Fluorogold. *PLOS ONE*, *13*(10), e0205133. https://doi.org/10.1371/journal.pone.0205133

Zaborszky, L., Hoemke, L., Mohlberg, H., Schleicher, A., Amunts, K., & Zilles, K. (2008). Stereotaxic probabilistic maps of the magnocellular cell groups in human basal forebrain. *Neuroimage*, *42*(3), 1127–1141.

Zayia, L. C., & Tadi, P. (2020). Neuroanatomy, motor neuron. *StatPearls [Internet]*.

Zhang, G.-W., Shen, L., Zhong, W., Xiong, Y., Zhang, L. I., & Tao, H. W. (2018). Transforming Sensory Cues into Aversive Emotion via Septal-Habenular Pathway. *Neuron*, *99*(5), 1016-1028.e5. https://doi.org/10.1016/j.neuron.2018.07.023

Zheng, F., Nixdorf-Bergweiler, B. E., Edelmann, E., van Brederode, J. F., & Alzheimer, C. (2020). Muscarinic Modulation of Morphologically Identified Glycinergic Neurons in the Mouse PreBötzinger Complex. *Frontiers in Cellular Neuroscience*, *13*, 562.

Zhou, K., Cherra III, S. J., Goncharov, A., & Jin, Y. (2017). Asynchronous cholinergic drive correlates with excitation-inhibition imbalance via a neuronal Ca2+ sensor

protein. *Cell Reports*, *19*(6), 1117–1129.

Ahmed, N. Y., Knowles, R., & Dehorter, N. (2019). New Insights Into Cholinergic Neuron Diversity. *Frontiers in Molecular Neuroscience*, *12*, 204. https://doi.org/10.3389/fnmol.2019.00204

Ai, J., Epstein, P. N., Gozal, D., Yang, B., Wurster, R., & Cheng, Z. J. (2007). Morphology and topography of nucleus ambiguus projections to cardiac ganglia in rats and mice. *Neuroscience*, *149*(4), 845–860. https://doi.org/10.1016/j.neuroscience.2007.07.062

Allaway, K. C., & Machold, R. (2017). Developmental specification of forebrain cholinergic neurons. *Developmental Biology*, *421*(1), 1–7.

Alsahafi, Z., Dickson, C. T., & Pagliardini, S. (2015). Optogenetic excitation of preBötzinger complex neurons potently drives inspiratory activity *in vivo*: PreBötzinger complex optostimulation. *The Journal of Physiology*, *593*(16), 3673–3692. https://doi.org/10.1113/JP270471

Altschuler, S. M., Bao, X., & Miselis, R. R. (1991). Dendritic architecture of nucleus ambiguus motoneurons projecting to the upper alimentary tract in the rat. *The Journal of Comparative Neurology*, *309*(3), 402–414. https://doi.org/10.1002/cne.903090309

Anderson, T. M., Garcia, A. J., Baertsch, N. A., Pollak, J., Bloom, J. C., Wei, A. D., Rai, K. G., & Ramirez, J.-M. (2016). A novel excitatory network for the control of breathing. *Nature*, *536*(7614), 76–80. https://doi.org/10.1038/nature18944

Aserinsky, E. (1965). Periodic respiratory pattern occurring in conjunction with eye movements during sleep. *Science*, *150*(3697), 763–766.

Ashhad, S., & Feldman, J. L. (2019). *Network synchronization and synchrony propagation: Emergent elements of inspiration* [Preprint]. Neuroscience. https://doi.org/10.1101/664946

Ashhad, S., & Feldman, J. L. (2020). Emergent Elements of Inspiratory Rhythmogenesis: Network Synchronization and Synchrony Propagation. *Neuron*, *106*(3), 482-497.e4. https://doi.org/10.1016/j.neuron.2020.02.005

Ausborn, J., Koizumi, H., Barnett, W. H., John, T. T., Zhang, R., Molkov, Y. I., Smith, J. C., & Rybak, I. A. (2018). Organization of the core respiratory network: Insights from optogenetic and modeling studies. *PLoS Computational Biology*, *14*(4), e1006148.

Baertsch, N. A., Baertsch, H. C., & Ramirez, J. M. (2018). The interdependence of excitation and inhibition for the control of dynamic breathing rhythms. *Nature Communications*, *9*(1), 843. https://doi.org/10.1038/s41467-018-03223-x

Baertsch, N. A., & Ramirez, J.-M. (2019). Insights into the dynamic control of breathing revealed through cell-type-specific responses to substance P. *ELife*, *8*, e51350. https://doi.org/10.7554/eLife.51350

Baertsch, N. A., Severs, L. J., Anderson, T. M., & Ramirez, J.-M. (2019). A spatially dynamic network underlies the generation of inspiratory behaviors. *Proceedings of the National Academy of Sciences*, *116*(15), 7493–7502. https://doi.org/10.1073/pnas.1900523116

Ballantyne, D., & Richter, D. (1984). Post-synaptic inhibition of bulbar inspiratory neurones in the cat. *The Journal of Physiology*, *348*(1), 67–87.

Ballinger, E. C., Ananth, M., Talmage, D. A., & Role, L. W. (2016). Basal forebrain cholinergic circuits and signaling in cognition and cognitive decline. *Neuron*, *91*(6), 1199–1218.

Barmack, N., Baughman, R., & Eckenstein, F. (1992). Cholinergic innervation of the cerebellum of rat, rabbit, cat, and monkey as revealed by choline acetyltransferase activity and immunohistochemistry. *Journal of Comparative Neurology*, *317*(3), 233–249.

Bearer, E., Breakefield, X., Schuback, D., Reese, T., & LaVail, J. (2000). Retrograde

axonal transport of herpes simplex virus: Evidence for a single mechanism and a role for tegument. *Proceedings of the National Academy of Sciences*, *97*(14), 8146–8150.

Bellingham, M. C., & Funk, G. D. (2000). Cholinergic modulation of respiratory brain-stem neurons and its function in sleep–wake state determination. *Clinical and Experimental Pharmacology and Physiology*, *27*(1–2), 132–137.

Bellingham, M. C., & Ireland, M. F. (2002). Contribution of cholinergic systems to state-dependent modulation of respiratory control. *Respiratory Physiology & Neurobiology*, *131*(1–2), 135–144. https://doi.org/10.1016/S1569-9048(02)00043-5

Benagiano, V., Virgintino, D., Flace, P., Girolamo, F., Errede, M., & Roncali, L. (2003). Choline acetyltransferase-containing neurons in the human parietal neocortex. *European Journal of Histochemistry*, *47*(3), 253–256.

Biancardi, V., Saini, J., Pageni, A., Prashaad M., H., Funk, G. D., & Pagliardini, S. (2020). Mapping of the excitatory, inhibitory, and modulatory afferent projections to the anatomically defined active expiratory oscillator in adult male rats. *Journal of Comparative Neurology*, cne.24984. https://doi.org/10.1002/cne.24984

Bieger, D., & Hopkins, D. A. (1987). Viscerotopic representation of the upper alimentary tract in the medulla oblongata in the rat: The nucleus ambiguus. *The Journal of Comparative Neurology*, *262*(4), 546–562. https://doi.org/10.1002/cne.902620408

Bittar, T. P., Pelaez, M. C., Silva, J. C. H., Quessy, F., Lavigne, A.-A., Morency, D., Blanchette, L.-J., Arsenault, E., Cherasse, Y., Seigneur, J., & others. (2021). Chronic Stress Induces Sex-Specific Functional and Morphological Alterations in Corticoaccumbal and Corticotegmental Pathways. *Biological Psychiatry*.

Bonis, J. M., Neumueller, S. E., Krause, K. L., Kiner, T., Smith, A., Marshall, B. D., Qian, B., Pan, L. G., & Forster, H. V. (2010). A role for the Kölliker-Fuse nucleus in cholinergic modulation of breathing at night during wakefulness and NREM sleep.

Journal of Applied Physiology, *109*(1), 159–170. https://doi.org/10.1152/japplphysiol.00933.2009

Bonsi, P., Cuomo, D., Martella, G., Madeo, G., Schirinzi, T., Puglisi, F., Ponterio, G., & Pisani, A. (2011). Centrality of striatal cholinergic transmission in basal ganglia function. *Frontiers in Neuroanatomy*, *5*, 6.

Boskovic, Z., Milne, M. R., Qian, L., Clifton, H. D., McGovern, A. E., Turnbull, M. T., Mazzone, S. B., & Coulson, E. J. (2018). Cholinergic basal forebrain neurons regulate fear extinction consolidation through p75 neurotrophin receptor signaling. *Translational Psychiatry*, *8*(1), 199. https://doi.org/10.1038/s41398-018-0248-x

Boutin, R. C., Alsahafi, Z., & Pagliardini, S. (2017). Cholinergic modulation of the parafacial respiratory group. *The Journal of Physiology*, *595*(4), 1377–1392.

Boutin, R. C. T., Alsahafi, Z., & Pagliardini, S. (2017). Cholinergic modulation of the parafacial respiratory group: Cholinergic modulation of active expiration. *The Journal of Physiology*, *595*(4), 1377–1392. https://doi.org/10.1113/JP273012

Brinkman, J. E., & Sharma, S. (2019). Physiology, respiratory drive. *StatPearls [Internet]*.

Burke, P. G. R., Kanbar, R., Basting, T. M., Hodges, W. M., Viar, K. E., Stornetta, R. L., & Guyenet, P. G. (2015). State-dependent control of breathing by the retrotrapezoid nucleus: RTN, breathing and sleep. *The Journal of Physiology*, *593*(13), 2909–2926. https://doi.org/10.1113/JP270053

Burton, M. D., Johnson, D. C., & Kazemi, H. (1997). The central respiratory effects of acetylcholine vary with CSF pH. *Journal of the Autonomic Nervous System*, *62*(1–2), 27–32. https://doi.org/10.1016/S0165-1838(96)00104-X

Burton, M. D., Nouri, M., & Kazemi, H. (1995). Acetylcholine and central respiratory control: Perturbations of acetylcholine synthesis in the isolated brainstem of the neonatal rat. *Brain Research*, *670*(1), 39–47. https://doi.org/10.1016/0006-8993(94)01249-H

Burton, M., Nouri, K., Baichoo, S., Samuels-Toyloy, N., & Kazemi, H. (1994). Ventilatory

output and acetylcholine: Perturbations in release and muscarinic receptor activation. *Journal of Applied Physiology*, *77*(5), 2275–2284.

Carlson, A. B., & Kraus, G. P. (2018). *Physiology, cholinergic receptors*.

Carroll, M. S., & Ramirez, J.-M. (2013). Cycle-by-cycle assembly of respiratory network activity is dynamic and stochastic. *Journal of Neurophysiology*, *109*(2), 296–305. https://doi.org/10.1152/jn.00830.2011

Case, D. T., Burton, S. D., Gedeon, J. Y., Williams, S.-P. G., Urban, N. N., & Seal, R. P. (2017). Layer- and cell type-selective co-transmission by a basal forebrain cholinergic projection to the olfactory bulb. *Nature Communications*, *8*(1), 652. https://doi.org/10.1038/s41467-017-00765-4

Castle, M. J., Gershenson, Z. T., Giles, A. R., Holzbaur, E. L. F., & Wolfe, J. H. (2014). Adeno-Associated Virus Serotypes 1, 8, and 9 Share Conserved Mechanisms for Anterograde and Retrograde Axonal Transport. *Human Gene Therapy*, *25*(8), 705–720. https://doi.org/10.1089/hum.2013.189

Caulfield, M. P. (1993). Muscarinic receptors—Characterization, coupling and function. *Pharmacology & Therapeutics*, *58*(3), 319–379.

Chokshi, V., Gao, M., Grier, B. D., Owens, A., Wang, H., Worley, P. F., & Lee, H.-K. (2019). Input-specific metaplasticity in the visual cortex requires Homer1a-mediated mGluR5 signaling. *Neuron*, *104*(4), 736–748.

Coddou, C., Bravo, E., & Eugenín, J. (2009). Alterations in cholinergic sensitivity of respiratory neurons induced by pre-natal nicotine: A mechanism for respiratory dysfunction in neonatal mice. *Philosophical Transactions of the Royal Society B: Biological Sciences*, *364*(1529), 2527–2535. https://doi.org/10.1098/rstb.2009.0078

Cui, Y., Kam, K., Sherman, D., Janczewski, W. A., Zheng, Y., & Feldman, J. L. (2016). Defining preBötzinger Complex Rhythm- and Pattern-Generating Neural Microcircuits In Vivo. *Neuron*, *91*(3), 602–614.

https://doi.org/10.1016/j.neuron.2016.07.003

Dani, J. A., & Bertrand, D. (2007). Nicotinic acetylcholine receptors and nicotinic cholinergic mechanisms of the central nervous system. *Annu. Rev. Pharmacol. Toxicol.*, *47*, 699–729.

Datta, S. (2009). Cholinergic Brainstem. In M. D. Binder, N. Hirokawa, & U. Windhorst (Eds.), *Encyclopedia of Neuroscience* (pp. 705–708). Springer Berlin Heidelberg. https://doi.org/10.1007/978-3-540-29678-2_1002

Dautan, D., Hacioğlu Bay, H., Bolam, J. P., Gerdjikov, T. V., & Mena-Segovia, J. (2016). Extrinsic sources of cholinergic innervation of the striatal complex: A whole-brain mapping analysis. *Frontiers in Neuroanatomy*, *10*, 1.

de Sousa Abreu, R. P., Bondarenko, E., & Feldman, J. L. (2021). Phase-and State-Dependent Modulation of Breathing Pattern by preBötzinger Complex Somatostatin Expressing Neurons. *BioRxiv*.

Dehkordi, O., Haxhiu, M. A., Millis, R. M., Dennis, G. C., Kc, P., Jafri, A., Khajavi, M., Trouth, C. O., & Zaidi, S. I. (2004). Expression of α-7 nAChRs on spinal cord–brainstem neurons controlling inspiratory drive to the diaphragm. *Respiratory Physiology & Neurobiology*, *141*(1), 21–34.

Del Negro, C. A., Funk, G. D., & Feldman, J. L. (2018). Breathing matters. *Nature Reviews Neuroscience*, *19*(6), 351–367. https://doi.org/10.1038/s41583-018-0003-6

Del Negro, C. A., Morgado-Valle, C., Hayes, J. A., Mackay, D. D., Pace, R. W., Crowder, E. A., & Feldman, J. L. (2005). Sodium and calcium current-mediated pacemaker neurons and respiratory rhythm generation. *Journal of Neuroscience*, *25*(2), 446–453.

del Toro, E. D., Juiz, J. M., Peng, X., Lindstrom, J., & Criado, M. (1994). Immunocytochemical localization of the α7 subunit of the nicotinic acetylcholine receptor in the rat central nervous system. *Journal of Comparative Neurology*, *349*(3), 325–342.

Dhingra, R. R., Furuya, W. I., Bautista, T. G., Dick, T. E., Galán, R. F., & Dutschmann, M. (2019). Increasing Local Excitability of Brainstem Respiratory Nuclei Reveals a Distributed Network Underlying Respiratory Motor Pattern Formation. *Frontiers in Physiology*, *10*, 887. https://doi.org/10.3389/fphys.2019.00887

Dhingra, R. R., Furuya, W. I., Dick, T. E., & Dutschmann, M. (2021). Response to: The post-inspiratory complex (PiCo), what is the evidence? *The Journal of Physiology*, *599*(1), 361–362.

Dick, T. E., Oku, Y., Romaniuk, J. R., & Cherniack, N. (1993). Interaction between central pattern generators for breathing and swallowing in the cat. *The Journal of Physiology*, *465*(1), 715–730.

Douglas, N. J. (2005). Respiratory physiology: Control of ventilation. In *Principles and practice of sleep medicine* (pp. 224–231). Elsevier.

Dringenberg, H. C., & Vanderwolf, C. (1998). Involvement of direct and indirect pathways in electrocorticographic activation. *Neuroscience & Biobehavioral Reviews*, *22*(2), 243–257.

Duarte, L. F., Farías, M. A., Álvarez, D. M., Bueno, S. M., Riedel, C. A., & González, P. A. (2019). Herpes simplex virus type 1 infection of the central nervous system: Insights into proposed interrelationships with neurodegenerative disorders. *Frontiers in Cellular Neuroscience*, *13*, 46.

Dutschmann, M., & Herbert, H. (2006). The Kölliker-Fuse nucleus gates the postinspiratory phase of the respiratory cycle to control inspiratory off-switch and upper airway resistance in rat. *European Journal of Neuroscience*, *24*(4), 1071–1084. https://doi.org/10.1111/j.1460-9568.2006.04981.x

Eger, E. I., Zhang, Y., Laster, M., Flood, P., Kendig, J. J., & Sonner, J. M. (2002). Acetylcholine receptors do not mediate the immobilization produced by inhaled anesthetics. *Anesthesia & Analgesia*, *94*(6), 1500–1504.

Ellenberger, H., & Feldman, J. (1990). Brainstem connections of the rostral ventral

respiratory group of the rat. *Brain Research*, *513*(1), 35–42.

Ellenberger, H. H. (1999). Nucleus ambiguus and bulbospinal ventral respiratory group neurons in the neonatal rat. *Brain Research Bulletin*, *50*(1), 1–13.

Eugenín, J., & Nicholls, J. G. (1997). Chemosensory and cholinergic stimulation of fictive respiration in isolated cns of neonatal opossum. *The Journal of Physiology*, *501*(2), 425–437. https://doi.org/10.1111/j.1469-7793.1997.425bn.x

Feldman, J. L., Del Negro, C. A., & Gray, P. A. (2013). Understanding the rhythm of breathing: So near, yet so far. *Annual Review of Physiology*, *75*, 423–452.

Feldman, J. L., & Kam, K. (2015). Facing the challenge of mammalian neural microcircuits: Taking a few breaths may help: Principles of mammalian microcircuits controlling breathing. *The Journal of Physiology*, *593*(1), 3–23. https://doi.org/10.1113/jphysiol.2014.277632

Fleming, P. J., Cade, D., Bryan, M. H., & Bryan, A. C. (1980). Congenital central hypoventilation and sleep state. *Pediatrics*, *66*(3), 425–428.

Franklin, K. B., Paxinos, G., & others. (2008). *The mouse brain in stereotaxic coordinates*.

French, I. T., & Muthusamy, K. A. (2018). A review of the pedunculopontine nucleus in Parkinson's disease. *Frontiers in Aging Neuroscience*, *10*, 99.

Fukuda, Y., & Loeschcke, H. H. (1979). A cholinergic mechanism involved in the neuronal excitation by H+ in the respiratory chemosensitive structures of the ventral medulla oblongata of rats in vitro. *Pflügers Archiv*, *379*(2), 125–135.

Fuller, P. M., Saper, C. B., & Lu, J. (2007). The pontine REM switch: Past and present. *The Journal of Physiology*, *584*(3), 735–741.

Furuya, W. I., Bassi, M., Menani, J. V., Colombari, E., Zoccal, D. B., & Colombari, D. S. A. (2020). Modulation of hypercapnic respiratory response by cholinergic transmission in the commissural nucleus of the solitary tract. *Pflügers Archiv - European Journal of Physiology*, *472*(1), 49–60. https://doi.org/10.1007/s00424-019-02341-9

Gang, S., Sato, Y., Kohama, I., & Aoki, M. (1995). Afferent projections to the Bötzinger complex from the upper cervical cord and other respiratory related structures in the brainstem in cats: Retrograde WGA-HRP tracing. *Journal of the Autonomic Nervous System*, *56*(1–2), 1–7.

Garfield, A. S., Patterson, C., Skora, S., Gribble, F. M., Reimann, F., Evans, M. L., Myers, M. G., & Heisler, L. K. (2012). Neurochemical Characterization of Body Weight-Regulating Leptin Receptor Neurons in the Nucleus of the Solitary Tract. *Endocrinology*, *153*(10), 4600–4607. https://doi.org/10.1210/en.2012-1282

Gilbert, K. A., & Lydic, R. (1990). Parabrachial neuron discharge in the cat is altered during the carbachol-induced REM sleep-like state (DCarb). *Neuroscience Letters*, *120*(2), 241–244.

Gilbert, K. A., & Lydic, R. (1994). Pontine cholinergic reticular mechanisms cause state-dependent changes in the discharge of parabrachial neurons. *American Journal of Physiology-Regulatory, Integrative and Comparative Physiology*, *266*(1), R136–R150.

Goridis, C., Dubreuil, V., Thoby-Brisson, M., Fortin, G., & Brunet, J.-F. (2010). Phox2b, congenital central hypoventilation syndrome and the control of respiration. *Seminars in Cell & Developmental Biology*, *21*(8), 814–822.

Grace, K. P., Hughes, S. W., & Horner, R. L. (2013). Identification of the mechanism mediating genioglossus muscle suppression in REM sleep. *American Journal of Respiratory and Critical Care Medicine*, *187*(3), 311–319.

Grace, K. P., Hughes, S. W., & Horner, R. L. (2014). Identification of a pharmacological target for genioglossus reactivation throughout sleep. *Sleep*, *37*(1), 41–50.

Gray, P. A., Hayes, J. A., Ling, G. Y., Llona, I., Tupal, S., Picardo, M. C. D., Ross, S. E., Hirata, T., Corbin, J. G., Eugenin, J., & Del Negro, C. A. (2010). Developmental Origin of PreBotzinger Complex Respiratory Neurons. *Journal of Neuroscience*, *30*(44), 14883–14895. https://doi.org/10.1523/JNEUROSCI.4031-10.2010

Gray, P. A., Janczewski, W. A., Mellen, N., McCrimmon, D. R., & Feldman, J. L. (2001). Normal breathing requires preBötzinger complex neurokinin-1 receptor-expressing neurons. *Nature Neuroscience*, *4*(9), 927–930.

Greer, J., Smith, J., & Feldman, J. (1991). Role of excitatory amino acids in the generation and transmission of respiratory drive in neonatal rat. *The Journal of Physiology*, *437*(1), 727–749.

Gremel, C. M., Chancey, J. H., Atwood, B. K., Luo, G., Neve, R., Ramakrishnan, C., Deisseroth, K., Lovinger, D. M., & Costa, R. M. (2016). Endocannabinoid Modulation of Orbitostriatal Circuits Gates Habit Formation. *Neuron*, *90*(6), 1312–1324. https://doi.org/10.1016/j.neuron.2016.04.043

Gut, N. K. (2016). The pedunculopontine tegmental nucleus—A functional hypothesis from the comparative literature. *Movement Disorders*, *31*(5), 10.

Guthrie, S. (2007). Patterning and axon guidance of cranial motor neurons. *Nature Reviews Neuroscience*, *8*(11), 859–871.

Guyenet, P. G. (2005). Regulation of Ventral Surface Chemoreceptors by the Central Respiratory Pattern Generator. *Journal of Neuroscience*, *25*(39), 8938–8947. https://doi.org/10.1523/JNEUROSCI.2415-05.2005

Haery, L., Deverman, B. E., Matho, K. S., Cetin, A., Woodard, K., Cepko, C., Guerin, K. I., Rego, M. A., Ersing, I., Bachle, S. M., Kamens, J., & Fan, M. (2019). Adeno-Associated Virus Technologies and Methods for Targeted Neuronal Manipulation. *Frontiers in Neuroanatomy*, *13*, 93. https://doi.org/10.3389/fnana.2019.00093

Harris, K. D., Dashevskiy, T., Mendoza, J., Garcia III, A. J., Ramirez, J.-M., & Shea-Brown, E. (2017). Different roles for inhibition in the rhythm-generating respiratory network. *Journal of Neurophysiology*, *118*(4), 2070–2088.

Hasselmo, M. E., & McGaughy, J. (2004). High acetylcholine levels set circuit dynamics for attention and encoding and low acetylcholine levels set dynamics for consolidation. *Progress in Brain Research*, *145*, 207–231.

Haxhiu, M. A., Van Lunteren, E., Van De Graaff, W. B., Strohl, K. P., Bruce, E. N., Mitra, J., & Cherniack, N. S. (1984). Action of nicotine on the respiratory activity of the diaphragm and genioglossus muscles and the nerves that innervate them. *Respiration Physiology*, *57*(2), 153–169.

Heijden, M. E., & Zoghbi, H. Y. (2020). Development of the brainstem respiratory circuit. *WIREs Developmental Biology*, *9*(3). https://doi.org/10.1002/wdev.366

Helseth, A. R., Hernandez-Martinez, R., Hall, V. L., Oliver, M. L., Turner, B. D., Caffall, Z. F., Rittiner, J. E., Shipman, M. K., King, C. S., Gradinaru, V., & others. (2021). Cholinergic neurons engage the integrated stress response for dopamine modulation and skill learning. *Science (New York, NY)*, *372*(6540).

Herman, A. M., Ortiz-Guzman, J., Kochukov, M., Herman, I., Quast, K. B., Patel, J. M., Tepe, B., Carlson, J. C., Ung, K., Selever, J., Tong, Q., & Arenkiel, B. R. (2016). A cholinergic basal forebrain feeding circuit modulates appetite suppression. *Nature*, *538*(7624), 253–256. https://doi.org/10.1038/nature19789

Horner, R. L. (2008a). Neuromodulation of hypoglossal motoneurons during sleep. *Respiratory Physiology & Neurobiology*, *164*(1–2), 179–196.

Horner, R. L. (2008b). Pathophysiology of obstructive sleep apnea. *Journal of Cardiopulmonary Rehabilitation and Prevention*, *28*(5), 289–298.

Hülsmann, S. (2021). The post-inspiratory complex (PiCo), what is the evidence? *The Journal of Physiology*, *599*(1), 357–359.

Jacobs, A., Breakefield, X. O., & Fraefel, C. (1999). HSV-1-based vectors for gene therapy of neurological diseases and brain tumors: Part II. Vector systems and applications. *Neoplasia*, *1*(5), 402–416.

Janczewski, W. A., Tashima, A., Hsu, P., Cui, Y., & Feldman, J. L. (2013). Role of inhibition in respiratory pattern generation. *Journal of Neuroscience*, *33*(13), 5454–5465.

Jones, B. E. (1990). Immunohistochemical study of choline acetyltransferase-

immunoreactive processes and cells innervating the pontomedullary reticular formation in the rat. *Journal of Comparative Neurology*, *295*(3), 485–514.

Kallurkar, P. S., Grover, C., Picardo, M. C. D., & Del Negro, C. A. (2020). Evaluating the burstlet theory of inspiratory rhythm and pattern generation. *Eneuro*, *7*(1).

Kallurkar, P. S., Picardo, M. C. D., Sugimura, Y. K., Saha, M. S., Smith, G. D. C., & Del Negro, C. A. (2021). *Transcriptomes of Electrophysiologically Recorded Dbx1-derived Inspiratory Neurons of the preBötzinger Complex in Neonatal Mice* [Preprint]. Neuroscience. https://doi.org/10.1101/2021.08.01.454659

Kam, K., Worrell, J. W., Janczewski, W. A., Cui, Y., & Feldman, J. L. (2013). Distinct inspiratory rhythm and pattern generating mechanisms in the preBötzinger complex. *Journal of Neuroscience*, *33*(22), 9235–9245.

Kamiya, H., Itoh, K., Yasui, Y., Ino, T., & Mizuno, N. (1988). Somatosensory and auditory relay nucleus in the rostral part of the ventrolateral medulla: A morphological study in the cat. *Journal of Comparative Neurology*, *273*(3), 421–435.

Kinney, H. C., Filiano, J. J., Sleeper, L. A., Mandell, F., Valdes-Dapena, M., & White, W. F. (1995). Decreased muscarinic receptor binding in the arcuate nucleus in sudden infant death syndrome. *Science*, *269*(5229), 1446–1450.

Koizumi, H., Mosher, B., Tariq, M. F., Zhang, R., Koshiya, N., & Smith, J. C. (2016). Voltage-Dependent Rhythmogenic Property of Respiratory Pre-Bötzinger Complex Glutamatergic, Dbx1-Derived, and Somatostatin-Expressing Neuron Populations Revealed by Graded Optogenetic Inhibition. *Eneuro*, *3*(3), ENEURO.0081-16.2016. https://doi.org/10.1523/ENEURO.0081-16.2016

Krishnan, V., Stoppel, D. C., Nong, Y., Johnson, M. A., Nadler, M. J., Ozkaynak, E., Teng, B. L., Nagakura, I., Mohammad, F., Silva, M. A., & others. (2017). Autism gene Ube3a and seizures impair sociability by repressing VTA Cbln1. *Nature*, *543*(7646), 507–512.

Kubin, L. (2001). Carbachol models of REM sleep: Recent developments and new

directions. *Archives Italiennes de Biologie*, *139*(1), 147–168.

Kubin, L., & Fenik, V. (2004). Pontine cholinergic mechanisms and their impact on respiratory regulation. *Respiratory Physiology & Neurobiology*, *143*(2–3), 235–249. https://doi.org/10.1016/j.resp.2004.04.017

Lai, J., Shao, X. M., Pan, R. W., Dy, E., Huang, C. H., & Feldman, J. L. (2001). RT-PCR reveals muscarinic acetylcholine receptor mRNA in the pre-Bötzinger complex. *American Journal of Physiology-Lung Cellular and Molecular Physiology*, *281*(6), L1420–L1424. https://doi.org/10.1152/ajplung.2001.281.6.L1420

Lazaridis, I., Tzortzi, O., Weglage, M., Märtin, A., Xuan, Y., Parent, M., Johansson, Y., Fuzik, J., Fürth, D., Fenno, L. E., & others. (2019). A hypothalamus-habenula circuit controls aversion. *Molecular Psychiatry*, *24*(9), 1351–1368.

Levy, J., Facchinetti, P., Jan, C., Achour, M., Bouvier, C., Brunet, J., Delzescaux, T., & Giuliano, F. (2019). Tridimensional mapping of Phox2b expressing neurons in the brainstem of adult *Macaca fascicularis* and identification of the retrotrapezoid nucleus. *Journal of Comparative Neurology*, cne.24713. https://doi.org/10.1002/cne.24713

Li, F., Jiang, H., Shen, X., Yang, W., Guo, C., Wang, Z., Xiao, M., Cui, L., Luo, W., Kim, B. S., & others. (2021). Sneezing reflex is mediated by a peptidergic pathway from nose to brainstem. *Cell*.

Li, P., Janczewski, W. A., Yackle, K., Kam, K., Pagliardini, S., Krasnow, M. A., & Feldman, J. L. (2016). The peptidergic control circuit for sighing. *Nature*, *530*(7590), 293–297. https://doi.org/10.1038/nature16964

Li, X., Yu, B., Sun, Q., Zhang, Y., Ren, M., Zhang, X., Li, A., Yuan, J., Madisen, L., Luo, Q., Zeng, H., Gong, H., & Qiu, Z. (2018). Generation of a whole-brain atlas for the cholinergic system and mesoscopic projectome analysis of basal forebrain cholinergic neurons. *Proceedings of the National Academy of Sciences*, *115*(2), 415–420. https://doi.org/10.1073/pnas.1703601115

Lim, S. A. O., Kang, U. J., & McGehee, D. S. (2014). Striatal cholinergic interneuron regulation and circuit effects. *Frontiers in Synaptic Neuroscience*, *6*, 22.

Lydic, R., & Baghdoyan, H. A. (1993). Pedunculopontine stimulation alters respiration and increases ACh release in the pontine reticular formation. *American Journal of Physiology-Regulatory, Integrative and Comparative Physiology*, *264*(3), R544–R554.

Magalhães, K. S., da Silva, M. P., Mecawi, A. S., Paton, J. F., Machado, B. H., & Moraes, D. J. (2021). Intrinsic and synaptic mechanisms controlling the expiratory activity of excitatory lateral parafacial neurones of rats. *The Journal of Physiology*.

Maley, B. E. (1996). Immunohistochemical Lòcalization of Neuropeptides and Neurotransmitters in the Nucleus Solitarius. *Chemical Senses*, *21*(3), 367–376. https://doi.org/10.1093/chemse/21.3.367

Mallard, C., Tolcos, M., Leditschke, J., Campbell, P., & Rees, S. (1999). Reduction in choline acetyltransferase immunoreactivity but not muscarinic-m2 receptor immunoreactivity in the brainstem of SIDS infants. *Journal of Neuropathology and Experimental Neurology*, *58*(3), 255–264.

Marcus, C. L. (2001). Sleep-disordered breathing in children. *American Journal of Respiratory and Critical Care Medicine*, *164*(1), 16–30.

Masamizu, Y., Okada, T., Kawasaki, K., Ishibashi, H., Yuasa, S., Takeda, S., Hasegawa, I., & Nakahara, K. (2011). Local and retrograde gene transfer into primate neuronal pathways via adeno-associated virus serotype 8 and 9. *Neuroscience*, *193*, 249–258. https://doi.org/10.1016/j.neuroscience.2011.06.080

McKay, L. C., Janczewski, W. A., & Feldman, J. L. (2005). Sleep-disordered breathing after targeted ablation of preBötzinger complex neurons. *Nature Neuroscience*, *8*(9), 1142–1144.

Mena-Segovia, J. (2016). Structural and functional considerations of the cholinergic brainstem. *Journal of Neural Transmission*, *123*(7), 731–736.

https://doi.org/10.1007/s00702-016-1530-9

Mena-Segovia, J., & Bolam, J. P. (2017). Rethinking the Pedunculopontine Nucleus: From Cellular Organization to Function. *Neuron*, *94*(1), 7–18. https://doi.org/10.1016/j.neuron.2017.02.027

Meredith, G., Blank, B., & Groenewegen, H. (1989). The distribution and compartmental organization of the cholinergic neurons in nucleus accumbens of the rat. *Neuroscience*, *31*(2), 327–345.

Mesulam, M., Mufson, E., Wainer, B., & Levey, A. (1983). Central cholinergic pathways in the rat: An overview based on an alternative nomenclature (Ch1–Ch6). *Neuroscience*, *10*(4), 1185–1201.

Metz, B. (1966). Hypercapnia and acetylcholine release from the cerebral cortex and medulla. *The Journal of Physiology*, *186*(2), 321–332.

Minces, V., Pinto, L., Dan, Y., & Chiba, A. A. (2017). Cholinergic shaping of neural correlations. *Proceedings of the National Academy of Sciences*, *114*(22), 5725–5730.

Mitchell, R., Loeschcke, H., Severinghaus, J., Richardson, B., & Massion, W. (1963). Regions of respiratory chemosensitivity on the surface of the medulla. *Annals of the New York Academy of Sciences*, *109*(2), 661–681.

Moehle, M. S., Pancani, T., Byun, N., Yohn, S. E., Wilson, G. H., Dickerson, J. W., Remke, D. H., Xiang, Z., Niswender, C. M., Wess, J., Jones, C. K., Lindsley, C. W., Rook, J. M., & Conn, P. J. (2017). Cholinergic Projections to the Substantia Nigra Pars Reticulata Inhibit Dopamine Modulation of Basal Ganglia through the M4 Muscarinic Receptor. *Neuron*, *96*(6), 1358-1372.e4. https://doi.org/10.1016/j.neuron.2017.12.008

Montandon, G., Liu, H., & Horner, R. L. (2016). Contribution of the respiratory network to rhythm and motor output revealed by modulation of GIRK channels, somatostatin and neurokinin-1 receptors. *Scientific Reports*, *6*(1), 1–15.

Monteau, R., Morin, D., & Hilaire, G. (1990). Acetylcholine and central chemosensitivity: In vitro study in the newborn rat. *Respiration Physiology*, *81*(2), 241–253. https://doi.org/10.1016/0034-5687(90)90049-5

Moore, J. D., Deschênes, M., Furuta, T., Huber, D., Smear, M. C., Demers, M., & Kleinfeld, D. (2013). Hierarchy of orofacial rhythms revealed through whisking and breathing. *Nature*, *497*(7448), 205–210.

Moore, J. D., Kleinfeld, D., & Wang, F. (2014). How the brainstem controls orofacial behaviors comprised of rhythmic actions. *Trends in Neurosciences*, *37*(7), 370–380.

Morgado-Valle, C., Fernandez-Ruiz, J., Lopez-Meraz, L., & Beltran-Parrazal, L. (2015). Substitution of extracellular Ca2+ by Sr2+ prolongs inspiratory burst in pre-Bötzinger complex inspiratory neurons. *Journal of Neurophysiology*, *113*(4), 1175–1183.

Moser, N., Mechawar, N., Jones, I., Gochberg-Sarver, A., Orr-Urtreger, A., Plomann, M., Salas, R., Molles, B., Marubio, L., Roth, U., & others. (2007). Evaluating the suitability of nicotinic acetylcholine receptor antibodies for standard immunodetection procedures. *Journal of Neurochemistry*, *102*(2), 479–492.

Muñoz-Manchado, A. B., Gonzales, C. B., Zeisel, A., Munguba, H., Bekkouche, B., Skene, N. G., Lönnerberg, P., Ryge, J., Harris, K. D., Linnarsson, S., & others. (2018). Diversity of interneurons in the dorsal striatum revealed by single-cell RNA sequencing and PatchSeq. *Cell Reports*, *24*(8), 2179–2190.

Muñoz-Ortiz, J., Muñoz-Ortiz, E., López-Meraz, L., Beltran-Parrazal, L., & Morgado-Valle, C. (2019). The pre-Bötzinger complex: Generation and modulation of respiratory rhythm. *Neurología (English Edition)*, *34*(7), 461–468. https://doi.org/10.1016/j.nrleng.2018.05.006

Murakoshi, T., Suzue, T., & Tamai, S. (1985). A pharmacological study on respiratory rhythm in the isolated brainstem-spinal cord preparation of the newborn rat. *British Journal of Pharmacology*, *86*(1), 95–104.

Nattie, E. E., & Li, A. (1990). Ventral medulla sites of muscarinic receptor subtypes involved in cardiorespiratory control. *Journal of Applied Physiology*, *69*(1), 33–41.

Nattie, E., & Li, A. (2010). Central chemoreception in wakefulness and sleep: Evidence for a distributed network and a role for orexin. *Journal of Applied Physiology*, *108*(5), 1417–1424.

Nattie, E., & Li, A. (2011). Central chemoreceptors: Locations and functions. *Comprehensive Physiology*, *2*(1), 221–254.

Nattie, E., Wood, J., Mega, A., & Goritski, W. (1989). Rostral ventrolateral medulla muscarinic receptor involvement in central ventilatory chemosensitivity. *Journal of Applied Physiology*, *66*(3), 1462–1470.

Nectow, A. R., & Nestler, E. J. (2020). Viral tools for neuroscience. *Nature Reviews Neuroscience*, *21*(12), 669–681. https://doi.org/10.1038/s41583-020-00382-z

Newman, E. L., Gupta, K., Climer, J. R., Monaghan, C. K., & Hasselmo, M. E. (2012). Cholinergic modulation of cognitive processing: Insights drawn from computational models. *Frontiers in Behavioral Neuroscience*, *6*, 24.

Nieuwenhuis, B., Haenzi, B., Hilton, S., Carnicer-Lombarte, A., Hobo, B., Verhaagen, J., & Fawcett, J. W. (2021). Optimization of adeno-associated viral vector-mediated transduction of the corticospinal tract: Comparison of four promoters. *Gene Therapy*, *28*(1–2), 56–74. https://doi.org/10.1038/s41434-020-0169-1

Nurse, C. A. (2010). Neurotransmitter and neuromodulatory mechanisms at peripheral arterial chemoreceptors. *Experimental Physiology*, *95*(6), 657–667.

Oke, Y., Miwakeichi, F., Oku, Y., Hirrlinger, J., & Hülsmann, S. (2018). Cell type-dependent activation sequence during rhythmic bursting in the preBötzinger complex in respiratory rhythmic slices from mice. *Frontiers in Physiology*, *9*, 1219.

Okunomiya, T., Hioki, H., Nishimura, C., Yawata, S., Imayoshi, I., Kageyama, R., Takahashi, R., & Watanabe, D. (2020). Generation of a MOR-CreER knock-in mouse line to study cells and neural circuits involved in mu opioid receptor

signaling. *Genesis*, *58*(1), e23341.

Onimaru, H., & Homma, I. (2003). A Novel Functional Neuron Group for Respiratory Rhythm Generation in the Ventral Medulla. *The Journal of Neuroscience*, *23*(4), 1478–1486. https://doi.org/10.1523/JNEUROSCI.23-04-01478.2003

Onimaru, H., Ikeda, K., & Kawakami, K. (2008). CO2-sensitive preinspiratory neurons of the parafacial respiratory group express Phox2b in the neonatal rat. *Journal of Neuroscience*, *28*(48), 12845–12850.

Pagliardini, S., Greer, J. J., Funk, G. D., & Dickson, C. T. (2012). State-Dependent Modulation of Breathing in Urethane-Anesthetized Rats. *Journal of Neuroscience*, *32*(33), 11259–11270. https://doi.org/10.1523/JNEUROSCI.0948-12.2012

Pagliardini, S., Janczewski, W. A., Tan, W., Dickson, C. T., Deisseroth, K., & Feldman, J. L. (2011). Active Expiration Induced by Excitation of Ventral Medulla in Adult Anesthetized Rats. *Journal of Neuroscience*, *31*(8), 2895–2905. https://doi.org/10.1523/JNEUROSCI.5338-10.2011

Pagliardini, S., Ren, J., & Greer, J. J. (2003). Ontogeny of the Pre-Bötzinger Complex in Perinatal Rats. *The Journal of Neuroscience*, *23*(29), 9575–9584. https://doi.org/10.1523/JNEUROSCI.23-29-09575.2003

Peng, C., Yan, Y., Kim, V. J., Engle, S. E., Berry, J. N., McIntosh, J. M., Neve, R. L., & Drenan, R. M. (2019). Gene editing vectors for studying nicotinic acetylcholine receptors in cholinergic transmission. *European Journal of Neuroscience*, *50*(3), 2224–2238. https://doi.org/10.1111/ejn.13957

Picardo, M. C. D., Weragalaarachchi, K. T., Akins, V. T., & Del Negro, C. A. (2013). Physiological and morphological properties of Dbx1-derived respiratory neurons in the pre-Bötzinger complex of neonatal mice. *The Journal of Physiology*, *591*(10), 2687–2703.

Picciotto, M. R., Higley, M. J., & Mineur, Y. S. (2012). Acetylcholine as a Neuromodulator: Cholinergic Signaling Shapes Nervous System Function and Behavior. *Neuron*,

76(1), 116–129. https://doi.org/10.1016/j.neuron.2012.08.036

Poppi, L. A., Holt, J. C., Lim, R., & Brichta, A. M. (2020). A review of efferent cholinergic synaptic transmission in the vestibular periphery and its functional implications. *Journal of Neurophysiology*, *123*(2), 608–629.

Ramirez, J.-M., & Baertsch, N. (2018a). Defining the rhythmogenic elements of mammalian breathing. *Physiology*, *33*(5), 302–316.

Ramirez, J.-M., & Baertsch, N. A. (2018b). The Dynamic Basis of Respiratory Rhythm Generation: One Breath at a Time. *Annual Review of Neuroscience*, *41*(1), 475–499. https://doi.org/10.1146/annurev-neuro-080317-061756

Rekling, J. C., & Feldman, J. L. (1997). Bidirectional Electrical Coupling Between Inspiratory Motoneurons in the Newborn Mouse Nucleus Ambiguus. *Journal of Neurophysiology*, *78*(6), 3508–3510. https://doi.org/10.1152/jn.1997.78.6.3508

Ren, J., Qin, C., Hu, F., Tan, J., Qiu, L., Zhao, S., Feng, G., & Luo, M. (2011). Habenula "cholinergic" neurons corelease glutamate and acetylcholine and activate postsynaptic neurons via distinct transmission modes. *Neuron*, *69*(3), 445–452.

Richter, D. W., & Smith, J. C. (2014). Respiratory rhythm generation in vivo. *Physiology*, *29*(1), 58–71.

Rossi, J., Balthasar, N., Olson, D., Scott, M., Berglund, E., Lee, C. E., Choi, M. J., Lauzon, D., Lowell, B. B., & Elmquist, J. K. (2011). Melanocortin-4 Receptors Expressed by Cholinergic Neurons Regulate Energy Balance and Glucose Homeostasis. *Cell Metabolism*, *13*(2), 195–204. https://doi.org/10.1016/j.cmet.2011.01.010

Rothermel, M., Brunert, D., Zabawa, C., Diaz-Quesada, M., & Wachowiak, M. (2013). Transgene Expression in Target-Defined Neuron Populations Mediated by Retrograde Infection with Adeno-Associated Viral Vectors. *Journal of Neuroscience*, *33*(38), 15195–15206. https://doi.org/10.1523/JNEUROSCI.1618-13.2013

Ruggiero, D. A., Giuliano, R., Anwar, M., Stornetta, R., & Reis, D. J. (1990a). Anatomical

substrates of cholinergic-autonomic regulation in the rat. *Journal of Comparative Neurology*, *292*(1), 1–53.

Ruggiero, D. A., Giuliano, R., Anwar, M., Stornetta, R., & Reis, D. J. (1990b). Anatomical substrates of cholinergic-autonomic regulation in the rat. *Journal of Comparative Neurology*, *292*(1), 1–53.

Ruggiero, D., Pickel, V., Milner, T., Anwar, M., Otake, K., Mtui, E., & Park, D. (2019). Viscerosensory processing in nucleus tractus solitarii: Structural and neurochemical substrates. In *Nucleus of the solitary tract* (pp. 3–34). CRC Press.

Rybak, I. A. (n.d.). *Rhythmic Bursting in the Pre-Bötzinger Complex: Mechanisms and Models*. 23.

Saunders, A., & Sabatini, B. L. (2015). Cre Activated and Inactivated Recombinant Adeno-Associated Viral Vectors for Neuronal Anatomical Tracing or Activity Manipulation. *Current Protocols in Neuroscience*, *72*(1). https://doi.org/10.1002/0471142301.ns0124s72

Saxon, D. W., Robertson, G. N., & Hopkins, D. A. (1996). Ultrastructure and synaptology of the nucleus ambiguus in the rat: The semicompact and loose formations. *The Journal of Comparative Neurology*, *375*(1), 109–127. https://doi.org/10.1002/(SICI)1096-9861(19961104)375:1<109::AID-CNE7>3.0.CO;2-7

Schäfer, M. K.-H., Eiden, L. E., & Weihe, E. (1998). Cholinergic neurons and terminal fields revealed by immunohistochemistry for the vesicular acetylcholine transporter. I. Central nervous system. *Neuroscience*, *84*(2), 331–359. https://doi.org/10.1016/S0306-4522(97)00516-2

Schultz, B. R., & Chamberlain, J. S. (2008). Recombinant Adeno-associated Virus Transduction and Integration. *Molecular Therapy*, *16*(7), 1189–1199. https://doi.org/10.1038/mt.2008.103

Schwarzacher, S. W., Smith, J. C., & Richter, D. W. (1995). Pre-Botzinger complex in the

cat. *Journal of Neurophysiology*, *73*(4), 1452–1461. https://doi.org/10.1152/jn.1995.73.4.1452

Shao, X., & Feldman, J. (2000). Acetylcholine modulates respiratory pattern: Effects mediated by M3-like receptors in preBotzinger complex inspiratory neurons. *Journal of Neurophysiology*, *83*(3), 1243–1252.

Shao, X. M., & Feldman, J. L. (2001). Mechanisms underlying regulation of respiratory pattern by nicotine in preBotzinger complex. *Journal of Neurophysiology*, *85*(6), 2461–2467.

Shao, X. M., & Feldman, J. L. (2005). Cholinergic neurotransmission in the preBÖtzinger Complex modulates excitability of inspiratory neurons and regulates respiratory rhythm. *Neuroscience*, *130*(4), 1069–1081. https://doi.org/10.1016/j.neuroscience.2004.10.028

Shao, X. M., & Feldman, J. L. (2007). Efficient measurement of endogenous neurotransmitters in small localized regions of central nervous systems in vitro with HPLC. *Journal of Neuroscience Methods*, *160*(2), 256–263.

Shao, X. M., & Feldman, J. L. (2009). Central cholinergic regulation of respiration: Nicotinic receptors. *Acta Pharmacologica Sinica*, *30*(6), 761–770. https://doi.org/10.1038/aps.2009.88

Sherman, D., Worrell, J. W., Cui, Y., & Feldman, J. L. (2015). Optogenetic perturbation of preBötzinger complex inhibitory neurons modulates respiratory pattern. *Nature Neuroscience*, *18*(3), 408–414. https://doi.org/10.1038/nn.3938

Silva, J. N., Oliveira, L. M., Souza, F. C., Moreira, T. S., & Takakura, A. C. (2019). Distinct pathways to the parafacial respiratory group to trigger active expiration in adult rats. *American Journal of Physiology-Lung Cellular and Molecular Physiology*, ajplung.00467.2018. https://doi.org/10.1152/ajplung.00467.2018

Simmons, D. D., Bertolotto, C., Typpo, K., Clay, A., & Wu, M. (n.d.). *Differential development of cholinergic-like neurons in the superior olive: A light microscopic*

study. 11.

Sirieix, C., Gervasoni, D., Luppi, P.-H., & Léger, L. (2012). Role of the Lateral Paragigantocellular Nucleus in the Network of Paradoxical (REM) Sleep: An Electrophysiological and Anatomical Study in the Rat. *PLoS ONE*, *7*(1), e28724. https://doi.org/10.1371/journal.pone.0028724

Smith, J. C., Abdala, A. P. L., Borgmann, A., Rybak, I. A., & Paton, J. F. R. (2013). Brainstem respiratory networks: Building blocks and microcircuits. *Trends in Neurosciences*, *36*(3), 152–162. https://doi.org/10.1016/j.tins.2012.11.004

Smith, J. C., Abdala, A. P. L., Rybak, I. A., & Paton, J. F. R. (2009). Structural and functional architecture of respiratory networks in the mammalian brainstem. *Philosophical Transactions of the Royal Society B: Biological Sciences*, *364*(1529), 2577–2587. https://doi.org/10.1098/rstb.2009.0081

Smith, J., Ellenberger, H., Ballanyi, K., Richter, D., & Feldman, J. (1991). Pre-Botzinger complex: A brainstem region that may generate respiratory rhythm in mammals. *Science*, *254*(5032), 726–729. https://doi.org/10.1126/science.1683005

Sobrinho, C. R., Kuo, F.-S., Barna, B. F., Moreira, T. S., & Mulkey, D. K. (2016). Cholinergic control of ventral surface chemoreceptors involves Gq/inositol 1,4,5-trisphosphate-mediated inhibition of KCNQ channels: Cholinergic modulation of ventral surface chemoreceptors. *The Journal of Physiology*, *594*(2), 407–419. https://doi.org/10.1113/JP271761

Song, D., Wang, D., Yang, Q., Yan, T., Wang, Z., Yan, Y., Zhao, J., Xie, Z., Liu, Y., Ke, Z., Qazi, T. J., Li, Y., Wu, Y., Shi, Q., Lang, Y., Zhang, H., Huang, T., Wang, C., Quan, Z., & Qing, H. (2020). The lateralization of left hippocampal CA3 during the retrieval of spatial working memory. *Nature Communications*, *11*(1), 2901. https://doi.org/10.1038/s41467-020-16698-4

Souza, G. M. P. R., Kanbar, R., Stornetta, D. S., Abbott, S. B. G., Stornetta, R. L., & Guyenet, P. G. (2018). Breathing regulation and blood gas homeostasis after near

complete lesions of the retrotrapezoid nucleus in adult rats: Retrotrapezoid nucleus, breathing and PCO2 homeostasis. *The Journal of Physiology*, *596*(13), 2521–2545. https://doi.org/10.1113/JP275866

Spann, BryanM., & Grofova, I. (1992). Cholinergic and non-cholinergic neurons in the rat pedunculopontine tegmental nucleus. *Anatomy and Embryology*, *186*(3). https://doi.org/10.1007/BF00174143

Srivastava, A. (2016). In vivo tissue-tropism of adeno-associated viral vectors. *Current Opinion in Virology*, *21*, 75–80. https://doi.org/10.1016/j.coviro.2016.08.003

STEWART, W. C., & ANDERSON, E. A. (1968). Effect of a cholinesterase inhibitor when injected into the medulla of the rabbit. *Journal of Pharmacology and Experimental Therapeutics*, *162*(2), 309–318.

Stornetta, R. L., Macon, C. J., Nguyen, T. M., Coates, M. B., & Guyenet, P. G. (2013). Cholinergic neurons in the mouse rostral ventrolateral medulla target sensory afferent areas. *Brain Structure and Function*, *218*(2), 455–475. https://doi.org/10.1007/s00429-012-0408-3

Stornetta, R. L., Rosin, D. L., Wang, H., Sevigny, C. P., Weston, M. C., & Guyenet, P. G. (2003). A group of glutamatergic interneurons expressing high levels of both neurokinin-1 receptors and somatostatin identifies the region of the pre-Bötzinger complex: Somatostatin in the Pre-BötC. *Journal of Comparative Neurology*, *455*(4), 499–512. https://doi.org/10.1002/cne.10504

Sugimura, T., & Saito, Y. (2021). Distinct proportions of cholinergic neurons in the rat prepositus hypoglossi nucleus according to their cerebellar projection targets. *Journal of Comparative Neurology*, *529*(7), 1541–1552.

Sun, L., Tang, Y., Yan, K., Yu, J., Zou, Y., Xu, W., Xiao, K., Zhang, Z., Li, W., Wu, B., Hu, Z., Chen, K., Fu, Z. F., Dai, J., & Cao, G. (2019). Differences in neurotropism and neurotoxicity among retrograde viral tracers. *Molecular Neurodegeneration*, *14*(1), 8. https://doi.org/10.1186/s13024-019-0308-6

Takakura, A. C., Barna, B. F., Cruz, J. C., Colombari, E., & Moreira, T. S. (2014). Phox2b-expressing retrotrapezoid neurons and the integration of central and peripheral chemosensory control of breathing in conscious rats. *Experimental Physiology*, *99*(3), 571–585.

Takeshita, S., Sasa, M., Ishihara, K., Matsubayashi, H., Yajin, K., Okada, M., Izumi, R., Arita, K., & Kurisu, K. (1999). Cholinergic and glutamatergic transmission in medial vestibular nucleus neurons responding to lateral roll tilt in rats. *Brain Research*, *840*(1–2), 99–105.

Tan, W., Janczewski, W. A., Yang, P., Shao, X. M., Callaway, E. M., & Feldman, J. L. (2008). Silencing preBötzinger complex somatostatin-expressing neurons induces persistent apnea in awake rat. *Nature Neuroscience*, *11*(5), 538–540.

Tan, W., Pagliardini, S., Yang, P., Janczewski, W. A., & Feldman, J. L. (2010). Projections of preBötzinger Complex neurons in adult rats. *The Journal of Comparative Neurology*, *518*(10), 1862–1878. https://doi.org/10.1002/cne.22308

Tang, W., Ehrlich, I., Wolff, S. B. E., Michalski, A.-M., Wolfl, S., Hasan, M. T., Luthi, A., & Sprengel, R. (2009). Faithful Expression of Multiple Proteins via 2A-Peptide Self-Processing: A Versatile and Reliable Method for Manipulating Brain Circuits. *Journal of Neuroscience*, *29*(27), 8621–8629. https://doi.org/10.1523/JNEUROSCI.0359-09.2009

Teppema, L. J., & Baby, S. (2011). Anesthetics and control of breathing. *Respiratory Physiology & Neurobiology*, *177*(2), 80–92. https://doi.org/10.1016/j.resp.2011.04.006

Tervo, D. G. R., Hwang, B.-Y., Viswanathan, S., Gaj, T., Lavzin, M., Ritola, K. D., Lindo, S., Michael, S., Kuleshova, E., Ojala, D., Huang, C.-C., Gerfen, C. R., Schiller, J., Dudman, J. T., Hantman, A. W., Looger, L. L., Schaffer, D. V., & Karpova, A. Y. (2016). A Designer AAV Variant Permits Efficient Retrograde Access to Projection Neurons. *Neuron*, *92*(2), 372–382. https://doi.org/10.1016/j.neuron.2016.09.021

Thoby-Brisson, M. (2005). Emergence of the Pre-Botzinger Respiratory Rhythm Generator in the Mouse Embryo. *Journal of Neuroscience*, *25*(17), 4307–4318. https://doi.org/10.1523/JNEUROSCI.0551-05.2005

Threlfell, S., Lalic, T., Platt, N. J., Jennings, K. A., Deisseroth, K., & Cragg, S. J. (2012). Striatal Dopamine Release Is Triggered by Synchronized Activity in Cholinergic Interneurons. *Neuron*, *75*(1), 58–64. https://doi.org/10.1016/j.neuron.2012.04.038

Tokumaru, T. (1968). The nature of toxins of herpes simplex virus. *Archiv Für Die Gesamte Virusforschung*, *24*(1–2), 104–122.

Toor, R. U. A. S., Sun, Q.-J., Kumar, N. N., Le, S., Hildreth, C. M., Phillips, J. K., & McMullan, S. (2019). Neurons in the Intermediate Reticular Nucleus Coordinate Postinspiratory Activity, Swallowing, and Respiratory-Sympathetic Coupling in the Rat. *The Journal of Neuroscience*, *39*(49), 9757–9766. https://doi.org/10.1523/JNEUROSCI.0502-19.2019

Tupal, S., Rieger, M. A., Ling, G.-Y., Park, T. J., Dougherty, J. D., Goodchild, A. K., & Gray, P. A. (2014). Testing the role of preBötzinger Complex somatostatin neurons in respiratory and vocal behaviors. *European Journal of Neuroscience*, *40*(7), 3067–3077. https://doi.org/10.1111/ejn.12669

Ugolini, G., Kuypers, H., & Simmons, A. (1987). Retrograde transneuronal transfer of herpes simplex virus type 1 (HSV 1) from motoneurones. *Brain Research*, *422*(2), 242–256.

Van Dort, C. J., Zachs, D. P., Kenny, J. D., Zheng, S., Goldblum, R. R., Gelwan, N. A., Ramos, D. M., Nolan, M. A., Wang, K., Weng, F.-J., Lin, Y., Wilson, M. A., & Brown, E. N. (2015). Optogenetic activation of cholinergic neurons in the PPT or LDT induces REM sleep. *Proceedings of the National Academy of Sciences*, *112*(2), 584–589. https://doi.org/10.1073/pnas.1423136112

Varga, A. G., Maletz, S. N., Bateman, J. T., Reid, B. T., & Levitt, E. S. (2021). Neurochemistry of the Kölliker-Fuse nucleus from a respiratory perspective.

Journal of Neurochemistry, *156*(1), 16–37. https://doi.org/10.1111/jnc.15041

Volgin, D. V., Rukhadze, I., & Kubin, L. (2008). Hypoglossal premotor neurons of the intermediate medullary reticular region express cholinergic markers. *Journal of Applied Physiology*, *105*(5), 1576–1584.

Von Engelhardt, J., Eliava, M., Meyer, A. H., Rozov, A., & Monyer, H. (2007). Functional characterization of intrinsic cholinergic interneurons in the cortex. *Journal of Neuroscience*, *27*(21), 5633–5642.

WADA, E. (1989). Distribution of alpha 2. Alpha 3. Alpha 4 and beta 2 neuronal nicotinic receptor subunit hybridization histochemical study in the rat. *J. Comp. Neurol*, *284*, 314–335.

Wada, E., McKinnon, D., Heinemann, S., Patrick, J., & Swanson, L. W. (1990). The distribution of mRNA encoded by a new member of the neuronal nicotinic acetylcholine receptor gene family (α5) in the rat central nervous system. *Brain Research*, *526*(1), 45–53.

Wallén-Mackenzie, \AAsa, Wootz, H., & Englund, H. (2010). Genetic inactivation of the vesicular glutamate transporter 2 (VGLUT2) in the mouse: What have we learnt about functional glutamatergic neurotransmission? *Upsala Journal of Medical Sciences*, *115*(1), 11–20.

Wang, D., He, X., Zhao, Z., Feng, Q., Lin, R., Sun, Y., Ding, T., Xu, F., Luo, M., & Zhan, C. (2015). Whole-brain mapping of the direct inputs and axonal projections of POMC and AgRP neurons. *Frontiers in Neuroanatomy*, *9*, 40.

Wang, H.-L., & Morales, M. (2009). Pedunculopontine and laterodorsal tegmental nuclei contain distinct populations of cholinergic, glutamatergic and GABAergic neurons in the rat. *European Journal of Neuroscience*, *29*(2), 340–358. https://doi.org/10.1111/j.1460-9568.2008.06576.x

Wang, J., & Zhang, L. (2021). Retrograde axonal transport property of adeno-associated virus and its possible application in future. *Microbes and Infection*, *23*(8), 104829.

https://doi.org/10.1016/j.micinf.2021.104829

Wang, Y., Sanghvi, M., Gribizis, A., Zhang, Y., Song, L., Morley, B., Barson, D., Santos-Sacchi, J., Navaratnam, D. S., & Crair, M. (2020). Efferent feedback enforces bilateral coupling of spontaneous activity in the developing auditory system. *BioRxiv*.

Warner-Schmidt, J. L., Schmidt, E. F., Marshall, J. J., Rubin, A. J., Arango-Lievano, M., Kaplitt, M. G., Ibañez-Tallon, I., Heintz, N., & Greengard, P. (2012). Cholinergic interneurons in the nucleus accumbens regulate depression-like behavior. *Proceedings of the National Academy of Sciences*, *109*(28), 11360–11365.

Weiss, A. R., Liguore, W. A., Domire, J. S., Button, D., & McBride, J. L. (2020). Intra-striatal AAV2.retro administration leads to extensive retrograde transport in the rhesus macaque brain: Implications for disease modeling and therapeutic development. *Scientific Reports*, *10*(1), 6970. https://doi.org/10.1038/s41598-020-63559-7

Wessler, I., & Kirkpatrick, C. (2008). Acetylcholine beyond neurons: The non-neuronal cholinergic system in humans. *British Journal of Pharmacology*, *154*(8), 1558–1571.

Weston, M. C., Stornetta, R. L., & Guyenet, P. G. (2004). Glutamatergic neuronal projections from the marginal layer of the rostral ventral medulla to the respiratory centers in rats. *Journal of Comparative Neurology*, *473*(1), 73–85.

Winter, S. M., Fresemann, J., Schnell, C., Oku, Y., Hirrlinger, J., & Hülsmann, S. (2009). Glycinergic interneurons are functionally integrated into the inspiratory network of mouse medullary slices. *Pflügers Archiv-European Journal of Physiology*, *458*(3), 459–469.

Witten, I. B., Lin, S.-C., Brodsky, M., Prakash, R., Diester, I., Anikeeva, P., Gradinaru, V., Ramakrishnan, C., & Deisseroth, K. (2010). Cholinergic interneurons control local circuit activity and cocaine conditioning. *Science*, *330*(6011), 1677–1681.

Woolf, N. J. (1991). Cholinergic systems in mammalian brain and spinal cord. *Progress in Neurobiology*, *37*(6), 475–524.

Xu, M., Chung, S., Zhang, S., Zhong, P., Ma, C., Chang, W.-C., Weissbourd, B., Sakai, N., Luo, L., Nishino, S., & others. (2015). Basal forebrain circuit for sleep-wake control. *Nature Neuroscience*, *18*(11), 1641–1647.

Yang, C. F., & Feldman, J. L. (2018). Efferent projections of excitatory and inhibitory preBötzinger Complex neurons. *Journal of Comparative Neurology*, *526*(8), 1389–1402. https://doi.org/10.1002/cne.24415

Yang, C. F., Kim, E. J., Callaway, E. M., & Feldman, J. L. (2019). Monosynaptic projections to excitatory and inhibitory preBötzinger Complex neurons. *BioRxiv*, 694711. https://doi.org/10.1101/694711

Yao, F., Zhang, E., Gao, Z., Ji, H., Marmouri, M., & Xia, X. (2018). Did you choose appropriate tracer for retrograde tracing of retinal ganglion cells? The differences between cholera toxin subunit B and Fluorogold. *PLOS ONE*, *13*(10), e0205133. https://doi.org/10.1371/journal.pone.0205133

Zaborszky, L., Hoemke, L., Mohlberg, H., Schleicher, A., Amunts, K., & Zilles, K. (2008). Stereotaxic probabilistic maps of the magnocellular cell groups in human basal forebrain. *Neuroimage*, *42*(3), 1127–1141.

Zayia, L. C., & Tadi, P. (2020). Neuroanatomy, motor neuron. *StatPearls [Internet]*.

Zhang, G.-W., Shen, L., Zhong, W., Xiong, Y., Zhang, L. I., & Tao, H. W. (2018). Transforming Sensory Cues into Aversive Emotion via Septal-Habenular Pathway. *Neuron*, *99*(5), 1016-1028.e5. https://doi.org/10.1016/j.neuron.2018.07.023

Zheng, F., Nixdorf-Bergweiler, B. E., Edelmann, E., van Brederode, J. F., & Alzheimer, C. (2020). Muscarinic Modulation of Morphologically Identified Glycinergic Neurons in the Mouse PreBötzinger Complex. *Frontiers in Cellular Neuroscience*, *13*, 562.

Zhou, K., Cherra III, S. J., Goncharov, A., & Jin, Y. (2017). Asynchronous cholinergic

drive correlates with excitation-inhibition imbalance via a neuronal Ca2+ sensor protein. *Cell Reports*, *19*(6), 1117–1129.